3890

WAPD-PWR-PMM-491

METALLURGY AND CERAMICS

UNITED STATES ATOMIC ENERGY COMMISSION

RESUME OF URANIUM OXIDE DATA—VII

By
J. Belle
L. J. Jones

September 12, 1956

Bettis Plant
Westinghouse Electric Corporation
Pittsburgh, Pennsylvania

Technical Information Service Extension, Oak Ridge, Tenn.

Printed in USA. Price $3.75. Available from the Office of Technical Services, Department of Commerce, Washington 25, D. C.

AEC Technical Information Service Extension
Oak Ridge, Tennessee

DISCLAIMER

WAPD-PWR-PMM-491

RESUME' OF URANIUM OXIDE DATA - VII

J. Belle and L. J. Jones

September 12, 1956

Work performed under Contract No. AT-11-1-Gen-14

Bettis Plant Pittsburgh, Pa.

Operated for the U.S. Atomic Energy Commission by
Westinghouse Electric Corporation

RESUME' OF URANIUM OXIDE DATA - VII

J. Belle and L. J. Jones

Contributors

S. Aronson
A. B. Auskern
T. J. Burke
J. C. Clayton
R. E. Cowan
J. D. Eichenberg
E. S. Gamble
T. J. Kisiel
R. C. Koch
J. M. Markowitz
T. R. Padden
J. A. Roll
R. B. Roof, Jr.
B. E. Schaner
F. S. Susko

Preparation and Properties of UO_2

Powder Preparation

Work was continued on the preparation of pure UO_2, "activated" UO_2 and UO_2 containing additives and poisons for irradiation and fabrication tests as well as for investigations of their physical and chemical properties.

Poison Additives

Several methods of preparing poison calibration standards for the Reactivity Measurement Facility (RMF) were investigated. Powder mixtures of UO_2 plus metallic gold (0.25 w/o) were prepared by chemical addition and mechanical blending and were cold pressed into compacts. After sintering in hydrogen at 1700°C for 8 hours, the pellets retained only half the gold content (0.13 w/o). The entire gold content was retained, however, after argon sintering at 1550°C for 10 hours. Powder mixtures of UO_2 plus amorphous boron (200 ppm), boron carbide and boron nitride were prepared by blending and dry ball milling. On the first attempts considerable boron segregation was indicated by chemical analyses.

"Activated" UO_2

Attempts were made to prepare finely divided UO_2 by comminution processes other than ball milling. In one procedure, Mallinckrodt oxide slurries were mechanically ground at 45,000 rpm with stainless steel blades. In another technique, an aqueous UO_2 suspension was added to a stationary steel grinding tank filled with small stainless steel balls. An agitator kept the grinding bodies and the UO_2 charge in continuous interaction. However, after both these methods, the dried oxide powders were found to contain

considerable amounts of iron (0.5 to 3%).

In a third method, as-received Mallinckrodt powder was ground with a "Mikro Atomizer", a high-speed horizontal-shaft hammer mill. This instrument can continuously grind approximately 75 lbs. of oxide per hour. A batch of Mallinckrodt oxide which was ground with this instrument had substantially the same impurity content as the feed material.

Physical Measurements

Density Measurements

Density measurements of various types of UO_2 powders were continued. A comparison of helium and liquid measurements for a group of UO_2 powders is given in Table I. For the most part the liquid and helium density values are low and in close agreement, indicating that these powders contain little open porosity but an appreciable amount of closed porosity. Only in the case of UO_2 powders prepared by chemical precipitation and spray denitration are the liquid values lower (2 to 2.5%), suggesting the presence of small open pores. The high density oxides, except for the powders prepared by steam oxidation, have high O/U ratios (2.07 to 2.08).

A comparison of "real" and "apparent" density values of various UO_2 powders is given in Table II. As described in Resume' VI (WAPD-PWR-PMM-466) the apparent (bulk) density is measured according to a specified method of loading a container of known volume (4.84 cc). The oxides prepared through the crystal growth and spray denitration methods have the highest bulk densities.

Surface Area Measurements

Measurements of the total surface area of various types of UO_2 powders were continued. The results are given in Table III. In agreement with previous measurements, the specific surface of UO_2 made through chemical precipitation was high while those powders prepared by steam oxidation and reduction of the higher uranium oxides had relatively low total surfaces. The low surface area of NPHUR-1 and the rather high specific surface of ANL-2 might be due in part to the reduction temperatures. The dependence of UO_2 surface area on the temperature of preparation is shown more clearly in Table IV. UO_2 made by hydrogen reduction of UO_3 at 480°C had a specific surface of 24.7 m^2/cc; when the reduction temperature was increased to 1180°C, the surface decreased to 9.4 m^2/cc. The temperature of reduction did not seem to affect the density values. Those preparations with slightly greater densities had somewhat higher O/U ratios.

External surface area measurements by air permeability methods of various types of UO_2 powders were continued. The method of Gooden and Smith, described in Resume' VI, was used for the coarser UO_2 powders with external surfaces less than 6 m^2/cc. To estimate the external surfaces of the finer oxide powders, an apparatus based on that of Carman and Malherbe[1] was constructed. In this technique, a self-supporting pellet of UO_2 is formed in an

1. J. Soc. Chem. Ind., 69, 134 (1950)

accurately machined tube with a small hand press. The volume of air flowing through the sample is directly measured with a graduated tube. This apparatus is accurate for measuring powders with external surfaces between 3 and 60 m^2/cc. A comparison of the total (gas adsorption) and external (permeability) surface areas for a series of UO_2 powders is shown in Table V. The "roughness factors" range from 2 to 6, indicating varying amounts of porosity and particle irregularities.

Surface area measurements were made by the krypton adsorption technique on two compacts sintered to theoretical densities of 89 and 96%. The specific areas calculated were 0.037 m^2/g and 0.004 m^2/g, respectively, as compared with the value of 0.060 m^2 for the uncompacted powder. As expected, sintering has the effect of greatly decreasing the surface area.

Pore Size Distribution in UO_2 Compacts

Measurements of pore size distributions have been completed on four green UO_2 compacts using a high pressure mercury porosimeter. The results of the measurements are shown in Fig. 1. It is apparent from these curves that a pronounced difference exists between the pore size distributions of as-received and ball-milled Mallinckrodt UO_2 powders as well as between the different green densities of the individual powders. The compacts having higher green densities show a smaller total pore volume, a narrower range of pore sizes, and a smaller average pore size. The ball-milled powder has a narrower distribution of pore diameters and a smaller average pore diameter than the as-received UO_2. The effect of ball milling is thought to be a reduction and evening of the aggregate size which results in a uniform pore size during compaction. It may be shown from these curves that pellets of higher green densities contain larger volumes of small pores than do the pellets of lower green densities. This is caused by the compression of the large pores during compaction.

Measurements of pore size distribution over a wider range of green densities will be obtained. Studies will also be made on pellets sintered to varying densities. It is expected that the information obtained from these measurements can be correlated with other studies of the sintering process.

Fabrication and Sintering of UO_2

Characterization of UO_2 Powder Preparations

The pressing and sintering characteristics of eight different UO_2 powders were investigated. Shown in Table VI are the powder histories, surface areas, and densities of these preparations. The observed sintering characteristics are presented in Table VII. These include: (1) the condition of the pellets after sintering; (2) the density attained with compacts which were pressed to 65% theoretical density and sintered in H_2 at 1700°C for 64 hours; (3) the relative dependence of sintered density on pressed density; (4) the density attained after sintering for 8 hours at 1700°C; and (5) relative rank-

ings based on surface area, powder density, and fully sintered density. The following observations can be made from these data:

1. There is some correlation between high sintered density attained by the compact and both high surface area and high density of the powder. However, the UO_2 powder produced by steam oxidation has poor sintering characteristics even when the powder is made with high surface area and density.

2. The powder preparations which have good sintering characteristics are (1) UO_2 made from ammonium diuranate and not milled, (2) ball-milled Mallinckrodt UO_2, and (3) UO_2 prepared from ball-milled UO_3.

3. As-received Mallinckrodt oxide is markedly inferior to four of the powder types studied and ranks seventh in the group of eight powders.

Microscopic observations indicate that it may be the nature of the porosity distribution in the as-pressed compacts that determines sintering characteristics. This may be substantiated by additional information from pore size distribution measurements.

Ball Milling

It was reported in Resume' VI that ball-milled Mallinckrodt UO_2 contained 1 to 2 w/o zirconium as a result of ball-milling in a Zircaloy mill with Zircaloy balls. To determine if the zirconium contamination contributed to the desirable sintering characteristics of the powder, Mallinckrodt oxide was wet ball-milled in rubber-lined mills with uranium pellets as the grinding medium. From a comparison of the sintered density versus pressed density data from this powder with that of the same powder milled in the Zircaloy mill, it was concluded that there is no effect of the zirconium.

The decrease, due to milling, in the dependence of sintered density on pressed density has been found to be a good measure of the efficiency of the milling procedure. This relation was used to determine the relative efficiencies of wet and dry ball milling. Uranium pellets were used as the grinding medium in rubber-lined mills. As shown in Fig. 2, it was found that wet ball milling is more efficient. The wet ball-milled powder showed much less dependence of sintered density on pressed density and, for comparable pressed densities, it sintered to higher densities than did the dry ball-milled powder. The wet ball-milled powder can be sintered to a density above 96% of theoretical when pressed at only 2000 psi. To attain densities higher than 95% of theoretical with as-received Mallinckrodt powder, pressing pressures in excess of 227,000 psi are required.

Effect of "Mikro Atomizing"

Preliminary experiments indicate that the "Mikro Atomizer" shows excellent promise as an alternative for ball milling in the production of large quantities of readily sinterable UO_2 powder. Table VIII is a summary

of the densities obtained on compacts made with finely divided "mikro atomized" Mallinckrodt UO_2. Extruded rods made from this powder attained a density of 92.6% of theoretical after sintering in H_2 at 1725°C for 10 hours.

Effect of Steam on the Sintering of UO_2

It has been reported at various times that steam is beneficial for sintering UO_2 compacts. The exact role of steam in the sintering process, however, is not known. A statistically designed experiment to determine effects of steam on sintering of UO_2 is planned and will include sintering temperature, green density, and powder preparation, each at four levels of atmosphere conditions. The atmosphere combinations will be as follows:

Atmosphere	Heat	Soak	Cool
a_o	H_2	H_2	H_2
a_1	H_2	H_2O	H_2
a_2	H_2O	H_2	H_2O
a_3	H_2O	H_2O	H_2O

The densities of the sintered pellets will be measured by mercury displacement and will be used as the measured value in the statistical analysis. One replication of each treatment combination will be run. This will permit the estimation of the main effect and all interactions.

Effect of Various Oxide Additions on the Sintering of UO_2

Five common oxides were added to as-received Mallinckrodt UO_2 powder to determine the effect of these additives on the sintered density at various temperatures. The powder batches were prepared by dry mixing the additive (0.1, 0.5 and 1.0 w/o additives) with the UO_2 and 1 w/o PVA. The powders were agglomerated to a granular mix and pressed at a pressure of 80 tsi. Pellets which did not contain additives were prepared in a similar manner as controls for the experiment. The sintering temperatures used were 1400, 1500, 1600, and 1700°C (H_2 atmosphere) and the pellets were held at these temperatures for 10 hours. The results are shown in Figs. 3 and 4. In general, small quantities of CaO reduced the density but quantities over 0.5 w/o increased the density markedly. None of the other materials except Al_2O_3 at 1400°C had a very pronounced effect on the density of the UO_2. Since CaO in quantities greater than 0.5 w/o and TiO_2 in quantities over 0.05 w/o have been shown, from previous work, to increase the sintered density of UO_2, the possible effect of both additives was also investigated. Figs. 5 to 8 are photomicrographs which show the effects of both the independent additions and the combined additions of CaO and TiO_2 on the microstructure and sintered density of as-received Mallinckrodt UO_2. TiO_2 enlarges the grain size and appears to have a maximum effect at an addition of 0.5 w/o. CaO increases the density but does not increase the grain size. The additives in combination have their most beneficial effect at 0.25 w/o TiO_2 and 0.25 w/o CaO where a density of 94.6% of theoretical was obtained, compared with 82.5% with 0.5 w/o CaO and 87.8% with 0.5 w/o TiO_2. A density of

only 77.8% of theoretical is achieved with no addition.

An experiment was made to determine whether the precombined forms of CaO and TiO_2 (calcium titanates) would produce the same results as the individual additions. $CaTiO_2$ and Ca_3TiO_7 were prepared for this purpose from mixtures of $CaCO_3$ and TiO_2 heated together at temperatures of 1350 and 1550°C, respectively. Fig. 9 shows that although these materials do have a tendency to increase the sintered density of the UO_2 they do not do so to the extent of the individual additions. At 1700°C several of the pellets containing high percentages of the additives blistered and bloated. This was probably due to formation of a compound or a lower melting phase.

Fabrication of High Density UO_2 from Ammonium Diuranate

It was reported in Resume' V (WAPD-PWR-PMM-429) that high density UO_2 pellets were obtained by cold pressing ammonium diuranate powder, pre-sintering the powder in hydrogen at 800°C to convert it to UO_2, and sintering in hydrogen at 1700°C. Although high densities (96.7% of theoretical density) were obtained, cracks in the pellets were formed during the pre-sintering operation.

Recent attempts were made by both extrusion and cold pressing methods to obtain high density UO_2 directly from ammonium diuranate powder. The powder was successfully extruded in the form of hollow cylindrical rods of 0.300 in. O.D. and 0.059 in. I.D. with an average green density of 42% of theoretical. The as-prepared powder was first screened through an 80 mesh sieve and then granulated with additions of 1.0 w/o methocel binder, 0.1 w/o sterotex lubricant, and 19.5 w/o water. The damp granular mix was then placed in the hydraulic extrusion press and precompacted at 14,000 psi and a partial pressure of 1.5 cm Hg for three minutes. The mix was then extruded through stainless steel dies and the rods were cut to approximately 5-in. lengths and placed in plaster forms for drying. After oven-drying overnight at 80°C, the extrusions were sintered in hydrogen at 1600 and 1700°C. In both cases the sintered rods, fully converted to UO_2, were badly cracked and warped from excessive shrinkage.

In another experiment, ammonium diuranate powder was preheated in air at 180, 350, and 500°C. Pellets were then pressed from these preheated materials at 80 tsi. On sintering at 600 and 700°C, all of these pellets showed cracking to some extent. Those that had been heated to 500°C were cracked slightly, those that had the 350°C pretreatment were more cracked, while those from the 180°C group were cracked to a still greater degree.

It appears that the heating-up portion of the sintering process must be carefully controlled and the temperature raised at a very slow rate, particularly in the temperature range where decomposition occurs with evolution of gas.

A study was made of the effect on the sinterability of Mallinckrodt oxide compacts containing additions of ammonium diuranate powder up to 25 w/o in 5 w/o increments. Appropriate weights of the two constituents were blended

with 1 w/o PVA, agglomerated with 10 w/o water, and then dried and prepared for pressing by adding 0.2 w/o sterotex. After the powders were pressed at 80 tsi, the compacts were sintered in hydrogen for 10 hours at 1400, 1600, and 1725°C. It was found that at each sintering temperature the density decreased with an increase in ammonium diuranate content in a nearly linear manner (see Fig. 10). There was also evidence of a tendency for cracking in the form of hairline circumferential cracks in those pellets with the higher ADU content. If the 1725°C curve in Fig. 10 is extrapolated to the 100% UO_2 ordinate, the value for the sintered density agrees with an interpolated density from a previously obtained plot of sintered density versus pressed density for Mallinckrodt oxide.

Sintering of High O/U Ratio Uranium Oxides

Experiments are being conducted to determine whether uranium oxides having O/U ratios greater than 2.00 can be sintered while undergoing no loss of oxygen. Compacts with high O/U ratios were sintered at 1550°C for 10 hours in a flowing argon atmosphere. The oxide was found to have been reduced to a composition of $UO_{2.00}$. Similar compacts, when sintered at 1300 and 1400°C for 10 hours in static argon, reverted to the composition $UO_{2.10}$. From the weight changes of the pellets in the 1300 and 1400°C runs, an equilibrium partial pressure of oxygen was calculated to be approximately 150 mm Hg. The oxygen partial pressure during a run in flowing argon would be essentially zero. These results indicate that certain atmosphere and temperature combinations exist under which no loss of oxygen occurs, and that the high O/U ratio material can be successfully sintered. Future work will be directed toward the determination of the exact temperature and atmosphere requirements for the sintering of each composition.

Sintering Rates

An experiment has been initiated for the measurement of the rates at which UO_2 pellets are densified during sintering. The diameters of pellets will be measured as a function of time during sintering using a micrometer cathetometer. These data will be used for the determintion of shrinkage and densification rates and activation energies for the sintering process.

Stability of UO_2 in Water

Long term tests on the stability of UO_2 compacts in water have continued. Specimens have now been exposed for 214 days in degassed water at 650°F and for 177 days in degassed water maintained at a pH of 10.5 at 650°F. The appearance of the compacts remained unchanged. UO_2 compacts were observed and weighed after exposures of 60 days to 750°F steam. Hydrogen gas build-up was prevented by maintaining a continuous flow of steam through the autoclave. Most of the pellets were not changed significantly in either appearance or weight.

Kinetic Studies in Water

Apparatus has been constructed to study the oxidation of UO_2 in water

in which the concentration of dissolved oxygen is maintained constant and homogeneous throughout the body of the UO_2 powder. The technique involves forcing the inlet water into the autoclave through a series of stainless steel micrometallic filter elements. The rates of oxidation of UO_2 will be determined at temperatures of 100-300°C and at an oxygen concentration in the water of 25 cc O_2/kg H_2O (equivalent to 125 mm Hg partial pressure of oxygen). The results in water will be compared with oxidation data obtained in air for the same temperature range.

UO_2-O_2 Equilibrium and Kinetics

Kinetic Studies

Determination of the kinetics of oxidation of UO_2 in air and oxygen at temperatures of 160-350°C has been completed. It has been found that oxidation to U_3O_8 proceeds in two stages. The first stage, oxidation to $UO_{2.34}\pm0.02$, was discussed in Resume' VI. The second reaction step, the conversion of tetragonal $UO_{2.34}\pm0.02$ to U_3O_8, was studied at temperatures of 260-350°C. Below 260°C, the reaction rate was very slow. Sigmoidal rate curves were obtained, which is indicative of an autocatalytic reaction. A likely mechanism for the reaction is the formation of U_3O_8 nuclei on the surface of the particles and the inward growth of the new phase into the particles.

The analysis of Johnson and Mehl[2] was used to interpret the rate data. These authors derived an equation for the transformation of one solid phase into another for the case of a solid matrix composed of small grains where nucleation occurs solely on the grain boundaries. This analysis is readily applicable to a powder material with nucleation occurring on the surface of the particles. The basic assumptions used in the analysis are that nucleation occurs at a constant rate per unit untransformed surface and that the rate of linear growth of the new phase is constant. Since the equation obtained was too complex for a numerical solution the authors plotted a number of theoretical curves which could be compared to experimental rate curves. They found that the rate of reaction was more strongly influenced by the rate of growth of the new phase than by the rate of nucleation.

The rate curves that were obtained for the oxidation of $UO_{2.34}\pm0.02$ to U_3O_8 were compared to the theoretical curves of Johnson and Mehl. For the calculation of the growth constants, the experimental curves were compared to a theoretical curve in which the average number of nuclei forming on the surface of a particle is approximately 15. In Fig. 11, a number of points of the theoretical curve are superimposed on a typical experimental curve. It is seen that agreement is good until the reaction is approximately 70% complete. The discrepancy at higher degrees of conversion may be the result of simplifying assumptions used in deriving the theoretical equation. It is also possible that the diffusion of oxygen, which is ignored in this treatment, becomes an important rate-controlling step at high degrees of conversion. Fig. 12 is a plot of log G versus 1/T where G is the coefficient of linear growth. The activation energy for growth was found to be 35.4 ± 2 kcal/mole.

2. Trans. A.I.M.E., 135, 416 (1939)

X-Ray Studies

X-ray evidence obtained from the kinetic oxidation experiments was found to be in good agreement with the kinetic data. UO_2 samples that were oxidized for various times to various O/U ratios were subjected to X-ray diffraction analysis. Table IX lists the crystallographic data which were obtained from samples that had been oxidized at 230°C to several O/U ratios. There is no X-ray evidence for the first step oxidation product U_3O_7 until the O/U ratio becomes about 2.16. From an O/U ratio of 2.16 to an O/U ratio of 2.34, the oxidation product U_3O_7 increases in relative quantity (at the expense of UO_2) and also appears to have a regular change in lattice parameter, as shown in Fig. 13. The data of Table IX can be interpreted as corroborative evidence for the diffusion of oxygen into UO_2. If diffusion did not occur, i.e., if the oxygen atoms were concentrated on the surface of the particle in a "skin effect", then X-ray diffraction would detect the presence of U_3O_7 when the average O/U ratio was as low as 2.03 to 2.06. Failure to observe U_3O_7 in this range and actually not until about an O/U ratio of 2.16 leads to the conclusion that from the O/U ratio of 2.00 (starting material) to the average O/U ratio of 2.16 the oxygen atoms are diffused in the UO_2 material. A concentration gradient most likely exists from the surface to the center of the particle but the concentration at any point in the UO_2 is not sufficient to form U_3O_7. Above the average O/U ratio of 2.16 the oxygen atoms diffuse into the matrix, and increasing amounts of U_3O_7 are formed until at an O/U ratio of 2.33 to 2.34 the matrix is completely U_3O_7. This is substantiated by the observation that the line intensities become stronger for U_3O_7 and weaker for UO_2 as the O/U ratio increases from 2.16 to 2.33.

The limits of error for the lattice contents of the tetragonal portion of Fig. 13, i.e., $\pm$ 0.02 A, are rather large. In an effort to reduce the limit of error and also to study in more detail the variation of lattice constants with O/U ratio in the tetragonal region, samples were taken from an oxidation run at 275°C. This increase in temperature has the effect of producing tetragonal diffraction lines that are sharper than those that were obtained at 230°C. The sharper diffraction lines can be measured more precisely, and consequently the limits of error are reduced. This is evident from Table X and Fig. 14. It is interesting to note that the limit of error is a maximum at the low O/U ratio and decreases as the theoretical limit of U_3O_7 (O/U = 2.33) is approached. It is assumed that this effect at low O/U ratio is due to oxygen vacancies in the U_3O_7 lattice. As the O/U ratio increases, these vacancies are filled by the diffusing oxygen atoms, resulting in lattice regions sufficiently large to give increasingly sharp diffraction lines.

The appearance of the second step oxidation product U_3O_8 follows the normal two-phase region rule. As the O/U ratio increases from 2.36 to 2.67, U_3O_8 appears in increasing amounts and the quantity of U_3O_7 decreases. The X-ray patterns illustrating this phenomenon were taken on samples obtained from an oxidation run at 300°C. No changes in lattice parameter were observed in either U_3O_8 or U_3O_7.

Calculated diffusion coefficients from the kinetic experiments are the same for air and pure O_2 oxidation. This result suggests that nitrogen acts only as a diluent for the oxygen and has no major role in the mechanism of oxidation of UO_2. X-ray diffraction patterns taken on samples obtained from a pure O_2 oxidation run at 230°C show similar behavior to air oxidation at the same temperature. U_3O_7 begins to appear at an O/U ratio of about 2.13 and there is a lattice parameter variation until an O/U ratio of 2.33.

Equilibrium Measurements

Equilibrium pressures of oxygen over uranium oxide in the composition range UO_2-U_3O_8 are being determined with a quartz microbalance. Measurements of oxide composition as a function of pressure were made at temperatures of 800, 880, and 975°C. The dependence on pressure was found to be slight in the pressure range 150 mm to 25 microns. The compositions were $UO_{2.65} \pm 0.005$, $UO_{2.647} \pm 0.005$, and $UO_{2.636} \pm 0.005$, respectively, at the three temperatures. These values are in fair agreement with the data obtained by Biltz and Muller.[3] However, they found a somewhat stronger dependence of composition on pressure. The composition $UO_{2.58}$ at 525°C, reported in Resume' VI, was in error. The erroneous value was due to reaction of the nichrome suspension wire, which has since been replaced by a platinum wire.

Diffusion Studies

Uranium Diffusion

In Resume' VI the experimental procedures used were outlined and two diffusion coefficients of U^{+4} in UO_2 were presented. Subsequent work has revealed that the diffusion coefficients reported are not correct. For one reason, the pellets which had been sintered to low densities (88 and 91% of theoretical) sintered further during the diffusion anneal. This would result in a modification of the boundary conditions from which the diffusion coefficient was calculated. Also, a systematic error was uncovered in the calculations, which resulted in values of the diffusion coefficient that were several orders of magnitude too large. Further experiments were made, however, on high density (97.5% of theoretical) UO_2. Additional sintering did not occur since this material remained dimensionally stable during the high temperature diffusion anneals. The anneals were made at 1010, 1095, 1560, 1640, 1670, 1700, and 1725°C. Complete isotopic analyses have not yet been completed.

For the bondary conditions employed in these experiments (the infinite solid with an instantaneous source of diffusing material deposited on the surface), the solution to the diffusion equation shows that a plot of log concentration against diffusion distance squared (log C vs. x^2) is a straight line. In all the experiments so far this has not been observed. What is observed is that the absolute value of the slope of the curve becomes smaller for increasing values of x^2. This implies that the diffusing material has moved a greater distance than that predicted by the solution for the diffusion

3. Z. Anorg. Chem. 163, 263 (1927)

equation. A diffusion coefficient calculated from such a curve by fitting the best straight line through the distribution results in a value that is too small near the original surface and too large at greater diffusion depths.

Diffusion coefficients have been calculated from similar nonlinear distributions when reasons for the anomalous behavior were known. For example, deviations in slope, and consequent variations in D, have been shown to be due to slight changes in the stoichiometric composition of the lattice.[4] In the case of UO_2, since all diffusion anneals take place in a hydrogen atmosphere, it appears that there would be no consistent compositional variation throughout the diffusion couple. The deviation from linearity can be attributed to contributions from grain boundary diffusion, as was done by Slifkin, et al,[5] in a study of self-diffusion in crystalline silver. From an analysis of Fischer,[6] they were able to separate the grain boundary contribution from lattice diffusion. At high temperatures the relationship between log C and x^2 was found by Slifkin et al, to be linear, indicating that only volume diffusion processes are present.

The temperature region where grain boundary diffusion effects appear to confound those of volume diffusion seems to be around 0.7 Tm (Tm is the absolute melting point). This is in the region where diffusion measurements have been made on UO_2. If it is assumed that the two effects, grain boundary and volume diffusion, are present in UO_2, then a volume diffusion coefficient can be calculated from the log C vs. x^2 plot using the points near the original surface. This has been done for diffusion anneals carried out at 1560 and 1670°C. The diffusion coefficients calculated from these runs are 1.8×10^{-14} and 2.8×10^{-13} cm^2/sec, respectively. Since a reliable calculation of the activation energy cannot be made from only two points and a temperature range of 110°, only an estimate can be given. The activation energy so estimated is of the order of 150 kcal/mole.

Oxygen Diffusion

A quantity of UO_2 enriched in O^{18} was prepared by the high pressure steam oxidation method. Mass spectrographic analysis of the material showed the O^{18} enrichment to be about 7 times normal, which is the enrichment of the water from which the UO_2 was prepared. A series of diffusion anneals has been completed for the temperature range 850 to 1050°C. The diffusion couples consisted of pellets of natural UO_2 upon which a thin layer of O^{18} enriched UO_2 was deposited. The analytical procedure for the determination of O^{18} in UO_2, however, is difficult. Only very small samples are available, and it is necessary to analyze the UO_2 from the solid phase directly, since solution

4. Anderson, J.S., and Richards, J.R., "The Self Diffusion of Lead in Lead Sulfide", J. Chem. Soc. 1946, p. 537.
5. Slifkin, L., Lazarus, D., and Tomizuka, T., "Self Diffusion in Pure Crystalline Silver", J. App. Phys., 23, 1952, 1032
6. J. C. Fischer, "Calculation of Diffusion Penetration Curves for Surface and Grain Boundary Diffusion", J. App. Phys. 22, 74, 1951

of the UO_2 would change the O^{18}/O^{16} ratio.

Another attempt at the determination of the self diffusion of oxygen in UO_2 will be made by an exchange reaction between UO_2 enriched in O^{18} and O^{16} in CO_2. Suitable apparatus has been constructed.

In-Pile Fission Gas Release Experiment

The in-pile fission gas release experiment, designed to study the emanation of inert gas fission products from sintered UO_2 bodies under irradiation, has continued in operation at the Brookhaven National Laboratory reactor. Six specimens have been irradiated to date:

Spec. No.	% U^{235}	Density (% Theoretical)	Shape	Powder Type
1	Nat.	92.7	plate	MCW as-recieved
2	Nat.	96.8	plate	MCW ball-milled
3	8.19	97.5	plate	EUR ball-milled
4	8.19	97.5	plate	EUR ball-milled
5	8.19	97.5	cylinder	EUR ball-milled
6	8.19	96.5	cylinder	EUR as-received

In operation, carrier gas flows over the irradiated specimen and passes into an out-of-pile analytical system, where the fission gases are separated and analyzed. The specimen temperature is controlled by an in-pile furnace. The experimental observation is the gamma activity of an aliquot of gas distilled from a charcoal filled cold trap through which the carrier gas stream passes after emerging from the pile. This observation may be related to the rate of gas emanation at the specimen surface by the equation

$$f = \frac{\alpha}{\epsilon q} \frac{e^{\lambda t_c} e^{\lambda t_p}}{(1-e^{-\lambda t_t})} \qquad (1)$$

where

f = surface flux, atoms sec^{-1}

α = observed activity, counts sec^{-1}

ϵ = counting efficiency

q = branching ratio of decay scheme

λ = decay constant, sec^{-1}

t_c = time lapse before counting, sec

t_p = transit time, specimen to trap, sec

t_t = trapping time, sec

Data from specimen No. 5 has been analyzed to determine the diffusion coefficients for Kr^{87} and Xe^{135} as a function of temperature. For this purpose the following equation was used:

$$\frac{f}{A} = D\,\frac{\mathbb{D}}{2R\lambda}\left[\sinh R\sqrt{\frac{\lambda}{D}}\tanh a\sqrt{\frac{\lambda}{D}} + R\sqrt{\frac{\lambda}{D}}\tanh a\sqrt{\frac{\lambda}{D}} - \cosh R\sqrt{\frac{\lambda}{D}} + 1\right] \quad (2)$$

f = total surface flux, atoms sec^{-1}

A = surface area, cm^2

$\mathbb{D}$ = fission source function, atoms cm^{-3} sec^{-1}

λ = decay constant, sec^{-1}

D = diffusion coefficient, cm^2 sec^{-1}

R = recoil range, cm

a = specimen thickness, cm

Fig. 15 is a graph of equation (2) for the four fission products, Kr^{85m}, Kr^{87}, Xe^{133}, and Xe^{135}. Equation (2) was derived for the case of a plane slab within which fission occurs at a constant rate and from which diffusing material disappears both by decay and recoil, the latter effect occuring only near the surface. As a result, equation (2) does not account for the fission product atoms which have recoiled out of the body and become entrapped in the region around the slab. In an experiment, such recoil atoms will eventually find their way, by some mechanism, into the primary diffusion stream and thus may contribute substantially to the total experimental observation. It is at present not possible to determine the magnitude of this effect, although, as discussed later, an experimental attempt to separate primary and secondary diffusion is being undertaken.

The fission source function, $\mathbb{D}$, used in equation (2) is defined by

$$\mathbb{D}_i = \eta\,\sigma\,\phi\,\psi_i$$

where

η = atom density of U^{235}, cm^{-3}

σ = fission cross section for U^{235}, cm^2

ϕ = neutron flux, cm^{-2} sec^{-1}

ψ_i = fission yield for the ith fission product

In the present experiment the determination of the neutron flux, ϕ, is to be

accomplished by analyzing a specimen after irradiation for one or more long-lived fission products such as Cs^{137}; this analysis has not yet been made. The value of ϕ used in calculating the curves of Fig. 15 is therefore an approximate value obtained from BNL personnel.

In view of these circumstances, the data which follow are intended to do no more than indicate orders of magnitude; the numerical values cannot be taken seriously.

Use of Fig. 15 to determine D resulted in the following values:

T	Kr^{87}		Xe^{135}	
°C	f/A $cm^{-2}sec^{-1}$	D cm^2sec^{-1}	f/A $cm^{-2}sec^{-1}$	D cm^2sec^{-1}
70	2.6×10^{4}	1.3×10^{-13}	5.3×10^{4}	1.3×10^{-14}
160	2.5×10^{4}	1.3×10^{-13}	4.9×10^{4}	1.3×10^{-14}
350	3.2×10^{4}	2.0×10^{-13}	4.2×10^{4}	7.9×10^{-13}
550	7.1×10^{4}	7.9×10^{-13}	7.6×10^{4}	2.5×10^{-14}

The data given above are plotted in Fig. 16 as log D vs. $1/T$. From the slopes of the curves it was determined that the activation energies for diffusion are 2300 cal/mole and 530 cal/mole for Kr^{87} and Xe^{135}, respectively. The latter results are subject to considerable error because of the scatter of the data, but the magnitude of the activation energy is probably of the right order, at least for this temperature range. A tentative conclusion from these data is that although the barrier height for diffusion is relatively low, only a relatively small fraction of the diffusing atoms can be found in the appropriate excited state at any instant.

In order to establish the relative importance of recoil atoms stopped by the carrier gas, as opposed to those which continue through the gas to embed themselves in the solid material around the specimen, a series of measurements was made on the activity coming from specimen No. 5 at a series of carrier gas pressures from 20 to 400 mm Hg, a range which included the normal operating pressure of the system. No change in the activity was observed over this range, allowing the conclusion that very few of the recoil atoms are stopped by the gas. This is in accord with data on stopping power of gases.[7]

In the immediate future two experiments are being undertaken. To separate the primary diffusion (from UO_2) and secondary diffusion (from recoil atoms embedded in the specimen surroundings), an experiment is being planned in which the specimen will consist of a stack of UO_2 plates with small separations between the surfaces. Such a specimen will multiply the area out of which primary diffusion can occur by a factor depending on the number of plates used. The plates will be fabricated of appropriate thickness so that the total height

7. W. M. Good and E. O. Woolan, Phys. Rev., 101, 249 (1956).

of the stack is fixed regardless of the number of plates used. Comparison of data for several such specimens should permit a separation of primary and secondary diffusion.

In addition, a series of cylindrical specimens made of as-received EUR powders, pressed and sintered to various densities from 80 to 97% of theoretical, will be placed in the apparatus to pin down the effect of porosity on emanation.

UO_2 Dissolution Rates

Studies on the removal of UO_2 pellets from Zircaloy-2 subassemblies were continued. Sintered UO_2 pellets of similar density and dimensions were mounted in Kelon (an acid resistant plastic) and the exposed ends ground and polished to a smooth known surface. The mounts were immersed in nitric acid in a constant temperature bath and the dissolution observed visually. When the smooth known surfaces were etched off by the acid, the mounts were removed and the acid solutions analyzed for their uranium content by polarographic techniques. Preliminary rates of solution for various temperatures and nitric acid concentrations are reported in Table XI. Since only one end of the pellets was exposed to the acid, the surface area was constant and the rates of solution were dependent on the temperature and acid strength.

Nickel Plating UO_2 Pellets for a Possible Fission Recoil Retention Coating

To facilitate the handling of the Zircaloy cladding for re-use, it would be desirable to place a suitable barrier between the fuel and the inside of the cladding to prevent fission recoils from entering the Zircaloy. By use of the Kanigen process, it was found possible to place a thin coating of Nickel on the surface of sintered UO_2 bodies. The plating solution which was used consisted of 15 gm $NiCl_2.6H_2O$, 5 gm sodium citrate, 5 gm sodium hypophosphite, and 5 gm ammonium chloride dissolved in 500 cc of distilled water. The pellets were cleaned in alcohol and marked with a 2S aluminum rod in several places to sensitize the surface and catalyze the reaction. The prepared pellets were then placed in the solution and maintained at a temperature of 90 to 95°C for sufficient time to produce the plating thickness desired. It was found that a two-hour plating time will produce a plate thickness of approximately 0.001 in. Chemical analysis of a typical nickel coating applied by this process showed that the coating contained 7.6 w/o phosphorous, probably present as nickel phosphide.

Four sintered UO_2 pellets plated in this manner were corrosion tested for 400 hours in 750°F steam at 2000 psi. The average corrosion rate, as a weight gain, was 0.00053 $mg/cm^2/hr$. At the completion of the test, the pellets were covered with a thin, brown, strongly adherent corrosion film. Less than 0.005 ppm nickel were found in the autoclave water at the conclusion of the test.

UO_2 Irradiation Program

MTR-WAPD-14-9, 10, and 11 Irradiation of Steam Oxidized and MCW UO_2 Samples

These experiments involved the irradiation of cold pressed and cold pressed and sintered samples of steam oxidized and MCW UO_2. The samples were irradiated at very low burnup rates, with the maximum calculated central temperature being of the order of only 1000°C. The results of the fission monitors included with the samples, together with a description of the samples, are shown in Table XII.

No dimensional changes occurred as a result of the irradiation. It is planned to puncture several of the samples and determine the amount of fission gas released. Although these samples have received quite low burnups, the amounts of fission gas released should provide data on the parameters relating to fabrication histories of the specimen.

MTR-WAPD 14-13 (WAPD 14 Met 6B) Irradiation of Hot Pressed UO_2 Samples

This experiment involved the irradiation of four 0.413 in. OD rods, two containing 93% dense hot pressed steam oxidized UO_2 and two containing 90% dense hot pressed MCW UO_2. The samples were irradiated in position L-58 of the Materials Testing Reactor for 168 days at an estimated flux of 2.5×10^{14} nv. The results from the UO_2 fission monitors included with the samples are shown below.

Top of Pile	19H	6,900 MWD/T
	18H	13,500 MWD/T
	15H	10,900 MWD/T
	14H	4,400 MWD/T

Post-irradiation dimensional measurements on the above samples indicated that no dimensional changes have occurred as a result of the irradiation.

Specimens 15H and 18H were punctured and the amount of Kr^{85} released has been determined. Specimen 15H contained steam oxidized UO_2 which had been hot pressed to 93.8% theoretical density. Specimen 18H was composed of MCW UO_2 which had been hot pressed to 90.1% of theoretical density. The amounts of Kr^{85} released from these two specimens were 5.0 and 8.9% of the respective total content calculated from the above fission monitor data. These data are compared to those for specimens having similar physical properties in the following table:

Specimen	Fabrication	% Theoretical Density	Est. Center Temp. (°C)	Burnup (MWD/T)	% Release of Kr^{85}
18H	MCW-H.P.	90.1	1850	13,500	8.9
16H	MCW-H.P.	91.4	1240	1,500	3.1
15H	S.O.-H.P.	93.8	1580	10,900	3.0
6H	S.O.-H.P.	93.0	1300	275	0.43

Comparison of the two pairs of specimens having roughly equal densities shows that specimens 18H and 15H released appreciably greater quantities of gas than did specimens 16H and 6H, respectively. The controlling parameter acting here may be either the higher temperatures at which specimens 18H and 15H operated in-pile or the appreciably longer burnup to which they were subjected, or a combination of these two factors. On the basis of these specimens, it is not possible to determine the relative importance of these parameters. However, this information will be derived from the statistical irradiations program described below.

MTR-WAPD 14-21, 24, 25 UO_2 - 0.2 w/o TiO_2 Rods

These tests consist of UO_2-0.2 w/o TiO_2 pellets clad with Zircaloy-2 and encapsulated in NaK. The fuel material in WAPD 14-21 was extruded, that in WAPD 14-24 was slip cast, and that in WAPD 14-25 was pressed and sintered in both the ground and unground conditions.

Experiment WAPD 14-21 was removed from the L-57 position in MTR on July 2 after 12 weeks of irradiation to a burnup of 2550 MWD/T, and returned to the Bettis hot laboratory. One train of WAPD 14-25 was removed from position L-51 SE on August 13 after three weeks of irradiation to a burnup of 600 MWD/T, yielding to a test of higher priority. Another train from WAPD 14-25 will remain in test for an additional nine weeks of irradiation.

WAPD 14-22 and 23 X-ray Diffraction Effects on Irradiated Uranium Oxides

The sixteen samples of various uranium oxides have been irradiated for one MTR cycle at a flux of approximately 5×10^{13} nv. The samples have been returned to the Bettis Plant, but as yet the fission monitors have not been analyzed. The samples will be mounted in Kelon and X-ray diffraction patterns will be obtained as soon as the double crystal X-ray spectrometer is in operation.

MTR-19 Met-4 Irradiation Cycling of Natural UO_2 Rods

This experiment involved the cycling of full length UO_2 rods, having varying end and diametral clearances, into and out of a maximum neutron flux of 1×10^{14} nv over a period of 12 weeks. During this time, the specimens were subjected to over 7500 power cycles and a maximum burnup of 1250 MWD/T.

The release of Kr^{85} from four of these specimens having different end and diametral clearances has been measured at room temperature and while the specimens have been held at 1000°C for 48 hr. The fractional release from these specimens, based on estimates of the total Kr^{85} present, is shown in the following table:

Specimen	Density	Estimated Burnup	% Release at Puncture	% Release at 1000°C
I-4	91.8%	490	0.3	0.02
J-4	92.6%	490	0.2	0.04
K-4	92.2%	720	0.1	0.02
N-2-11-4	91.7%	490	0.3	0.02

These values are considered to be accurate to no better than 50%, due to the uncertainity in the burnup estimates. Therefore, analyses are being performed on these specimens to obtain experimental values for total Kr^{85}. The analysis for specimen K-4 has been completed, yielding a value of 0.29% loss at puncture and 0.05% at 1000°C. This indicates that the burnup estimate of K-4 was too high by somewhat greater than a factor of two. Upon completion of the remainder of these analyses, any effect of variations in end or diametral clearance on fission gas release should be evident.

MTR-WAPD 25-2 Power Cycling of PWR Reference UO_2 Fuel Rods

This test, consisting of two full-length PWR reference fuel rods, one of which is defected with a 5 mil hole through the cladding, is running at design flow and thermal conditions in the hot water loop facility installed in the L-42 position in the MTR. The samples are being power cycled at 25 minute intervals between two regions having a thermal neutron flux ratio of seven. The test is scheduled to run until September 24 (a total of three reactor cycles), at which time a maximum exposure of 1400 MWD/T is expected.

MTR-WAPD 29-1 Density of UO_2 vs. Fission Product Release to Hot Water

The WAPD 29-1 experiment consists of the irradiation of two defected clad UO_2 fuel elements in the dynamic cycling facility in the VH-3 position in the MTR. One of the defected rods will be fabricated from UO_2 pellets of reference density and the other from pellets of 98% theoretical density. The rods are to be inserted alternately into the high flux position in the loop for a period dependent upon the half-life of the nuclide to be measured. The heat flux from each rod while it is in the high flux position will be approximately 400,000 Btu/hr-ft^2 during the fresh-fuel reactor conditions. The test is designed so that the defected specimen rods may be power cycled through a 14:1 power ratio on the average. The rate of release of fission products to the water will be determined for both the condition in which the high density fuel specimen is in the position of maximum flux and the alternate condition in which the reference density specimen is in the position of the maximum flux. It is expected that a substantial difference in the release rates will be observed, since it has been determined as part of the Brookhaven in-pile fission gas release experiment that the rate of fission gas release from UO_2 of 97% theoretical density is at least an order of magnitude lower than the rate from UO_2 of reference (92-94%) density. (See Resume' V, WAPD-PWR-PMM-429).

Two non-defected specimens, one of high density and one of reference density, will be irradiated with the defected specimens. Post-irradiation

measurements of fission gas release will be performed on these specimens to determine the correlation between fission product release to the water through a defect and the fission gas release as determined by these post-irradiation measurements.

MTR-WAPD-30-2 Second PWR Bundle Proof Test

Because the previous bundle proof test did not operate at the level of PWR conditions, a second bundle proof test is being planned to follow the AlW test in the WAPD-30 loop. A preliminary proposal (WAPD-IPC-213) has been submitted. In order to be sure that the test is operated at the proper conditions, the enrichment of the fuel will not be established until AlW completes a flux analysis of the loop. At present, loop equipment and Zircaloy components are being fabricated.

In order to maximize the use of in-pile loops, aluminum alloy samples will be tested along with the bundle. The alloys are M388-H14 (Al-1Ni-0.5 Fe), M400-H14 (Al-1Ni-1Fe), and X2219-T6 (Al-6 Cu). Two 1/8" plate samples of each alloy will be tested both in an irradiated and a non-irradiated region of the loop. These samples are currently being corrosion tested for 28 days in 600°F water.

HIR-WAPD 114A Statistical Irradiation Experiment

As originally conceived, this experiment involved the irradiation of cold pressed samples of $UO_{2.0}$, $UO_{2.1}$, $UO_{2.25}$, and $UO_{2.67}$, together with sintered $UO_{2.0}$ samples of various densities. To produce $UO_{2.1}$ and $UO_{2.25}$ in the quantities required, the most satisfactory method has been to mix appropriate mixtures of $UO_{2.0}$ and $UO_{2.67}$ powders, place in a Vycor bulb, evacuate and seal the bulb, and subsequently heat treat for two weeks at 800°C followed by an air cool. Therefore, the requisite 3200 grams of enriched material for this portion of the experiment were placed in a total of 36 Vycor bulbs and inserted in one muffle furnace at 800°C for heat treatment. After one week, a guard noticed that the door of the furnace was blown open and that glass and UO_2 were spread over the floor. After the furnace had cooled down, all but two of the 36 bulbs were found to have been broken. The uranium oxide powder had seriously contaminated the heat treating laboratory, and four men worked full time for a week to decontaminate the room. Also, the 3200 grams of material (including 185 grams of U^{235}) were scrapped. As the same heat treatments had been successfully performed in the past and have been successfully performed since the accident, the reasons for the accident have not been ascertained. However, it was deemed adviseable to report on this accident so that the various other installations will be forewarned if similar work is anticipated. Because of the difficulty involved in making $UO_{2.1}$ and $UO_{2.25}$, the experiment has been modified and will no longer include these materials.

CR-WAPD-Met-10 (X-1-f test) Sixth Chalk River UO_2 Defect Test

All five X-1-f rods have been sectioned. These are reference rods,

defected and non-defected, containing 6.88% enriched, 95% dense UO_2 pellets which had been tested in the Chalk River X-1 loop for 40 days to 1800 MWD/T. A summary of test data and results is presented in Table XIII.

Specimens 1-4 showed evidence of center melting in the UO_2 (see Figs. 17-21). Specimen 5 displayed grain growth in the pellets at the high flux end (see Fig. 22), indicating center temperatures approaching the melting poing of UO_2 but no obvious structural changes in the pellets at the opposite end. According to calculations of the heat flux required to produce UO_2 melting (see Table XIII), there should have been no changes in specimens 2 and 5.

One possibility pointed out by these discrepancies is that the heat fluxes reported for these tests are lower than actual conditions. Two independent calculations were made to study this possibility. Metallographic observations on specimen 4 revealed a ZrO_2 film at the cladding interface (see Fig. 23) which had a maximum thickness of 0.0081 in. and an average thickness of 0.0058 in. This average thickness is equivalent to a weight gain of 200 mg/dm^2. Extrapolating Zircaloy-2 oxidation data[8] for 200 mg/dm^2 and 40 days corrosion time, an interface temperature of 875°F was obtained. From this, a heat flux of 7-9 x 10^5 $Btu/hr/ft^2$ was estimated, as compared to 5 x 10^5 $Btu/hr-ft^2$ reported for X-1-f-4.

From the metallographic sample of specimen 4, it was possible to determine the location of two structural points whose tempteratures were known. These are: (1) the point where the UO_2 grains begin to increase in size, indicating temperatures above the sintering temperature at 1700°C, and (2) the point where melting begins (m.p. 2800°C). Applying the temperature distribution equation to these two determinations, a heat flux of 1 x 10^6 $Btu/hr/ft^2$ was obtained. UO_2 samples from each of the specimens are being processed for chemical analysis. This will further aid in establishing the flux level of this test.

Attempts were made to calculate the volume expansion that occurs in UO_2 upon melting. Comparing the volume of the shrinkage crater to the volume of the molten zone in each specimen, values from 0.1 to 11% were obtained. The latter high value was obtained from the section at the defect in the highest flux of the test, where the large shrinkage crater may be partly due to localized leaching of fission products from the UO_2 (see Fig. 20). The crater in this rod (specimen 4) reduced rapidly in size in the pellets further from the defect, with the bottom pellet reducing to a crater equivalent to 1.5% of the molten zone volume (see Fig. 21). By summing the assembled diametral clearance, diametral change in the cladding, thermal expansion in the cladding, and the strain required to overcome clad restraint, and subtracting the expansion in the pellet (assuming 2800°C for the molten zone and an average temperature of 1900°C in the unmelted ring of the pellet) for each rod, volume expansions due to melting of 0-2% were obtained.

8. The Metallurgy of Zirconium, ed. by B. Lustman and F. Kerze, Jr. p. 633.

Experimental values for axial growth of the rods are much lower than those calculated for a pellet center temperature at the melting point. Interference between the pellets and cladding at operating temperatures were calculated to be 0.210 and 0.270 in., while the measured axial growth after irradiation is 0.018-0.076 in.

Fig. 24 shows the molten zone of specimen 4. The structure is columnar and fairly compact except for some radial cracking, in sharp contrast to the molten structure found in the prior X-1-e test, which consisted of 100% dense grains interspersed by large voids (see Fig. 14, Resume V (WAPD-PWR-PMM-429). This is probably due to the higher degree of superheating in the latter specimen.

CR-WAPD-Met-11 & 12 (X-1-g and X-1-h) Seventh and Eighth Chalk River UO_2 Defect Tests

The X-1-g test section was temporarily removed from Chalk River on July 11 and replaced by X-1-h (formerly designated X-1-g') in order to obtain a higher level of water activity for testing of the PWR Fuel Element Failure Detection System. The higher water activity obtained is due to the larger diametral clearances in the defected rods of X-1-h. The X-1-h test will be removed and the X-1-g re-installed when sufficient data for the detection system is obtained.

A back-up to the X-1-h test, designated X-1-i, has been prepared and shipped to Chalk River. This consists of 5 reference rods containing natural UO_2, with one rod of 0.008 in. diametral clearance, defected with two 0.005 in. holes near each end and 90° apart. If this test is utilized, it is expected that sufficient fission products will be swept out of the defected rod by natural convection to provide a check for the detection system.

WAPD-CR-5 (CT-1) PWR Bundle Proof Test

A probing device has been constructed for the hot laboratory cells for measuring rod spacing in the CR-5 bundles. The data obtained to date have been erratic, and work is being directed toward improving the probe. Preliminary measurements taker from photographs indicate little change in rod spacing after irradiation. The photographs reveal some badly bowed rods in the bundle. It is to be pointed out that this was the original condition of the bundles, which were fabricated in the early stages of bundle development and were not within present PWR dimensional tolerances. The average rod spacing before irradiation is as follows:

Bundle Design	Average Rod Spacing ($\bar{X}$)	Statistical Variation (3σ)	No. of readings
Tube Sheet	0.0600"	0.0286"	200
Egg Crate	0.0557"	0.0300"	200

It is expected that the bundle proof test presently being planned for the WAPD-30 loop will not exceed values of 0.010 in. for 3σ variation in rod spacing.

TABLE I

COMPARISON OF HELIUM AND LIQUID DENSITIES OF UO_2 POWDERS

Method of Preparation	O/U	Displacing Fluid	Density (g/cc)
Hydrogen reduction of $UO_3.2H_2O$	2.01	Helium	10.25 ± 0.05
		CCl_4	10.25 ± 0.03
Direct hydrogen reduction of uranium peroxide	2.08	Helium	11.00 ± 0.1
		CCl_4	10.78 ± 0.03
Hydrogen reduction of UO_3 hydrate crystals grown hydrothermally in an autoclave	2.01	Helium	10.25 ± 0.05
		CCl_4	10.37 ± 0.03
Hydrogen reduction of UO_3 made by denitration in a fluidized bed	2.02	Helium	10.13 ± 0.1
		CCl_4	9.94 ± 0.03
Fluidized bed denitration and UO_3 reduction	2.07	Helium	10.54 ± 0.05
		CCl_4	10.28 ± 0.03
Air pyrolysis of uranium metal to U_3O_8; hydrogen reduction to UO_2	2.01	Helium	10.02 ± 0.1
		CCl_4	10.07 ± 0.03
Controlled low pressure steam oxidation of uranium metal	2.02	Helium	10.85 ± 0.1
		CCl_4	10.91 ± 0.03
Uncontrolled low pressure steam oxidation of uranium metal	2.03	Helium	10.92 ± 0.05
		CCl_4	10.85 ± 0.03

TABLE II

COMPARISON OF REAL AND APPARENT DENSITIES OF UO_2 POWDERS

Method of Preparation	Real Density (pR) (g/cc)	Apparent Density (pA) (g/cc)	Void Volume/g (1/PA-1/pR)
Direct hydrogen reduction of uranium peroxide	11.00	1.34	0.66
Air pyrolysis of UNH to UO_3; hydrogen reduction to UO_2 at 1180°C	10.24	1.84	0.45
Air pyrolysis of uranium metal to U_3O_8; hydrogen reduction to UO_2	10.02	1.93	0.42
Hydrogen reduction of $UO_3.2H_2O$	10.25	2.12	0.37
Uncontrolled steam oxidation of uranium metal	10.92	2.47	0.31
Hydrogen reduction of UO_3 made by denitration in a fluidized bed	10.13	3.85	0.16
Fluidized bed denitration and UO_3 reduction	10.54	4.19	0.14
Hydrogen reduction of UO_3 hydrate crystals grown hydrothermally in an autoclave	10.25	4.63	0.12

TABLE III

GAS ADSORPTION SURFACE AREA MEASUREMENTS ON UO_2 POWDERS

Code	Method of Preparation	Preparation Temperature (°C)	Specific Surface (m^2/cc)
NPUR-1	Direct hydrogen reduction of uranium peroxide	900	28.4
ANL-1	Hydrogen reduction of UO_3 made by denitration in a fluidized bed	800	9.5
ANL-2	Fluidized bed denitration and UO_3 reduction	700	30.6
IR-1	Air pyrolysis of U metal to U_3O_8; hydrogen reduction to UO_2	800	5.8
NOL-9	Controlled low pressure steam oxidation of U metal	700*	2.4
NOL-13	Uncontrolled low pressure steam oxidation of U metal	400	9.0
CR-2	Hydrogen reduction of $UO_3.2H_2O$	800	8.8
NPHUR-1	Hydrogen reduction of UO_3 hydrate crystals grown hydrothermally in an autoclave	1750	0.5

* vacuo drying temperature

TABLE IV

EFFECT OF TEMPERATURE OF PREPARATION ON TOTAL SURFACE AREA OF UO_2 POWDERS

Method of Preparation: hydrogen reduction of UO_3
Reduction time: sixteen hours

Reduction Temperature (°C)	O/U	Real Density (g/cc)	Specific Surface (m^2/cc)
480	2.04	10.44	24.7
580	2.03	10.44	17.8
690	2.03	10.38	18.1
805	2.02	10.32	13.8
920	2.02	10.38	13.2
1180	2.01	10.24	9.4

TABLE V

COMPARISON OF TOTAL AND EXTERNAL SPECIFIC SURFACES OF UO_2 POWDERS

Method of Preparation	Total Surface (Sg) (m^2/cc)	Porosity	Permeability External Surface (Sp) (m^2/cc)	Roughness Factor (Sg/Sp)
Uncontrolled low pressure steam oxidation of uranium foil	9.0	0.645	2.7	3.3
Air pyrolysis of uranium foil to U_3O_8; hydrogen reduction to UO_2	5.8	0.645	3.0	1.9
Air pyrolysis of UNH to UO_3; hydrogen reduction to UO_2 (1180°C)	9.4	0.645	3.6	2.6
Hydrogen reduction of $UO_3.2H_2O$	8.8	0.645	4.1	2.2
Direct hydrogen reduction of uranium peroxide	28.4	0.651	9.8	2.9
Ignition of ammonia precipitated diuranate to U_3O_8; hydrogen reduction to UO_2	59.9	0.731	12.9	4.6
Ignition of urea precipitated diuranate to U_3O_8; hydrogen reduction to UO_2	60.4	0.768	10.3	5.9
Direct hydrogen reduction of ammonia precipitated diuranate	37.4	0.771	13.9	2.7
Direct hydrogen reduction of urea precipitated diuranate	42.1	0.750	12.6	3.3
Wet ball-milled Mallinckrodt oxide	53.1	0.534	17.1	3.1

TABLE VI

CHARACTERISTICS OF UO_2 POWDERS

	Powder Surface Area (m^2/cc)	Powder Density (g/cc)		Preparation History
NURS 3-6	17.5	He	10.68	MCW UO_3 wet ball-milled in dilute H_2SO_4, reduced to UO_2 with H_2.
NAIR-2	60.4	He CCl_4	11.34 10.47	ADU precipitated with urea, ignited to U_3O_8 in air, reduced in H_2 to UO_2. Product pyrophoric, stabilized by heating in H_2 at 900°C.
MA-6	53.1	He	10.23	Wet ball-milled MCW powder (Zircaloy mill and balls).
NAIR-1	59.9	He He CCl_4	10.88 11.12 10.77	ADU Precipitated with NH_4OH, ignited to U_3O_8 in air, reduced with H_2 to UO_2. Product pyrophoric, stabilized by heating in H_2 at 800°C.
NAIR-1R	-	-	-	NAIR-1 powder heated in H_2 at 900°C
NUR 29-31	15.0	CCl_4	10.34	Air pyrolysis of UNH to UO_3; hydrogen reduction of dry ball-milled UO_3 to UO_2.
NHOL-2	22.6	He	10.98	Steam at 300-400°C on finely divided U from UH_3; UO_2 heated in H_2 at 750-820°C for 31 hours.
MCW As-Received	6.4	He	10.16	- -
NOH 20-24	12.9	He CCl_4	10.92 10.75	U Metal foil steam oxidized in autoclave at 343°C.

TABLE VII

SINTERING CHARACTERISTICS OF UO_2 POWDERS

Powder	Compact Condition After Sintering (based on pressed density)		Highest Sintered Density (64 hours 1700°C H_2) 65% TDG	Density Reached in 8 hours in H_2 at 1700°C. Pressed Density	Sintered Density	Dependence of Sintered Den. on Pressed Den.	Relative Rank Surface Area	Density
NURS-3-6	Good	55%						
	Slight	65%						
	Cracks		98.9%T	57.5%T	96.4%T	Slight	5	5
NAIR-2	Good	55%						
	Good	65%	98.7%T	55.3%T	95.4%T	Slight	1-2	1-2
MA-6	Good	55%						
	Good	65%	98.1%T	55.1%T	96.4%T	None	3	7
NAIR-1	Bad	55%T						
	Cracked	65%T	97.9%T	55.1%T	96.8%T	Slight	1-2	1-2
NAIR-1	Good	55%T						
	Bad	65%T	97.6%T	-	-	Slight	-	-
NUR-29-31	Good	55%T						
	Good	55%T	96.7%T	55.0%T	87.4%T	Medium	6	6
NHOL-2	Cracks	55T%						
	Good	65%T	94.7%T	55.3%T	79.2%T	Marked	4	3
MCW As-Rec.	Good	55%T						
	Good	65%T	92.7%T	55.0%T	78.5%T	Medium	8	8
NOH-20-24	Flakey	55%T						
	Good	65%T	79.2%T	55.2%T	58.1%T	Marked	7	4

TABLE VIII

DENSITIES OBTAINED WITH "MICRO ATOMIZED" MCW UO_2

Sintering Conditions (Hydrogen)	Density, Per Cent Theoretical* Compaction Pressure, TSI		
	60	80	100
1600°C for 5 hr.	94.6	94.7	95.3
1600°C for 10 hr.	94.2	94.7	95.3
1725°C for 5 hr.	95.4	96.1	96.1
1725°C for 10 hr.	95.2	96.4	96.3

* Average of 5 measurements

Table IX

LATTICE PARAMETER VARIATION AS A FUNCTION OF O/U RATIO FOR OXIDATION OF UO_2 AT 230°C IN AIR

Oxidation Time	O/U Ratio	Crystallographic Data
None	2.01	Cubic, $a_o = 5.472 \pm 0.0031$
15 min.	2.10	Cubic, $a_o = 5.467 \pm 0.0021$
2 hr.	2.24	Tetragonal, $a_o = 5.41 \pm 0.03$, $c_o = 5.50 \pm 0.03$
4 hr.	2.30	Tetragonal, $a_o = 5.41 \pm 0.02$, $c_o = 5.55 \pm 0.02$
18 hr.	2.34	Tetragonal, $a_o = 5.38 \pm 0.01$, $c_o = 5.55 \pm 0.01$

Table X

LATTICE PARAMETER VARIATION AS A FUNCTION OF O/U RATIO FOR OXIDATION OF UO_2 AT 275°C IN AIR

Oxidation Time	O/U Ratio	Crystallographic Data
None	2.01	Cubic, $a_o = 5.472 \pm 0.003$
20 min.	2.24	Tetragonal, $a_o = 5.43 \pm 0.01$, $c_o = 5.50 \pm 0.01$
40 min.	2.27	Tetragonal, $a_o = 5.410 \pm 0.008$, $c_o = 5.517 \pm 0.009$
1 hr.	2.30	Tetragonal, $a_o = 5.404 \pm 0.009$, $c_o = 5.520 \pm 0.007$
1 hr.	2.32	Tetragonal, $a_o = 5.398 \pm 0.005$, $c_o = 5.534 \pm 0.005$
2.5 hr.	2.34	Tetragonal, $a_o = 5.387 \pm 0.002$, $c_o = 5.549 \pm 0.002$

Table XI

SOLUTION RATES OF SINTERED UO_2 PELLETS IN HNO_3

Densities: 93.3-93.6%

Surface Area: 0.10 sq. in.

HNO_3 Concentration (N)	Temperature (°C)	Rate (mg/min)
15.7	21.0	0.6
15.7	26.5	0.7
15.7	44.0	13.6
15.7	48.0	13.8
14.1	32.0	1.5
7.9	33.0	0.6
7.9	46.0	2.0
1.6	23.5	0.003
1.6	25.8	0.003
1.6	47.0	0.03

Table XII

Experiments MTR-WAPD 14-9, 10, & 11
Burnup Data

Expt. No.	Irradiation Facility	Sample No.	Type of Material*	Diameter	Burnup (MWD/T)	Average Flux** nv x 10^{-13}	Flux at 40 MW** nv x 10^{-13}
14-9	A-36 NE	7	S.O. - CP	0.500"	600	1.0	1.2
"	"	8	" "	"	2370	5.3	5.9
"	"	12C	MCW - CP	"	1800	3.8	4.2
"	"	13C	" "	"	2240	5.2	5.8
14-10	All SW	42S	MCW-CP & S	0.400"	890	1.9	2.1
"	"	43S	" "	"	2200	5.7	6.5
"	"	50S	S.O. - CP & S	"	2780	8.2	9.4
"	"	51S	" "	"	1650	3.8	4.4
14-11	All NW	53S	S.O. - CP & S	0.500"	590	1.2	1.3
"	"	54S	" "	"	1320	2.9	3.4
"	"	56S	MCW - CP & S	"	1410	3.2	3.6
"	"	57S	" "	"	1050	2.2	2.6

* S.O. = High pressure steam oxidized UO_2
MCW = Mallinckrodt UO_2
CP = Cold pressed
CP & S = Cold pressed and sintered

** Samples were in-pile when power level was changed from 30 MW to 40 MW. Flux data for 40 MW in operation is an estimate from the available data.

Table XIII

CR-WAPD-Met-10 Test Data

Specimen No.		1	2	3	4	5
Defect Diameter (in)		0.005	0.005	none	0.005	none
Assembled Nominal Clearances (in)	- Diametral	0.008	0.0015	0.008	0.008	0.003
	- Axial	0.060	0.000	0.060	0.060	0.000
Dimensional Increases due to Irradiation (in)	- Diametral	nil	0.002 (0.48%)	0.001 (0.24%)	0.0025 (0.24%)	0.002 (0.48%)
	- Axial	0.020 (0.2%)	0.076 (0.75%)	0.018 (0.2%)	not recorded	0.061 (0.6%)
Reported Max. Heat Flux ($Btu/hr-ft^2$)	- Top	360,000	460,000	505,000	500,000 (D)	440,000
	- Bottom	440,000(D)*	495,000(D)	505,000	450,000	375,000
Calculated heat flux to initiate melting (UO_2 m.p. 5000°F)		353,000	684,000	529,000	353,000	684,000
Diameter of molten zone (in)		0.170-0.200	0.170-0.175	0.135-0.170	0.210-0.170	Grain growth in top pellets of specimen
Diameter of shrinkage crater (in)		0.007-0.012	nil-.005	0.008-0.015	0.025-0.090	

*(D) - defected end of specimen

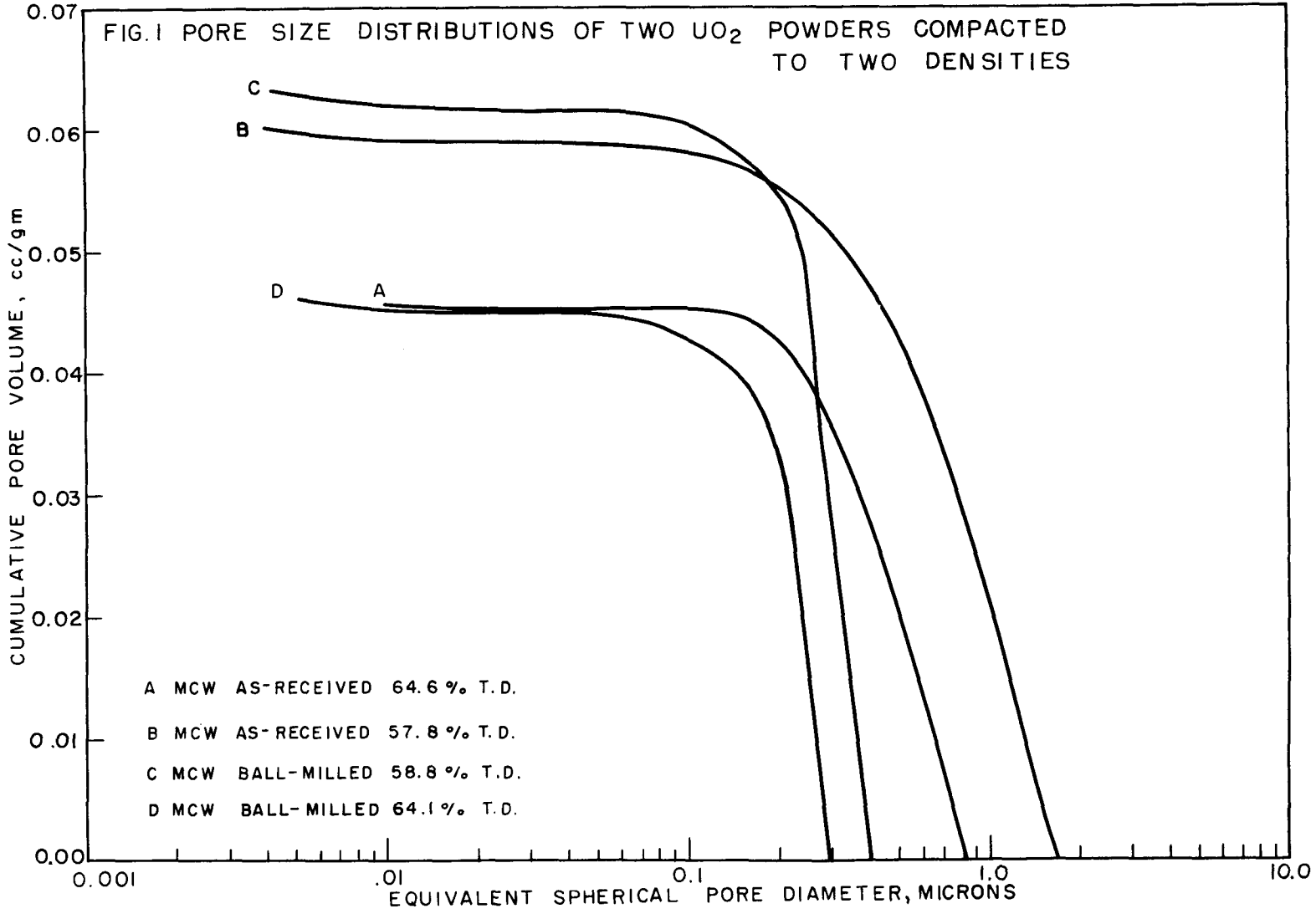
FIG. 1 PORE SIZE DISTRIBUTIONS OF TWO UO_2 POWDERS COMPACTED TO TWO DENSITIES
C
B
D
A
A MCW AS-RECEIVED 64.6 % T.D.
B MCW AS-RECEIVED 57.8 % T.D.
C MCW BALL-MILLED 58.8 % T.D.
D MCW BALL-MILLED 64.1 % T.D.
CUMULATIVE PORE VOLUME, cc/gm
0.07
0.06
0.05
0.04
0.03
0.02
0.01
0.00
0.001
.01
0.1
1.0
10.0
EQUIVALENT SPHERICAL PORE DIAMETER, MICRONS

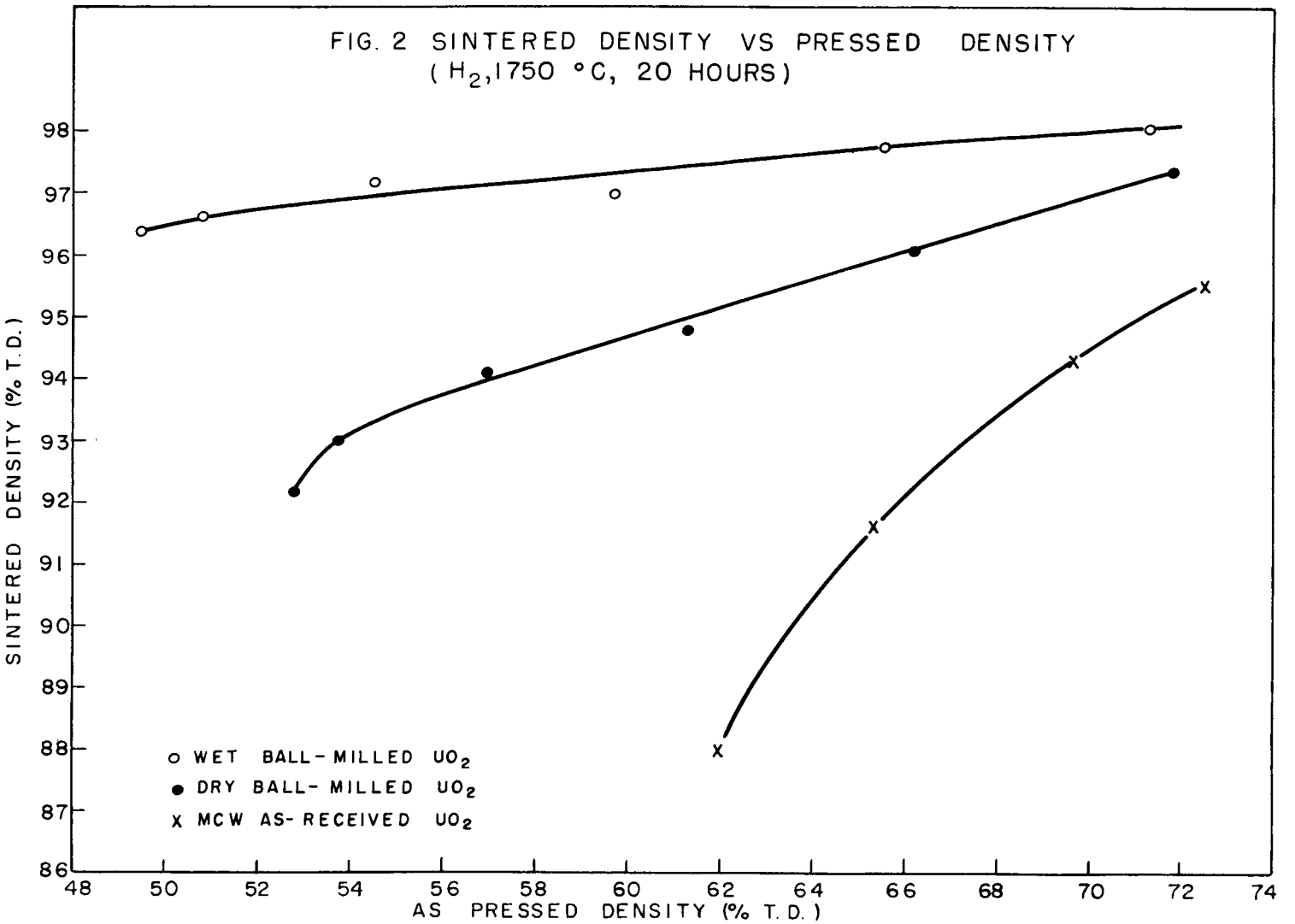
FIG. 2 SINTERED DENSITY VS PRESSED DENSITY
(H_2, 1750 °C, 20 HOURS)
SINTERED DENSITY (% T.D.)
AS PRESSED DENSITY (% T.D.)
98
97
96
95
94
93
92
91
90
89
88
87
86
48
50
52
54
56
58
60
62
64
66
68
70
72
74
o WET BALL-MILLED UO_2
● DRY BALL-MILLED UO_2
x MCW AS-RECEIVED UO_2

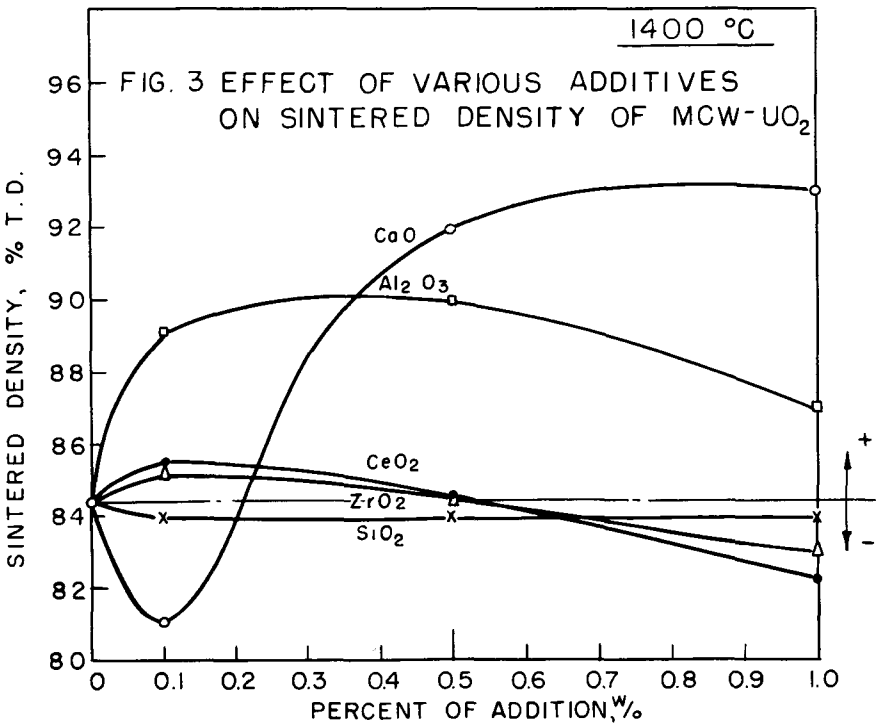

FIG. 3 EFFECT OF VARIOUS ADDITIVES ON SINTERED DENSITY OF MCW-UO_2

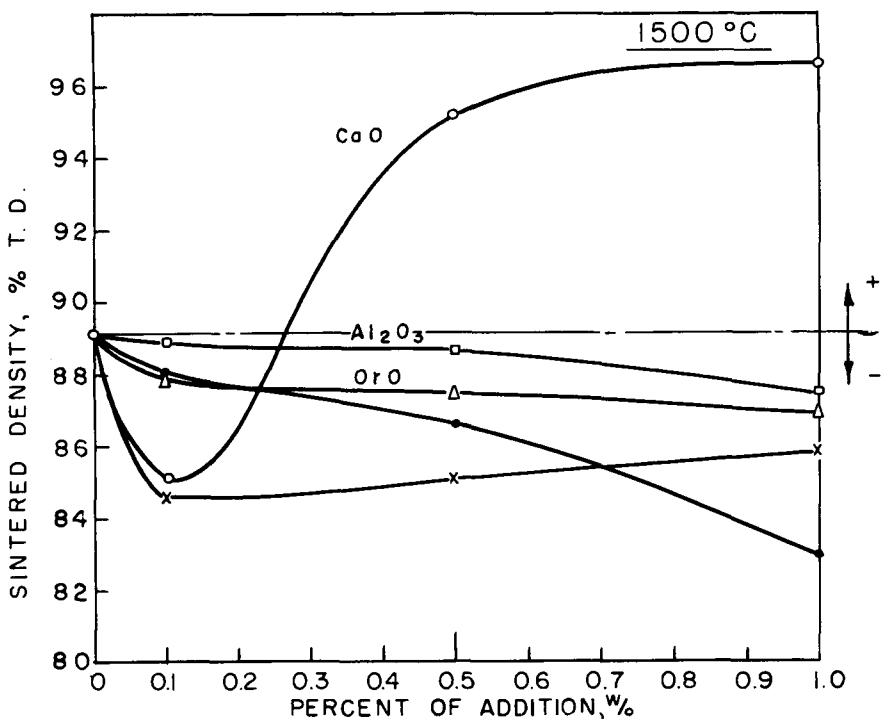

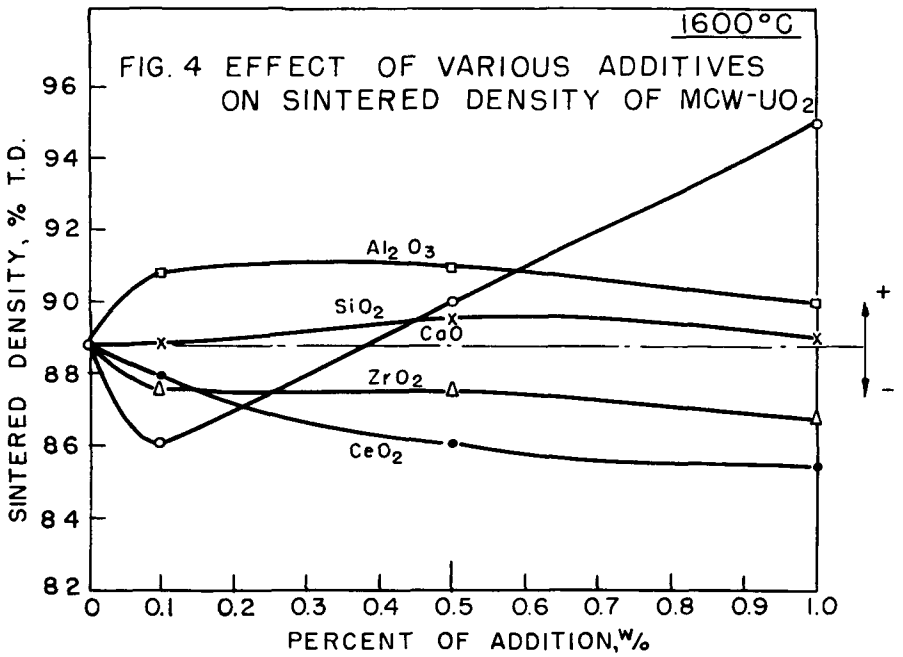

FIG. 4 EFFECT OF VARIOUS ADDITIVES ON SINTERED DENSITY OF MCW-UO_2

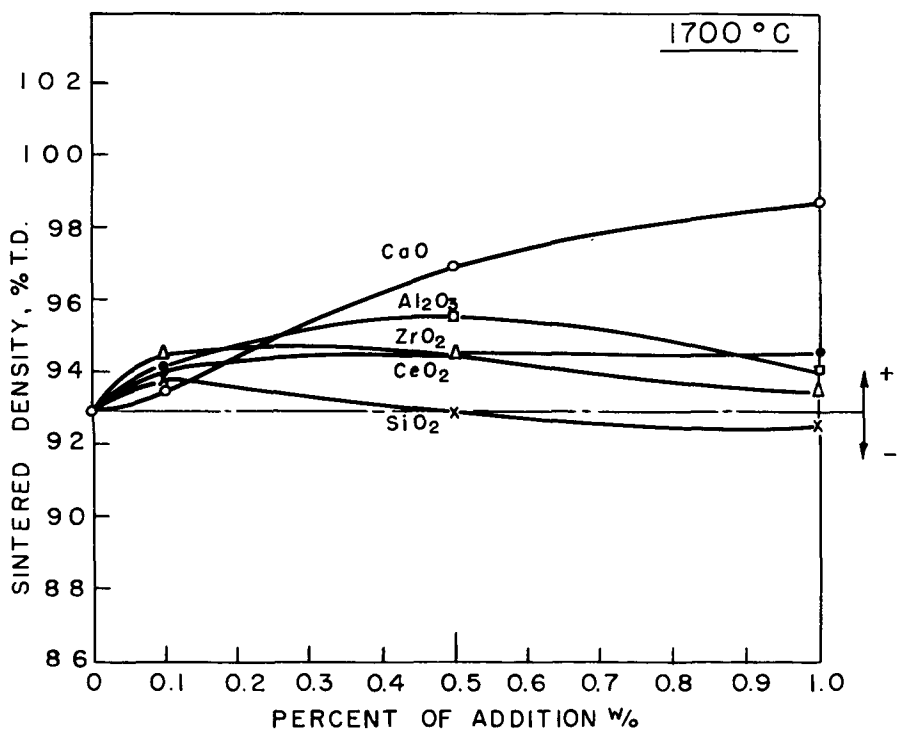

1400°C

1600°C

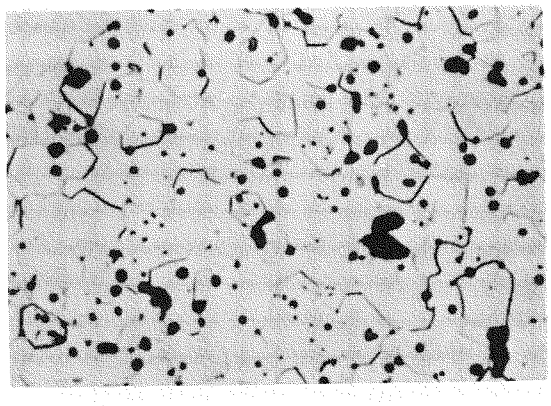

0.05 w/o TiO_2

0.05 w/o CaO

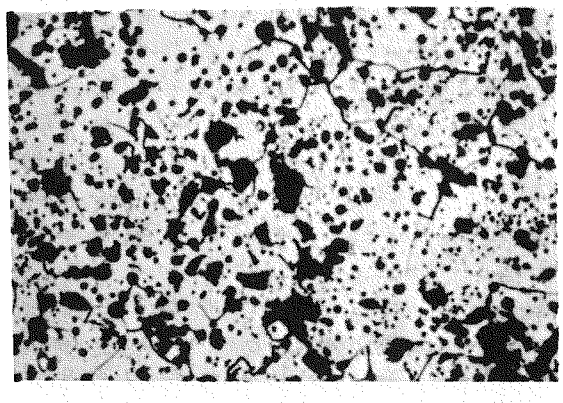

89.4 T.D.S.

93.5 T.D.S.

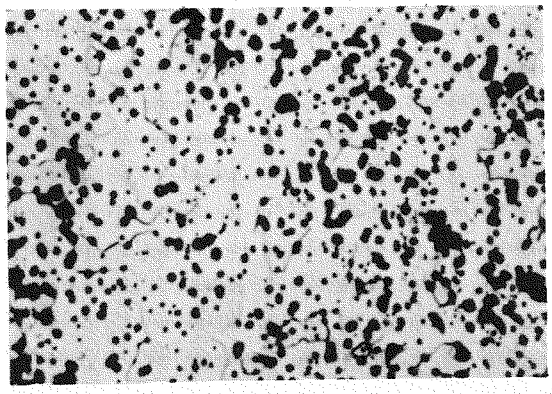

0.25 w/o TiO_2

0.25 w/o CaO

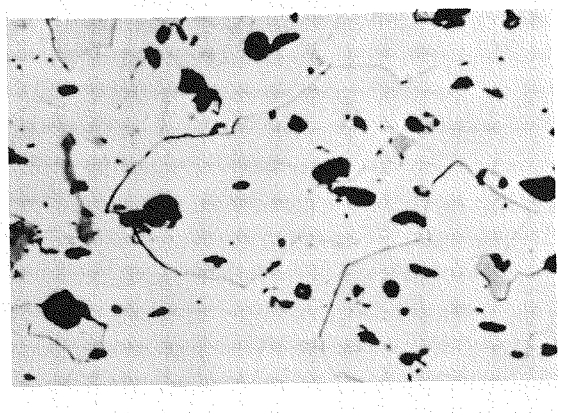

94.6% T.D.S.

98.6% T.D.S.

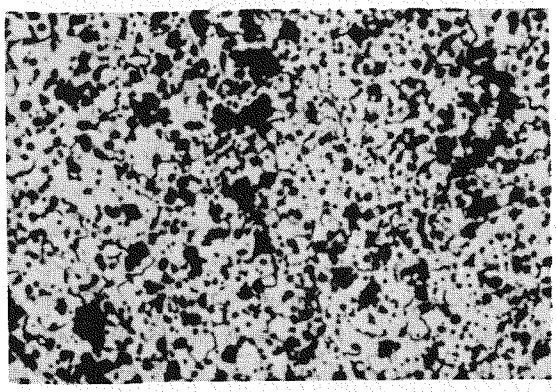

0.5 w/o TiO_2

0.5 w/o CaO

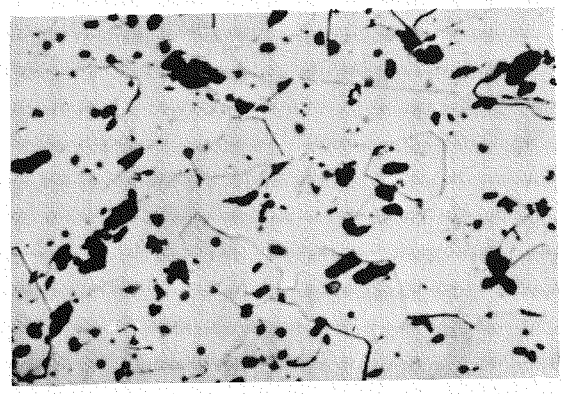

86.9% T.D.S.

98.4% T.D.S.

FIG. 5: The effect of TiO_2 and CaO additions on the microstructure of sintered MCW-UO_2.

Sintered 10 hrs. in H_2 Magnification-450X

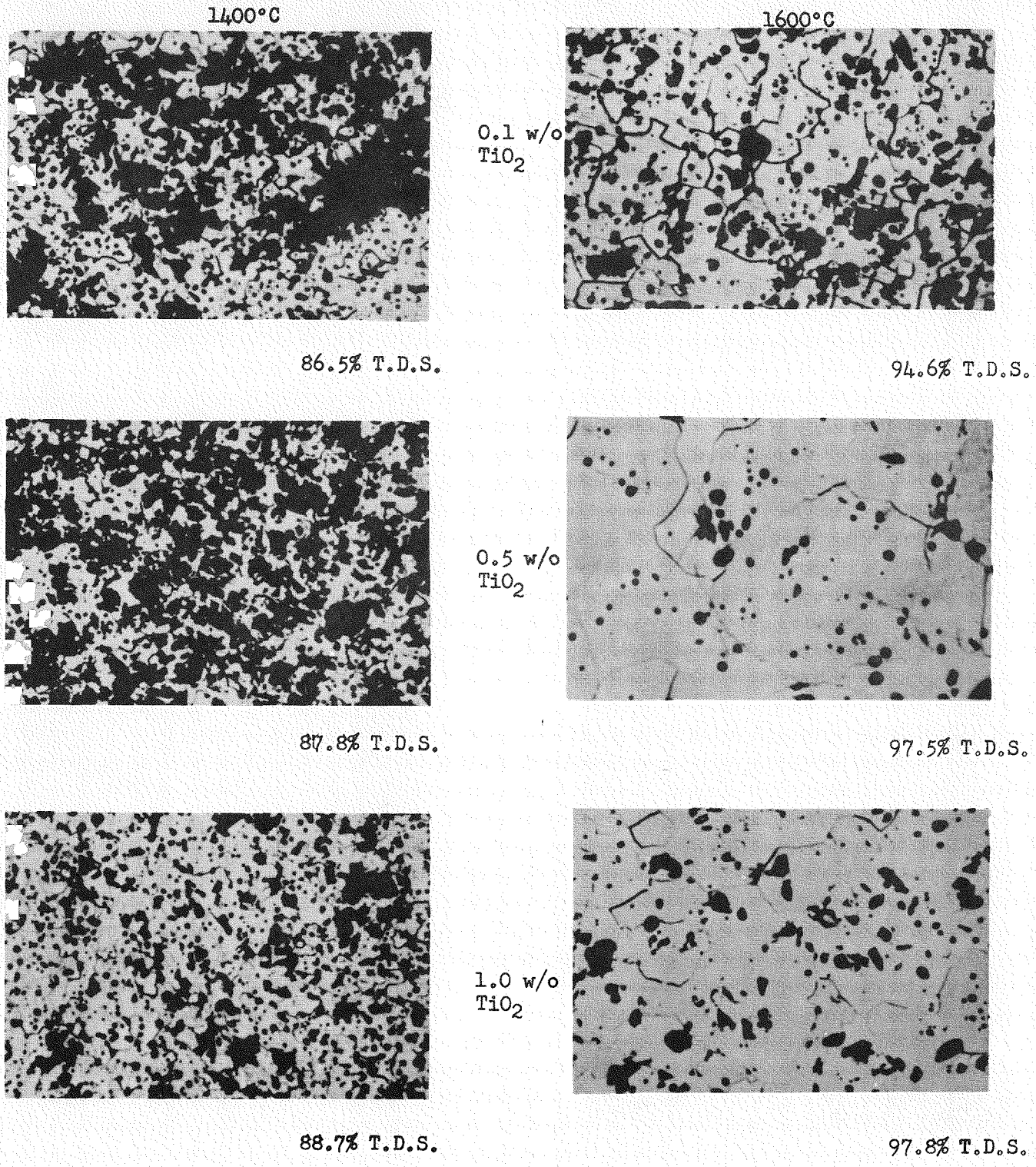

FIG. 6: Effect of TiO_2 additives on the microstructure of sintered MCW-UO_2.

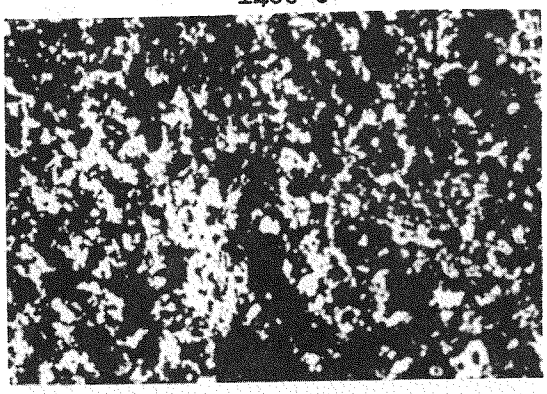

0.1 w/o CaO

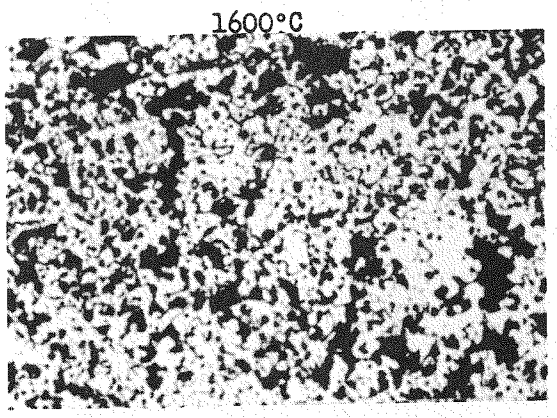

76.8% T.D.S.

86.6% T.D.S.

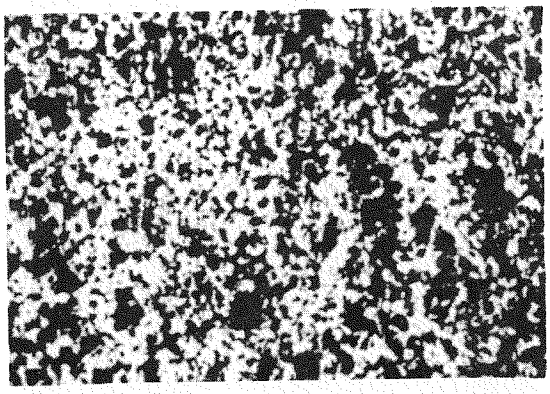

0.5 w/o CaO

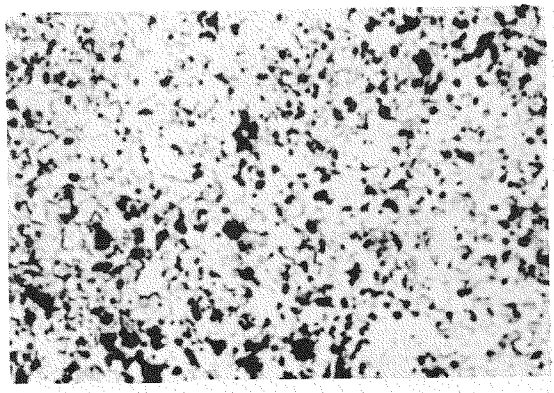

81.5% T.D.S.

91.5% T.D.S.

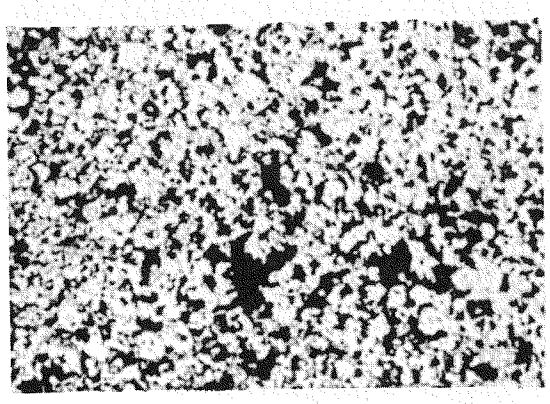

1.0 w/o CaO

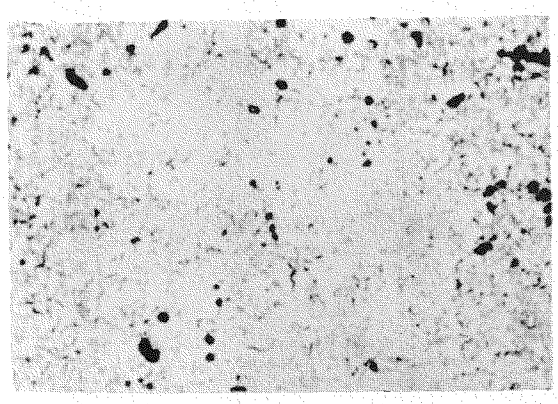

87.9% T.D.S.

95.0% T.D.S.

FIG. 7: Effect of CaO additives on the microstructure of sintered MCW-UO_2.

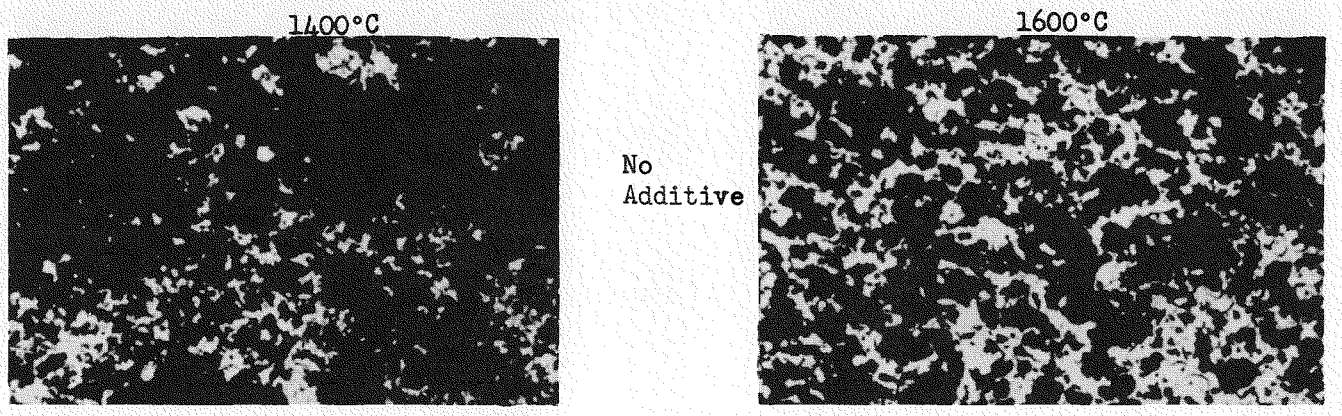

FIG. 8: Microstructure of Sintered UO_2.

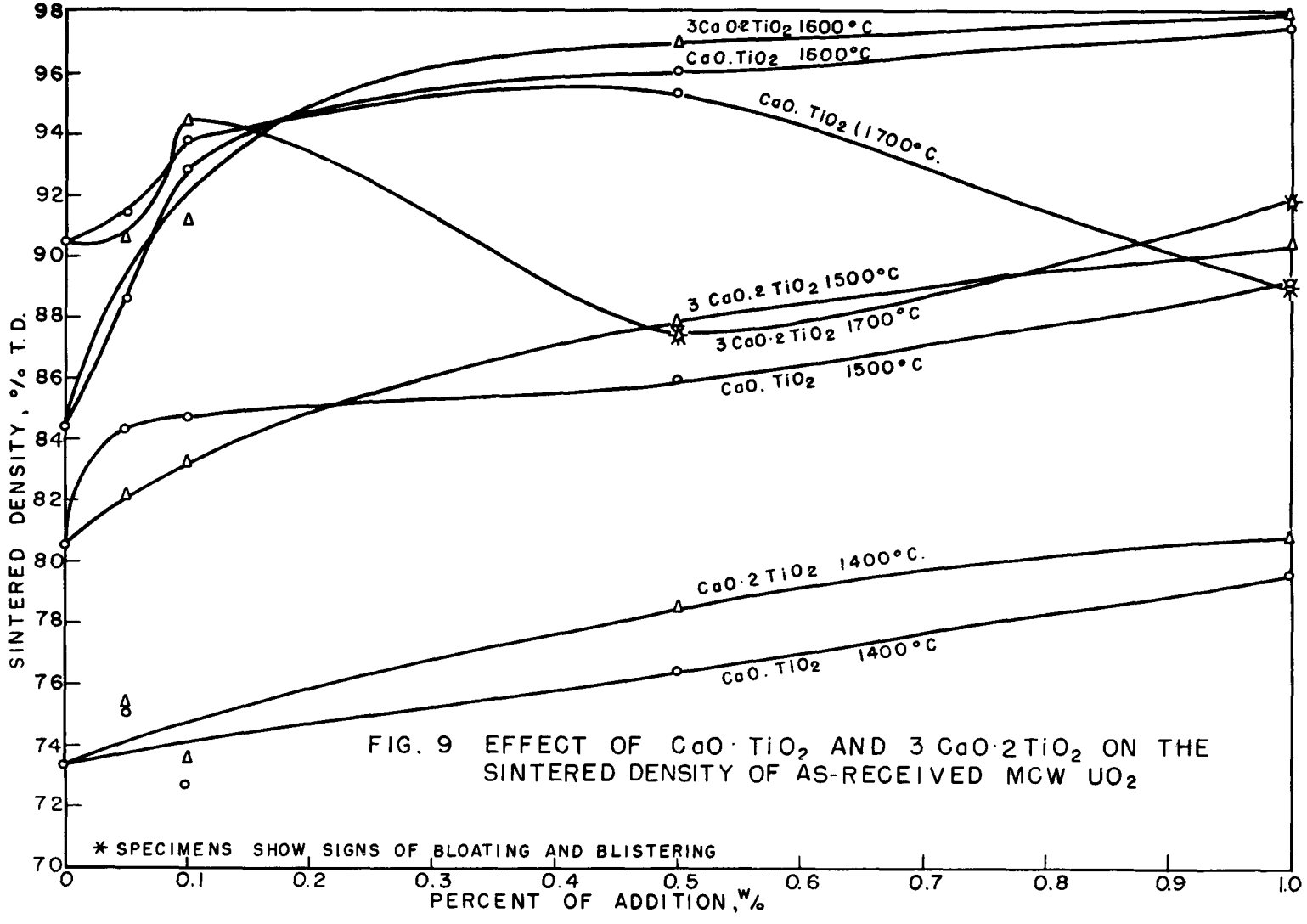

FIG. 9 EFFECT OF $CaO \cdot TiO_2$ AND $3\,CaO \cdot 2TiO_2$ ON THE SINTERED DENSITY OF AS-RECEIVED MCW UO_2

FIG. 10 SINTERED DENSITY VS COMPOSITION
MCW UO_2 - ADU (5-25 W/o)

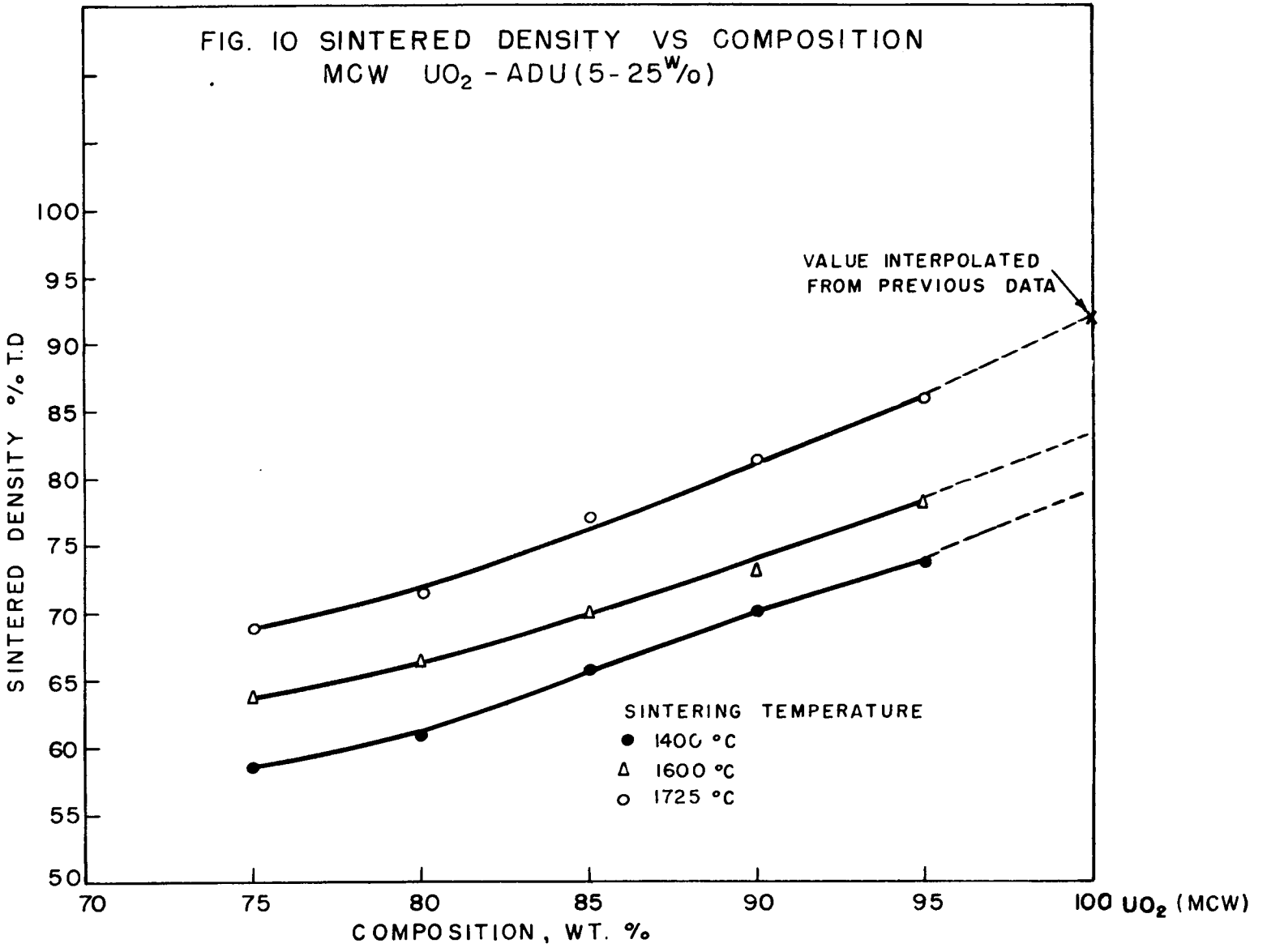

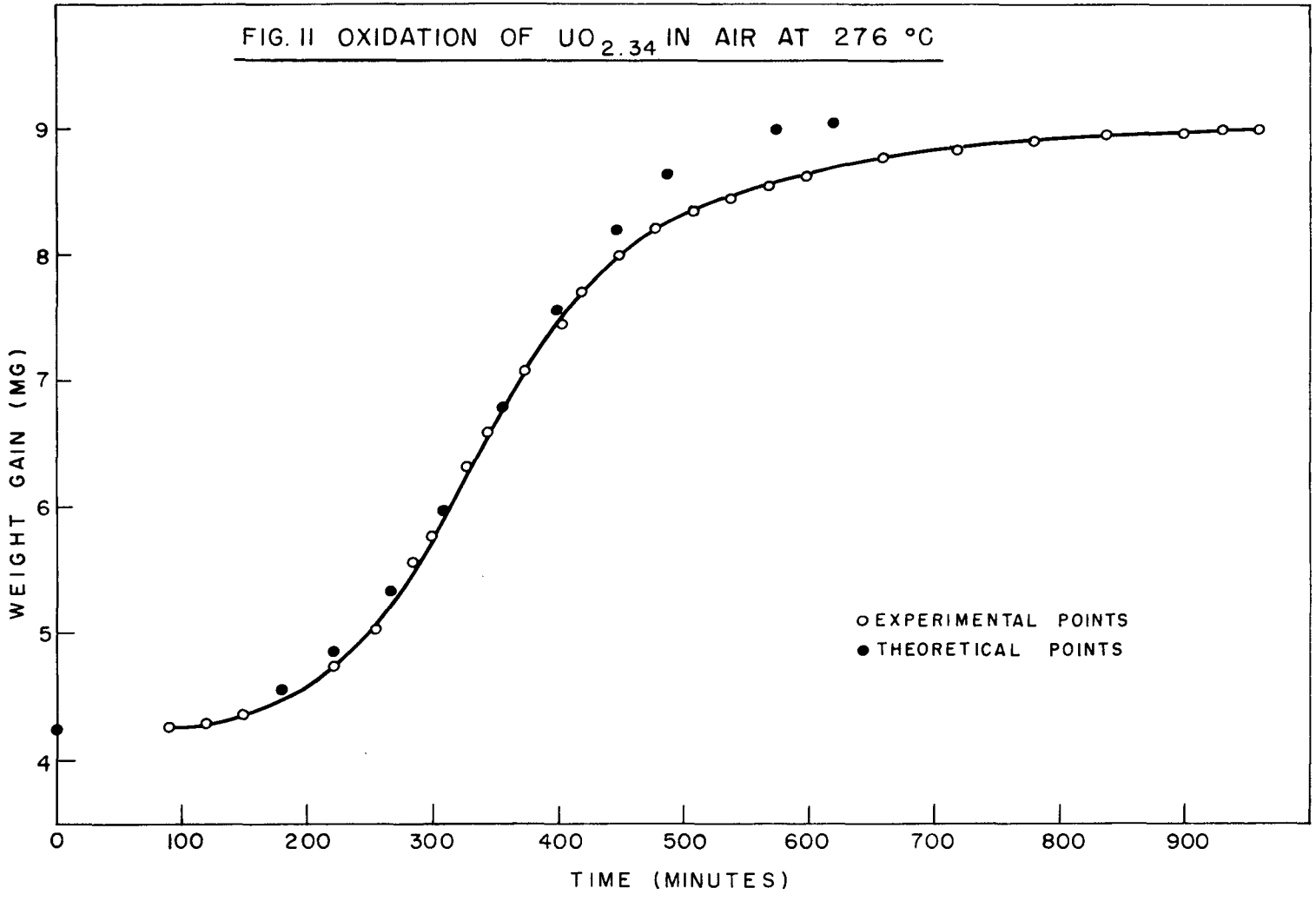
FIG. II OXIDATION OF $UO_{2.34}$ IN AIR AT 276 °C
WEIGHT GAIN (MG)
4
5
6
7
8
9
0
100
200
300
400
500
600
700
800
900
TIME (MINUTES)
○ EXPERIMENTAL POINTS
● THEORETICAL POINTS

FIG.12 GROWTH CONSTANT AS A FUNCTION OF TEMPERATURE

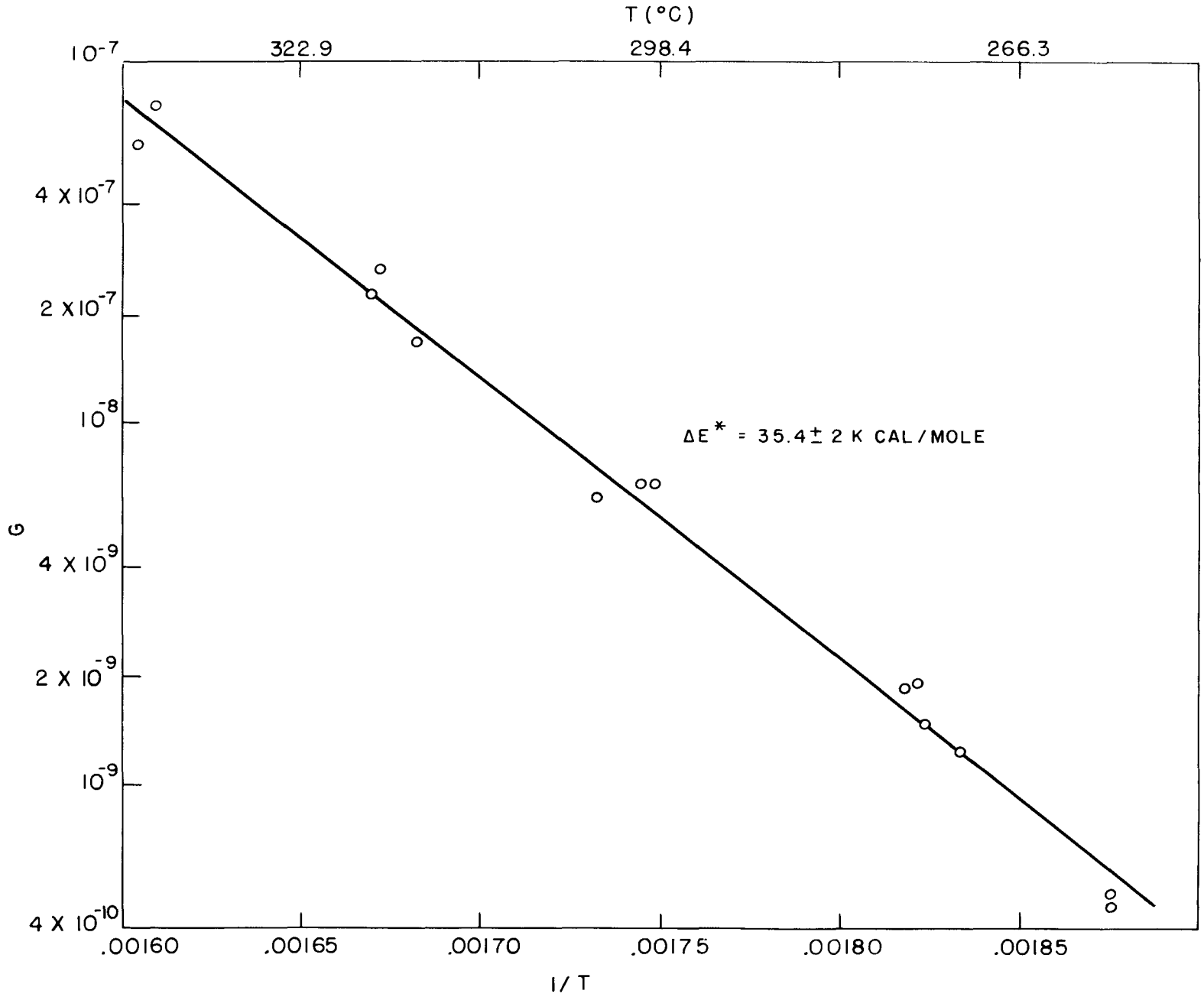

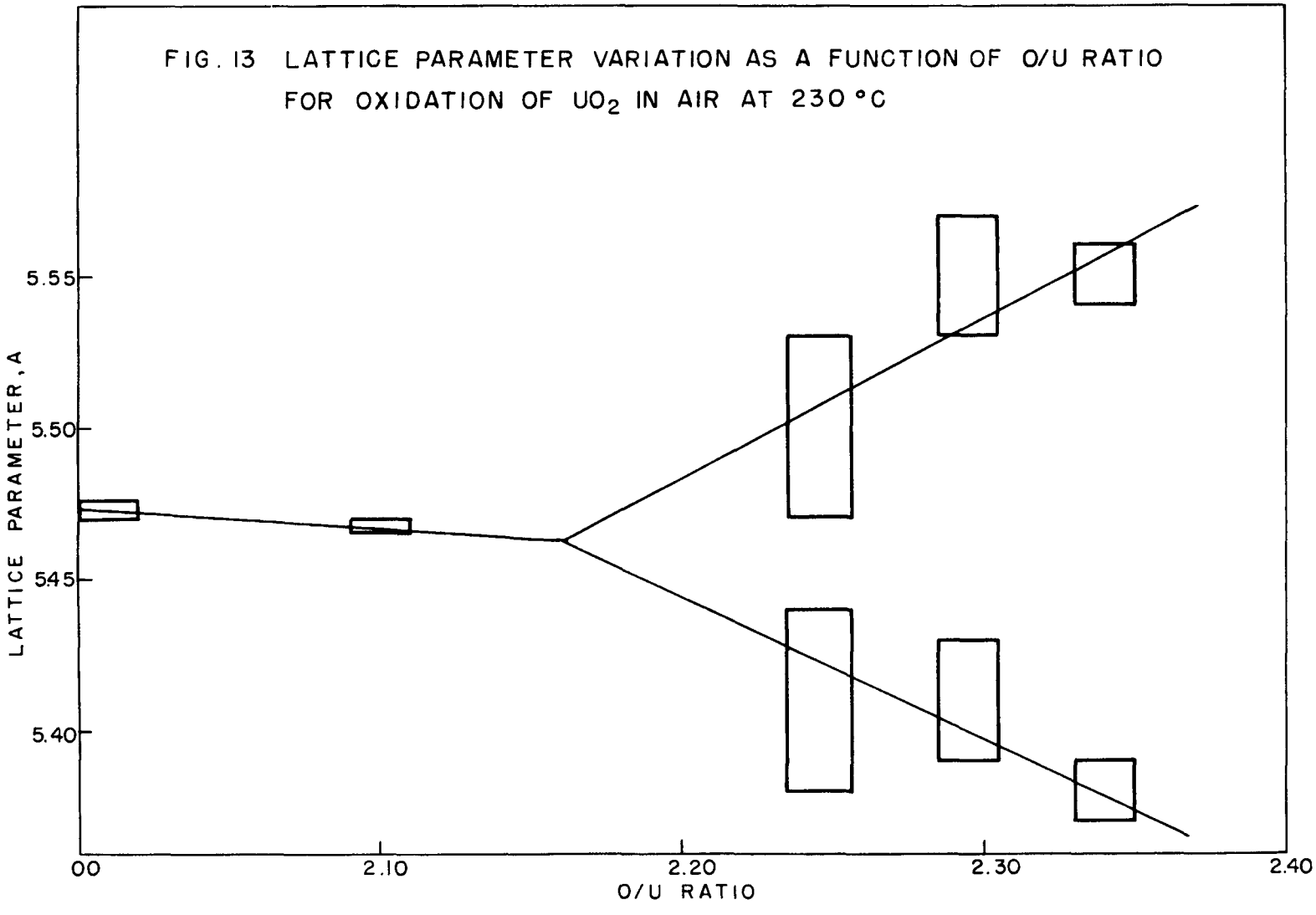

FIG. 13 LATTICE PARAMETER VARIATION AS A FUNCTION OF O/U RATIO FOR OXIDATION OF UO_2 IN AIR AT 230 °C

FIG. 14 LATTICE PARAMETER VARIATION AS A FUNCTION OF O/U RATIO FOR OXIDATION OF UO_2 IN AIR AT 275 °C

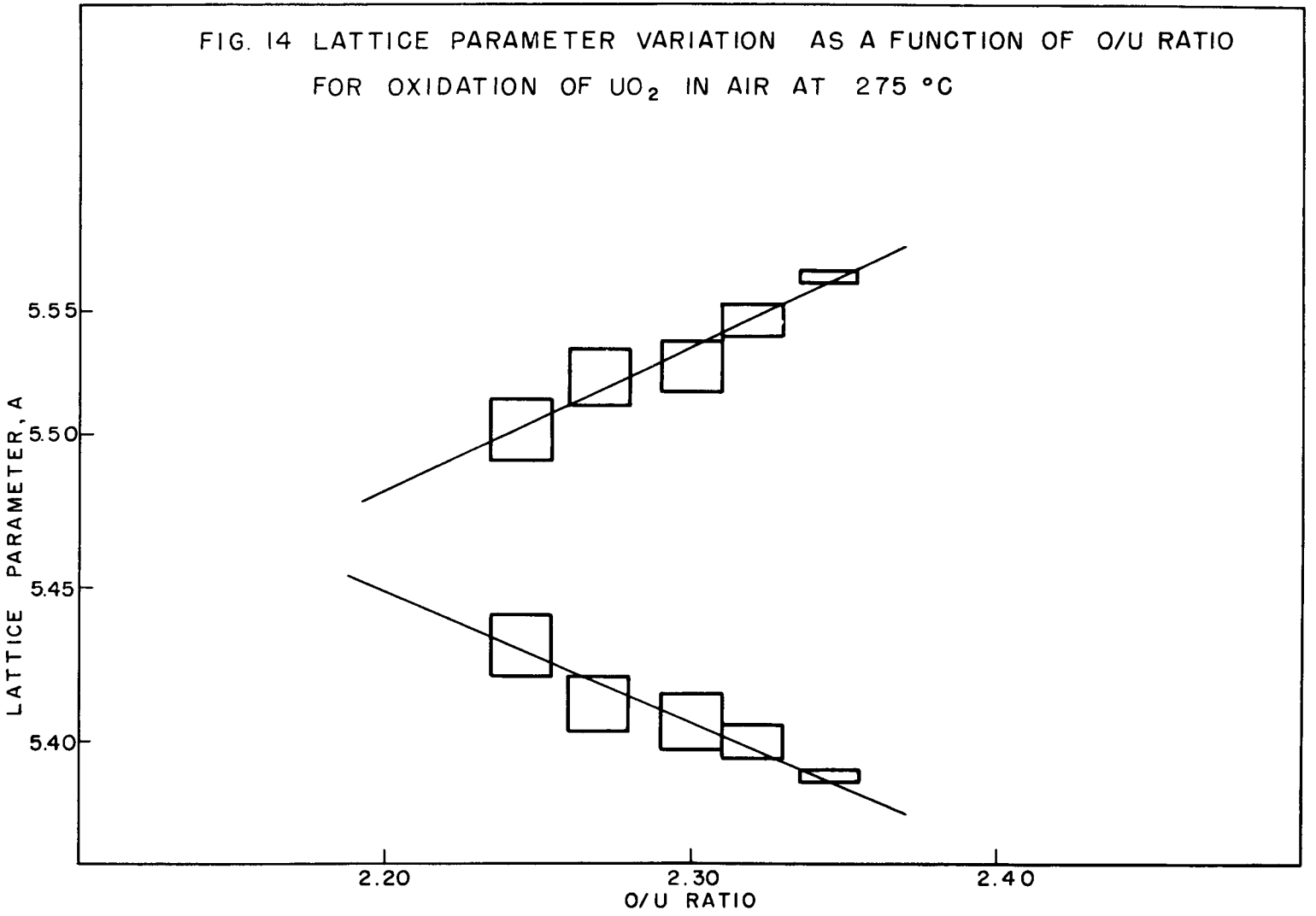

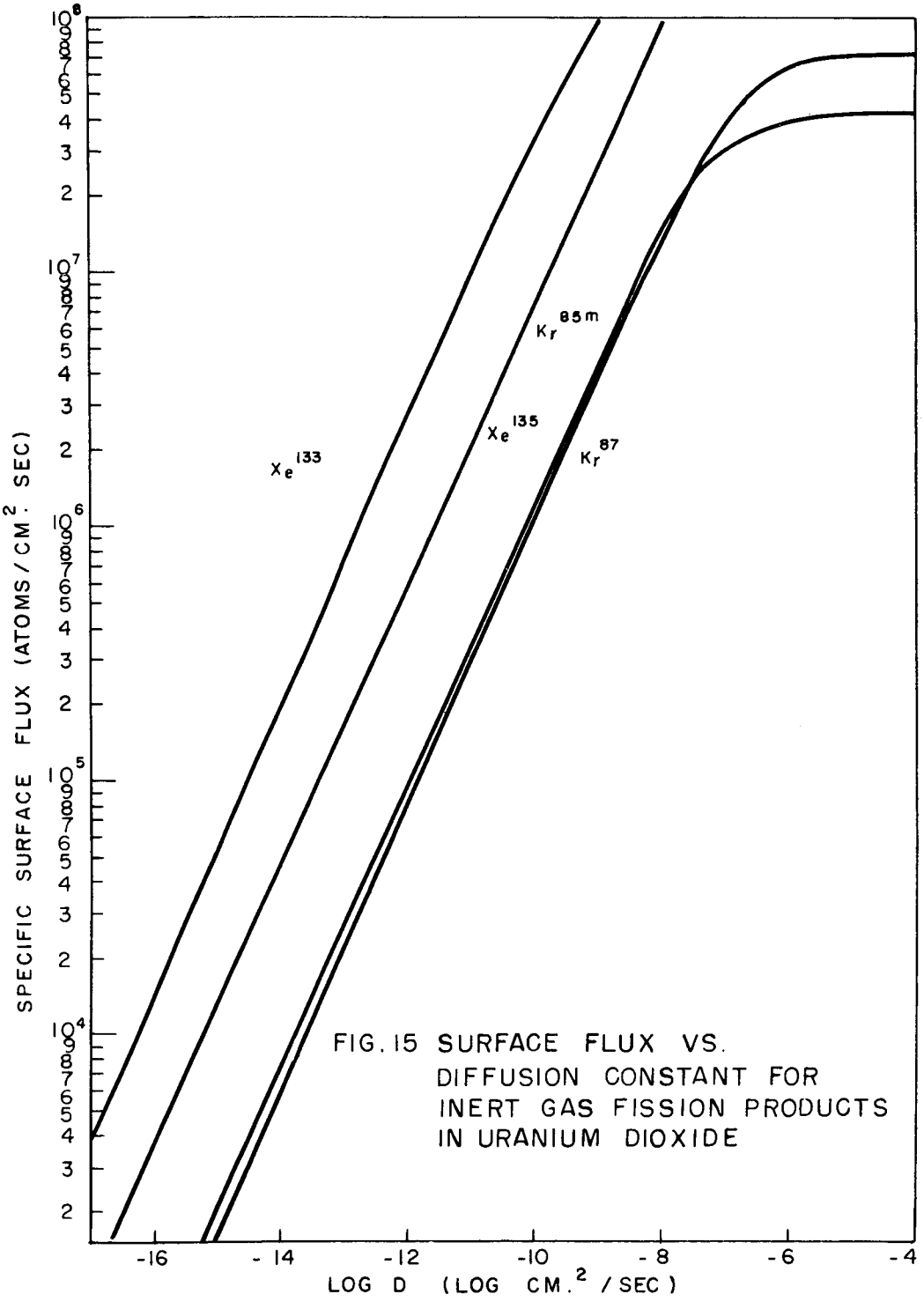

FIG. 15 SURFACE FLUX VS. DIFFUSION CONSTANT FOR INERT GAS FISSION PRODUCTS IN URANIUM DIOXIDE

FIG. 16 DIFFUSION OF FISSION GASES IN UO_2 AS A FUNCTION OF TEMPERATURE

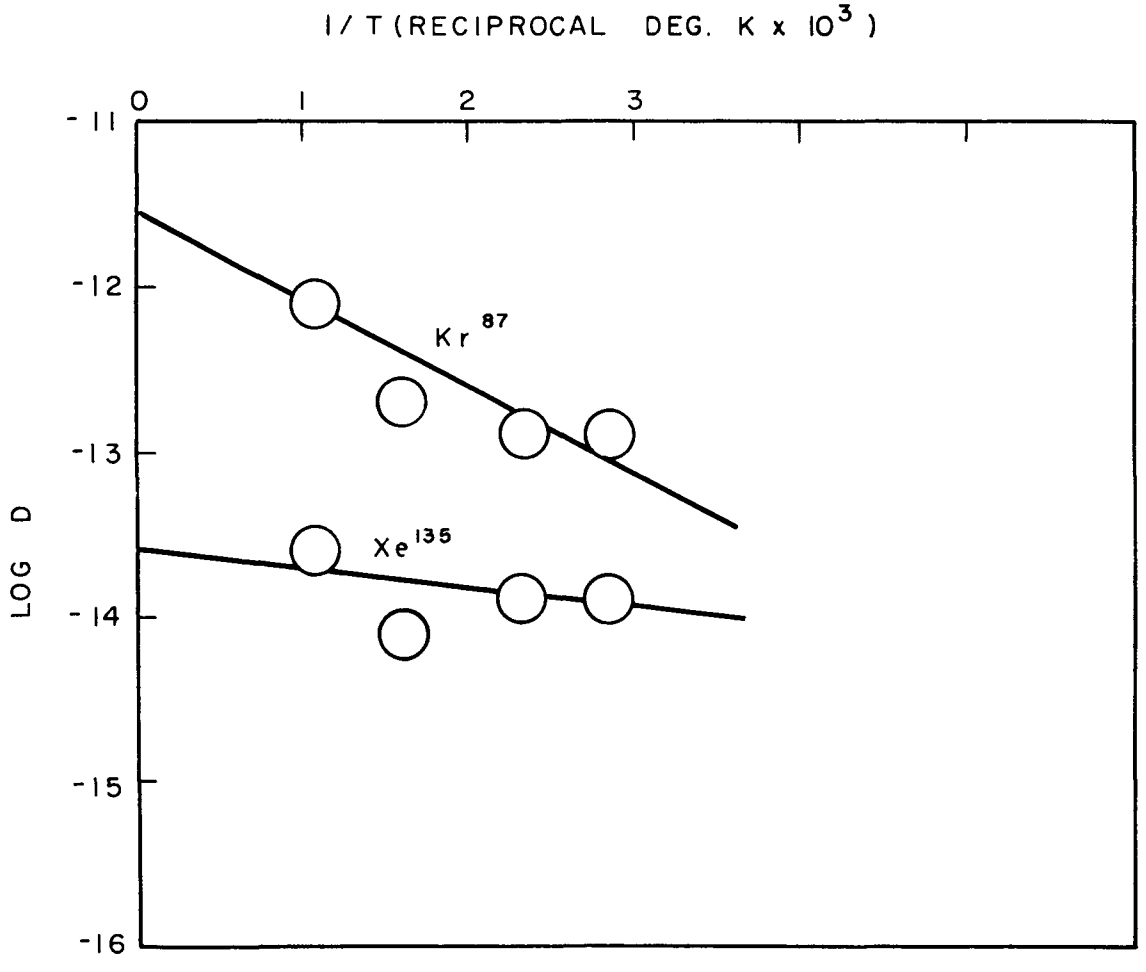

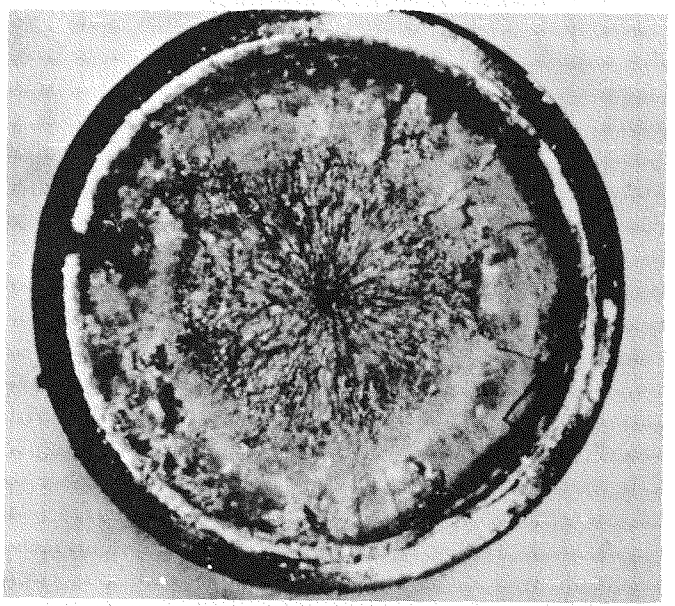

FIG. 17: Cross section of specimen No. 1 from the Sixth Chalk River UO_2 Defect Test. (Defected End) Defect-0.005 in. hole. Diam. Clearance-0.008 in. Est. Heat Flux - 440,000 Btu/ft^2/hr.

7.5X

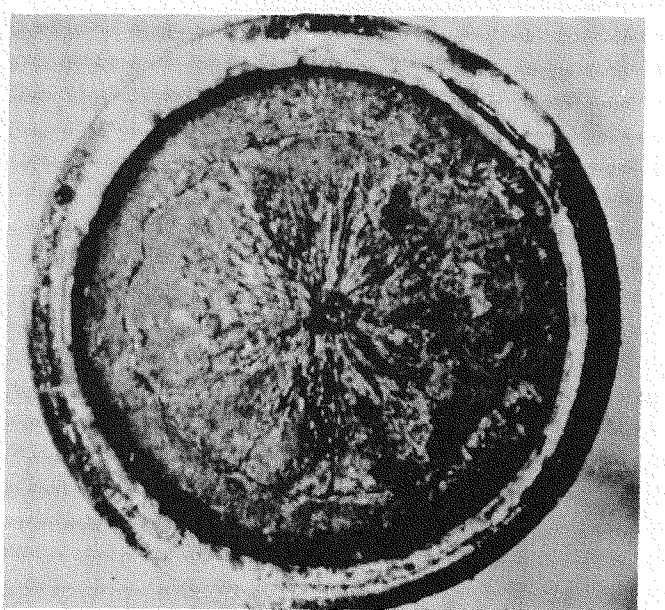

FIG. 18: Cross section of Specimen No. 2 from the Sixth Chalk River UO_2 Defect Test. (Defected End) Defect-0.005 in. hole. Diam. Clearance-0.0015 in. Est. Heat Flux - 495,000 Btu/ft^2/hr.

7.5X

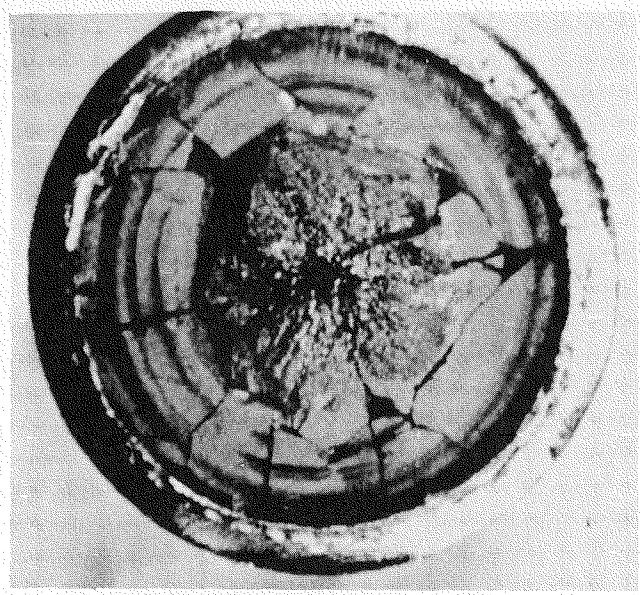

FIG. 19: Cross section of specimen No. 3 from the Sixth Chalk River UO_2 Defect Test. (No defect) Diam. Clearance - 0.008 in. Est. Heat Flux - 505,000 Btu/ft^2/hr.

7.5X

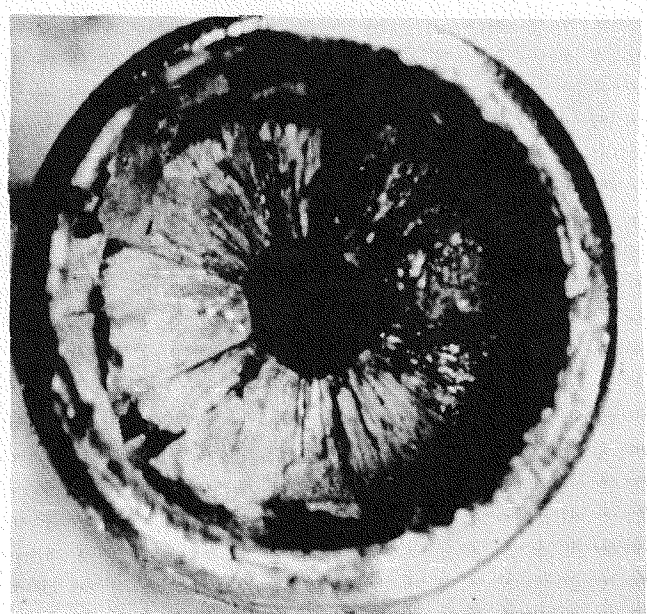

FIG. 20: Cross section of Specimen No. 4 from the Sixth Chalk River UO_2 Defect Test. (1st Pellet-Defected End) Defect-0.005 in. hole. Diam. Clearance - 0.008 in. Est. Heat Flux - 500,000 Btu/ft^2/hr.

7.5X

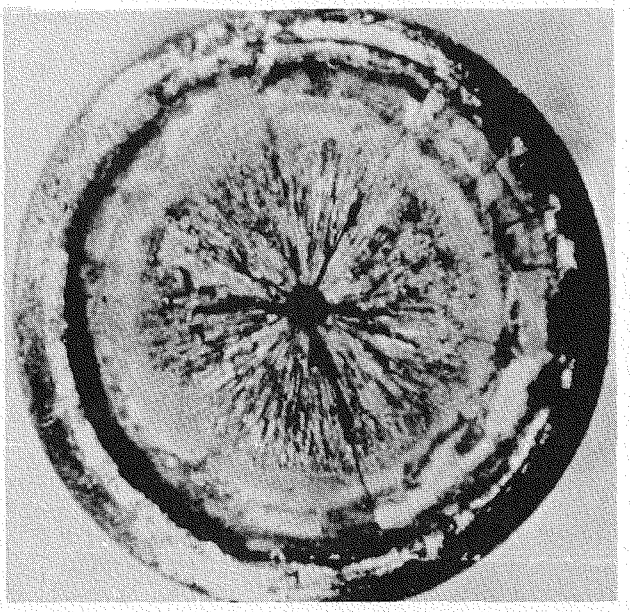

FIG. 21: Cross section of Specimen No. 4 from the Sixth Chalk River UO_2 Defect Test.(1st Pellet-Non-Defected End) Defect-0.005 in. hole. Diam. Clearance - 0.008 in. Est. Heat Flux - 450,000 Btu/ft^2/hr.

7.5X

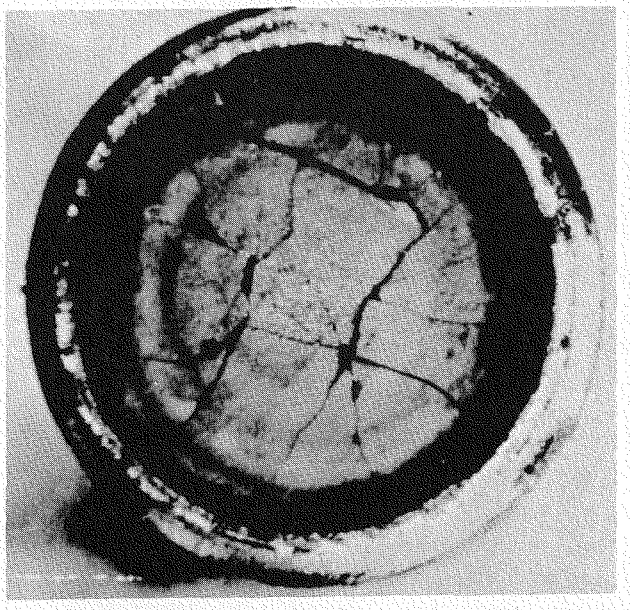

FIG. 22: Cross section of Specimen No. 5 from the Sixth Chalk River UO_2 Defect Test. (no defect-high flux end) Diam. Clearance - 0.003 in. Est. Heat Flux - 440,000 Btu/ft^2/hr.

7.5X

FIG. 23: ZrO_2 film at interface of UO_2 and Zircaloy-2 cladding of Specimen No. 4 from Sixth Chalk River UO_2 Defect Test.

370X

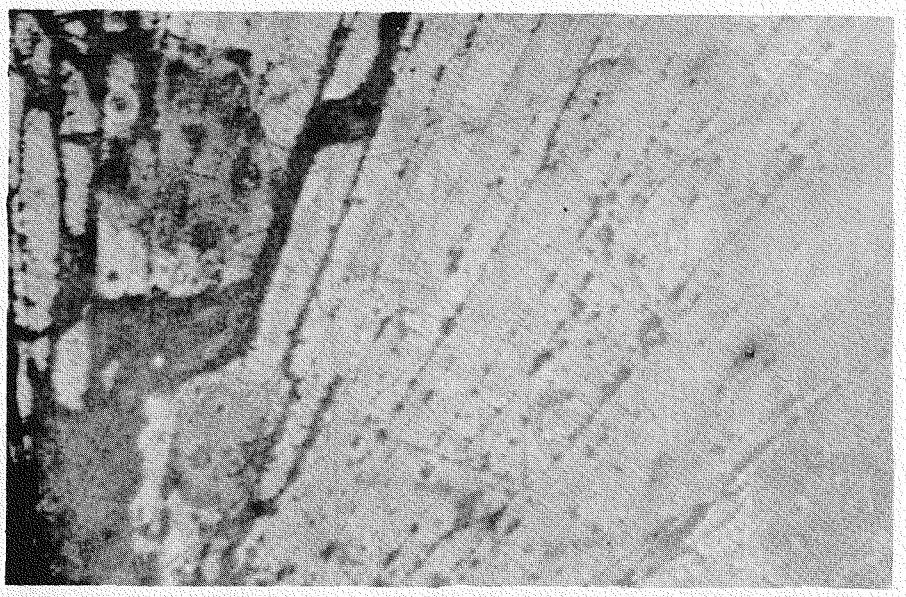

FIG. 24: Molten zone near center of UO_2 pellet from Specimen No. 4 from Sixth Chalk River UO_2 Defect Test. Part of shrinkage crater is shown at lower left.

65X

STUDIES CONCERNED WITH
URANIUM OXIDES IN PROGRESS
AT BATTELLE MEMORIAL INSTITUTE

September 4, 1956

STUDIES CONCERNED WITH URANIUM OXIDES IN PROGRESS AT BATTELLE MEMORIAL INSTITUTE

The studies previously reported have been continued or completed. The work on modified-uranium dioxide bodies was completed in July and is summarized in this report. The addition of refractory grade beryllia to uranium dioxide powder compacts improved the thermal-fracture resistance and did not adversely effect the corrosion resistance of the specimens. Although ceria additions were the most effective density promoters, they did not appreciably improve thermal-fracture resistance.

Experiments have been in progress in an attempt to determine the reactions responsible for the thermal activities in three preparations of uranium trioxide; (1) low-temperature Type III, (2) a high-temperature Type III, and (3) an amorphous uranium trioxide. In all weight-loss studies there was observed a greater weight loss than would be predicted by the conversion of uranium trioxide to U_3O_8 or to uranium dioxide. The temperature at which hydrogen reduction took place differed for the three preparations. Amorphous uranium trioxide was reduced in wet or dry hydrogen and exposed to air, oxygen, and nitrogen at room temperature. The oxygen/uranium ratio averaged 2.39 after exposure to air and a wide range of uranium/oxygen ratios resulted when uranium dioxide was exposed to oxygen.

The heating of specimens in which uranium dioxide is in intimate contact with zirconium has continued for 200 days at 950 and 1100 F and for 120 days at 1200 F. These specimens will be examined when healing is complete as a part of the study of the kinetics of the zirconium-uranium dioxide reaction. Analytical data describing the transfer of oxygen and uranium to the zirconium in an element heated 95 hr at 1600 F were considered from the viewpoint of diffusion of oxygen into zirconium. A model approximating the actual observed conditions was assumed

and equations representing this model were derived. The theoretical results agree quite well with results found experimentally. The data indicate that the uranium-rich layer (considered as a part of the first region in the diffusion zone) acts as an effective diffusion barrier. Experiments are now in progress that should clarify this point.

Studies of the electrical properties of uranium oxides have been continued in an attempt to establish the effect of interstitial oxygen on the uranium dioxide lattice. Magnetic susceptibility measurements suggest that incorporation of oxygen in this lattice increases the valence of the uranium atoms from the +4 to the +6 state. Ideally then, one uranium atom in four changes to give U_4O_9 and one in three to give U_3O_7. The electrical conductivity and thermoelectric power of these specimens have been studied as a function of temperature between 27 and 400 C. It is interesting to note that the initial activation energy decreases with increasing oxygen content in the p-type specimens. However, when the specimens became n-type, corresponding to the appearance of oxygen deficient U_4O_9 or U_3O_7, the activation energy increases with increasing oxygen content.

CERAMIC STUDIES

D. J. Bowers, A. G. Allison, and W. H. Duckworth

Work on modified-uranium dioxide bodies for the WAPD-PWR program was completed in July. The following summarizes this research.

Improvement in corrosion and thermal-fracture resistance of a uranium dioxide ceramic were sought through the use of selected additives of beryllia, ceria, silica, zirconia, silicon, silicon nitride, or beryllium. Nuclear considerations dictated that the modified bodies contain at least 80 volume per cent of uranium dioxide after sintering.

Sound specimens meeting this uranium dioxide content requirement were made with the beryllia, ceria, silica, or zirconia. These ceramics, with the exception of uranium dioxide silica, had as good resistance to 650 F water and 750 F steam as the unadulterated uranium dioxide ceramic.

Adding refractory-grade beryllia to the uranium dioxide powder compacts improved, by a factor of about 1.7, the thermal-fracture resistance of sintered specimens. Readily sinterable beryllia powder did not give this benefit. Variations in sintering treatment appreciably affected the thermal-fracture characteristics of the uranium dioxide-BeO specimens. Minor additions of titania or ceria to uranium dioxide beryllia powder compacts resulted in increased densities at lower sintering temperatures, but thermal-fracture resistance was not improved through their use.

Dense, strong specimens were made using ceria as the additive to uranium dioxide. Ceria was the most effective density promoter during sintering of the major additives studies. Uranium dioxide-ceria specimens, however, were only slightly better in thermal-fracture resistance than those of uranium dioxide alone.

Zirconia and uranium dioxide combinations had adequate density and strength, but the zirconia had a deleterious effect on the thermal-fracture resistance of uranium dioxide.

Uranium dioxide-silicon cermet specimens had low density and strength, presumably because of the formation of a reaction product. The reaction occurred on sintering in hydrogen, argon, or in a vacuum, and, to a lesser degree, on hot pressing. The reaction product was isolated, but not identified. It was unstable when resintered by itself and with uranium dioxide.

Satisfactorily dense and sound sintered compacts were not produced with either beryllium or silicon nitride as the additive.

A topical report, BMI-1117, covering the work in detail has been issued, (July 24, 1956).

RESUME OF URANIUM OXIDE INVESTIGATIONS

C. M. Schwartz, D. A. Vaughan, and J. R. Bridge

Investigation of the variations in oxide structures and properties that result from changes in processing was continued during the past three months. This work included thermal decomposition and hydrogen reduction studies of various preparations of uranium trioxide. As a measure of reactivity of uranium dioxide, its oxygen/uranium ratio after exposure to room-temperature air was determined by weight change on ignition to U_3O_8.

Uranium Trioxide Studies

As was reported previously, differential thermal analysis showed a marked effect of uranium trioxide preparation on its thermal activity in both air and hydrogen. During the past period attempts were made to determine the reactions responsible for the thermal activities in three preparations of uranium trioxide; (1) a low-temperature Type III, (2) a high-temperature Type III, and (3) an amorphous uranium trioxide. Weight loss and X-ray diffraction data were obtained on heating these preparations at selected temperatures as indicated by activity regions in the thermal analysis curves. In all of the weight-loss studies there was observed a greater weight loss than would be predicted by the conversion of uranium trioxide to U_3O_8 or to uranium dioxide. The excess is probably residual water or nitrate in the uranium trioxide. The conversion to U_3O_8 occurred in air at different temperatures, depending upon the uranium trioxide preparation. Likewise, in the hydrogen reduction studies, the temperature at which reduction took place differed for the three preparations. The amount of air reoxidation of uranium dioxide was greater for the specimen made from amorphous uranium trioxide which reduced at the lowest temperature.

Uranium Dioxide Studies

Amorphous uranium trioxide was reduced in wet or dry hydrogen and exposed to air, oxygen, or nitrogen at room temperature (Table 1). The oxygen/uranium ratio of the uranium dioxide after exposure to air was fairly high

(average = 2.39) whether the reduction was carried out in wet or dry hydrogen. A wide range of oxygen/uranium ratios resulted when uranium dioxide was exposed to oxygen. When reduced in wet hydrogen and exposed to nitrogen and then air, the oxygen/uranium ratio was about 2.15; but when reduced in dry hydrogen, the oxygen/uranium ratio was about 2.4. Experiments suggest that the as-reduced uranium dioxide is nearly stoichiometric. X-ray diffraction examination of all uranium dioxide preparations showed only a cubic phase, except that in one of the samples which had been exposed to oxygen, some U_3O_8 was present. High-temperature X-ray studies of these active uranium dioxide powders of variable oxygen/uranium ratios are in progress.

TABLE 1. OXYGEN/URANIUM RATIO OF URANIUM DIOXIDE MADE FROM AMORPHOUS URANIUM TRIOXIDE

Sample	Hydrogen Reductant	Oxygen/Uranium Ratio, Atmosphere After Reduction: Air	Oxygen	Nitrogen
213D	Dry	2.321		
214A	Ditto	2.437		
216B	"	2.376		
217B	"	2.472		
235A	"	2.289		
221A	Wet	2.321		
227A	Ditto	2.392		
215B	Dry		2.248	
222A	Ditto		2.377	
237A	"		2.172	
219A	Wet		2.307	
229A	Ditto		2.641	
225A	Dry			2.390
226A	Ditto			2.467
231A	Wet			2.137
233A	Ditto			2.169

KINETICS OF THE ZIRCONIUM-URANIUM DIOXIDE REACTION

M. W. Mallett, J. W. Droege, A. F. Gerds, and A. W. Lemmon

Zirconium-clad uranium oxide fuel elements are being considered for reactor use. The compatibility of these materials is being studied in the temperature range of 950 to 1600 F to aid in estimating the useful life of the elements in reactor service. Sandwich-type elements in which a plane surface of zirconium is in intimate contact with a plane surface of uranium dioxide are being used for the study.

The heating of the thin-walled elements at 950, 1100, and 1200 F is continuing. The elements being heated at 950 and 1100 F now have been on test for about 200 days; those being heated at 1200 F now have been on test for about 120 days.

Previously, an element that was heated at 1600 F for 500 hr produced voids in the uranium dioxide adjacent to the zirconium. In order to minimize this condition, a large element was prepared in which the wall thickness of the jacket was reduced from 1/8 to 1/16 in. Simultaneously the dead load on the heated element was increased to attempt to maintain the desired intimate contact between the components. This test has not been completed.

The analytical data describing the transfer of oxygen and uranium to the zirconium in an element heated for 95 hr at 1600 F were considered from the viewpoint of diffusion of oxygen into zirconium. A model was assumed which approximates the actual observed conditions. Equations representing this model were found. They described the diffusion from a constant initial concentration through a first region and past a boundary into a second region of unlimited thickness. This first region corresponds roughly to the two-phase area adjacent to the uranium dioxide and the thin uranium-rich phase. The second region corresponds to the oxygen diffusion affected and unaffected zirconium phase base metal. Using a portion of the experimental data, constants in the equations were evaluated. The computed numerical values for oxygen concentration versus

distance of penetration approximate the curve found experimentally. Although the model is probably not sufficiently valid to permit the evaluation of reliable diffusion constants or distribution coefficients, comparison with the diffusion constant for oxygen in Zircaloy 2 indicates that the uranium-rich layer (considered as part of the first region) acts as an effective diffusion barrier.

The 500 hr, 1600 F experiment now in progress should help to clarify this point. In addition, an experiment is being set up in which a 1-mil piece of uranium foil will be used to separate the zirconium from the uranium dioxide. This should aid in determining the role that uranium plays as a barrier for the diffusion of oxygen.

Uranium and oxygen analyses have been completed on thin layers machined in the zirconium of an element heated at 1450 F for 495 hr. The data are now being interpreted.

ELECTRICAL PROPERTIES OF URANIUM OXIDES

J. W. Moody, R. K. Willardson, and H. L. Goering

The electrical conductivity and thermoelectric power of uranium oxides in the uranium dioxide-U_3O_7 range have been studied as a function of temperature and of heat treatment. The materials studied were prepared from regular MCW uranium dioxide by exposure to dry oxygen at 180 C. After oxidation, oxygen to uranium ratios were determined by ignition to U_3O_8. Specimens for electrical measurements were hydrostatically pressed (without a binder) at 100,000 psi.

Initially, all the specimens prepared in the above manner were p-type and of relatively low conductivity. However, annealing the specimens at various elevated temperatures resulted in enhanced conductivities in all cases and the appearance of n-type conductivity in those specimens having oxygen/uranium ratios greater than 2.16. These results were discussed in some detail in the last resume. It will be sufficient to recall here that the effects of heat treatment were ascribed to an ordering of interstitial oxygen atoms in the uranium dioxide

lattice resulting in the appearance of phases, or compounds, other than uranium dioxide. The compounds identified in the range studied may be described, electrically, as:

(1) UO_{2+x}, a metal deficit semiconductor (p-type)

(2) U_4O_{9-y}, a metal excess semiconductor (n-type)

(3) U_3O_{7-z}, a metal excess semiconductor (n-type).

Phases corresponding to the representations U_4O_{9+y} and U_3O_{7+z} (p-type, metal deficit semiconductors) were not identified. The electrical measurements indicate that their existence occurs over an exceedingly small range, if at all.

The presence of all major phases were confirmed by X-ray powder techniques. Basically the crystal lattices is the same for all three compounds. Excess oxygen enters into interstitial positions in the fluorite structure of uranium dioxide, and in doing so, contracts the lattice. The results of the anneal-quench experiments suggest a temperature dependent oxygen solubility for which, at low temperatures, much of the oxygen is not incorporated in the lattice but is precipitated on grain boundaries. Under proper conditions, however, sufficient interstitial oxygen is accommodated in the uranium dioxide lattice to contract it a fixed amount to give U_4O_9 or to contract it preferentially to give the slightly tetragonal structure of U_3O_7.

The incorporation of interstitial oxygen in the uranium dioxide lattice is accompanied by an increase of valence by some of the uranium atoms. Magnetic susceptibility measurements suggest that the change is from the +4 and the +6 state. Ideally then, one uranium atom in four changes to give U_4O_9 and one in three to give U_3O_7. That these states are relatively stable is indicated by the fact that they may be quenched in and by the reproducibility of the anneal-quench experiments. However, prolonged aging at room temperature resulted in decreased conductivities of all the specimens studied. This suggests the reversibility of the phase transitions brought about by the anneals and the precipitation of oxygen along grain boundaries at low temperatures.

The electrical conductivity and thermoelectric power of these specimens were studied as a function of temperature between 27 and 400 C. In general, the conductivity of each specimen could be represented by an expression of the form:

$$\sigma = He^{-\Delta E/2KT} \qquad (1)$$

where ΔE is the energy necessary to free the charge carriers. Thus, the slope of the curve $\log\sigma = f(1/T)$ yielded a value of the activation energy. For some specimens a change of slope occurred at about 200 C and it was possible to calculate two activation energies. The values are listed in Table 2 where ΔE_1 represents the low temperature slope and ΔE_2 the slope obtained above 200 C. It is interesting to note that the initial activation energy decreases with increasing oxygen content for the p-type specimens. However, when the specimens become n-type, corresponding the appearance of oxygen deficient U_4O_9 or U_3O_7 the activation energy increases with increasing oxygen content. A comparison of these results with previous work suggests that an energy of 0.4 ev at high carrier concentrations to 0.6 ev at low carrier concentrations is required to free a positive carrier from interstitial oxygen in UO_{2+x}. On the other hand, the energy required to free a negative carrier from hexavalent uranium in U_4O_9 or U_3O_7 varies from 0.4 to 0.9 ev from high to low carrier concentrations. However, if the n-type specimens of high (0.9 ev) activation energies contained both donors and acceptors (say UO_{2+x} and U_3O_{7-z}) the effect is one of reducing the free carrier density and the carrier density changes more rapidly with temperature. When such a condition prevails, a calculation based on equation (1) might be in considerable error and the true activation energy may be lower by as much as a factor of two.

As noted in Table 2, the behavior of the maximum thermoelectric power was similar to that observed for the activation energies. That is, as oxygen was added to UO_{2+x} the thermoelectric power decreased. When the specimens became n-type the thermoelectric power increased as the oxygen/uranium ratio of 7/3 was

TABLE 2. ELECTRICAL DATA ON PRESSED URANIUM OXIDE SPECIMENS

Specimen	Oxygen/Uranium Ratio	Room Temperature Conductivity, $ohm^{-1}-cm^{-1}x10^4$	Slopes on Conductivity Curve, ev		Maximum Thermoelectric Power, per deg. C	Probable Phases Present
			ΔE_1	ΔE_2		
119	2.032	13.4	0.47	0.52	270 (P)	UO_{2+x}
154	2.074	34.6	0.42	--	130 (P)	a UO_{2+x} + b U_4O_9, a $>>$ b
178	2.160	48.5	0.38	0.49	77 (P)	a UO_{2+x} + b U_4O_9, a $\sim$ b
155	2.208	56.4	0.41	--	76 (N)	b U_4O_{9-y} + c U_3O_7, c $>$ b
174	2.264	48.0	0.41	0.42	84 (N)	U_3O_{7-z}
157	2.317	9.63	0.46	0.56	130 (N)	U_3O_{7-z}
188	2.353	4.45	0.56	--		---

approached. Such behavior is consistent with the appearance of U_4O_9 and U_3O_7 and offers strong evidence of their existence.

During the anneal-quench experiments it was noted that some of the specimens underwent a considerable volume shrinkage when annealed at temperatures above 600 C. The change of volume at any temperature was directly proportional to the amount of excess oxygen when it was present as UO_{2+x} (that is, up to oxygen/uranium ratios of about 2.14). If U_4O_9 or U_3O_7 were the major phases present a slight increase of volume was noted, due, perhaps, to excessive loss of oxygen and subsequent expansion of the lattice. In view of these results it was felt advisable to sinter the specimens under normal sintering conditions. Accordingly, the specimens were sintered for one hr at 1650 C in a hydrogen atmosphere. Several of the specimens cracked during the process (perhaps because of excessive handling beforehand) and all sintered to a density of about 80 per cent that of theoretical, the usual density to which normal MCW uranium dioxide sinters.

Electrical measurements were than made on several of the sintered specimens. These properties are summarized in Table 3.

TABLE 3. ELECTRICAL DATA ON SINTERED SPECIMENS OF URANIUM OXIDES

Specimen	Estimated Oxygen/Uranium Ratio	Room Temperature Conductivity (ohm^{-1}-cm^{-1}x10^4)	Slope of Conductivity Curve ΔE, ev	Maximum Thermoelectric Power
154	2.010	12	0.38	350
155	2.020	30	0.38	260
157	2.025	38	0.38	140

After sintering, all the specimens were p-type and their electrical properties are to be compared with those listed in Table 2. The changes in magnitude and type of conductivity and the approximate 0.4 ev slope of the conductivity curve are consistent with the loss of considerable oxygen during the sintering process. After sintering the composition of all the specimens could be represented as UO_{2+x}. The oxygen/uranium ratios listed in Table 3 are estimated from a comparison of the conductivities with previous experience.

Evidently the reducing atmosphere of the sintering process removes excess oxygen from the uranium dioxide lattice and the carriers arising from interstitial oxygen play no part in the sintering mechanism under reducing conditions. Yet the correlation between sintering characteristics and electrical conductivity noted during the anneal-quench experiments (when great care was taken to minimize loss of oxygen) appears important and suggests that, a p-type metallic impurity may improve the sintering characteristics.

At present experiments are now underway to characterize a more reactive uranium dioxide than normal MCW material. Such an oxide is prepared from the hydrogen reduction of amorphous uranium trioxide and sinters to a high density. Measurements similar to those performed on the "inactive" oxide will be made in an effort to distinguish the essential differences between the materials.

UO_2 PANEL REPORT

Corning Glass Works
Corning, New York

September 5, 1956

SUMMARY:

Since the June meeting of the UO_2 Panel work on modulus of rupture of UO_2 was completed. It was shown that there is an optimum firing time for a given firing temperature. The modulus of rupture for UO_2 is about 15,000 psi from room temperature to 1000°C. Most significant is the fact that thermal shock characteristics are greatly affected by surface treatment.

Work on TiO_2 additions was also completed. Such additions produce bodies with similar strength characteristics to those of UO_2 alone but at a much lower firing temperature. The presence of a liquid phase has been established.

A program on steam sintering produced a method for firing dense UO_2 pellets in a GLOBAR furnace with a minimum of hydrogen consumption. Of great interest is the fact that this method can produce pellets of either $UO_{2.03}$ or $UO_{2.19}$, depending on the cooling atmosphere used.

The work on cladding has been mostly of an exploratory nature on the fabrication of various pellet configurations. Corrosion tests in high temperature steam and water were also made of several potential cladding materials.

1. MODULUS OF RUPTURE MEASUREMENTS

The objective of this work was to determine the modulus of rupture of high density UO_2 bodies and to determine the factors affecting it (e.g. fabrication variables and surface finish).

The test bars were made from ballmilled MCW UO_2, pressed in a steel die at 6400 psi and hydrostatically repressed at 40,000 psi. They were fired in a Harper hydrogen-atmosphere furnace. All surfaces were fine-ground with #400 grit Al_2O_3 before modulus of rupture measurements were made. These measurements were made in H_2-He atmosphere at temperatures from room temperature to 1000°C.

The strength data given in each case represent an average value obtained for six bars. Table I shows the modulus of rupture values for specimens sintered at 1750°C from one to 20 hours. It also includes data on special bars made with 1400°C calcined UO_2. Results are also shown graphically in Figure I.

In general, the strength increases slightly with the testing temperature. The higher values obtained at 1000°C may be due to plastic deformation of the specimens which permits dissipation of the tension stress.

It should be noted that the bars fired for one hour have the highest strength. On the basis of these data this is the preferred firing time at 1750°C.

Figure I also shows a strength decrease for firing time to 5 hours and then remains essentially constant for higher times.

Examination of the broken bars shows that nearly all breaks originate either at or close to the surface. This suggested that surface conditions would greatly affect the strength characteristics of UO_2 bars. Accordingly, measurements were made on a series of bars whose surface had been given various types of finishes including polishing. Data are shown in Table 2. It is seen that a standard grind with #400 grit Al_2O_3 improves the strength over that of the "as-fired" surface and that a still finer grind (A0303-1/2) also improved the room temperature strength slightly. However, no further effect was noted on the polished bars.

Of particular interest is the fact that the A0303-1/2-ground and the polished bars could not be heated in present equipment without breaking. The fact that the polished bars showed the greatest tendency to shatter indicates that thermal shock resistance of these bodies is markedly affected by surface finishing operations. This phenomenon urgently requires more study because all UO_2 fuel pellets today are completely finished to meet tolerance requirements. As further evidence of the effect of surface finish on thermal shock resistance of UO_2 bodies it was found that bars ground in our standard manner would not withstand a regular 1750°C firing schedule in the Harper furnace without breaking while bars with the "as-fired" surface did not break under these conditions. It was believed possible that stresses were introduced by grinding which reduced strengths of the ware. Annealing the bars might therefore alleviate this situation. Accordingly, two sets of ground bars, fired for 1 hour at 1750°C, were heated to 500°C in the modulus of rupture equipment and then allowed to cool slowly (average rate 80°C/hour) to room temperature. Modulus of rupture data taken on these samples, with those of an equal number of control samples, are given in Table 3. A noticeable improvement in strength as a result of the annealing operation appears to confirm the assumption that tensile stresses are set up in the surfaces of the slabs as a result of the grinding operation. This could also account for the poor thermal shock resistance of the ground and polished bars.

Data presented in Table 4 shows the effect of firing temperature on modulus of rupture when the firing time is kept constant at 20 hours. This time was chosen because previous work indicated that good densities could be obtained at temperatures as low as 1500°C. Data are shown graphically in Figure II. This graph also shows that for this sintering time bars of maximum strength at room temperature are made at 1550°C. Table 4 shows that this high strength persists at measuring temperatures to 1000°C. A comparison of these strengths with those of bars fired for 1 hour at 1750°C and for 5 hours at 1750°C (calcined at 1400°C) (Table I) shows that they are all high and of the same order of magnitude. This indicates that bars with good strength characteristics can be made by long firings at low temperatures or short firings at high temperatues. There are thus optimum time and temperature combinations which will produce samples with the maximum strength.

Room temperature measurements of Young's Modulus are shown in Table 5 for pieces fired at 1750°C and from 1 to 20 hours. It is interesting to note that the value increases, reaching a constant value at and over five hour firing times. The room temperature modulus of rupture follows a similar pattern, decreasing to a constant value for firing times of five hours and above. (See Table I).

2. ADDITION OF TiO_2:

2.1 Effect of Carbowax Binders

Certain additives are known to increase the sinterability and to lower the sintering temperature of oxide ceramics. The objective of this work was to determine the effect of TiO_2 on the sintering of UO_2 and also its effect on modulus of rupture. During the preparation of modulus of rupture specimens using this additive, it was found that fired densities were 3 to 4% below expected values on pieces fired at 1750°C for one hour. This was traced to the use of Carbowax 20M binder, which apparently produced a bloating action. This is shown in Table 6.

2.2 Effect of TiO_2 on Modulus of Rupture Values

Modulus of rupture measurements were made on three different sets of samples prepared as outlined below.

2.2.1 Ballmilled MCW UO_2 with 0.1wt.% TiO_2 - Fired at 1750°C for 1 hour

The room temperature strength was high (17,000 psi) and decreased linearly with increase in temperature of measurement to 9000 psi at 1000°C. The samples had poor thermal shock characteristics. Many gross flaws appeared in the samples on heating to 1000°C.

2.2.2 Calcined Ballmilled UO_2 with 0.3wt.% TiO_2- Fired at 1750°C for 1 hour

The modulus of rupture was fairly constant at 14,000 psi from room temperature to 1000°C. Samples showed better thermal shock characteristics when heating in the furnace.

2.2.3 Ballmilled MCW UO_2 with 0.3wt.% TiO_2 - Fired at 1500°C for 1 hour

The strength was fairly constant at 15,000 psi from room temperature to 1000°C. This was the most satisfactory body produced with a TiO_2 addition.

Results of this work indicate that TiO_2 additions do not improve the modulus of rupture of UO_2 bodies. However, a UO_2 body with addition of 0.3 wt.% TiO_2, fired for 1 hour at 1500°C, has strength values as high as those of a standard UO_2 body fired for an equal time at 1750°C.

3. CERAMIC CLADDING:

The objective of this phase of the work is to improve the thermal shock, oxidation and abrasion resistance of UO_2 pellets. Work since the last panel report has been concerned with the fabrication of a number of different pellet shapes and body configurations. Some results have been obtained with bonded claddings.

A variety of body configurations were made, the most common (reported previously) being a UO_2 core coated with Al_2O_3. Other variations are (1) a hollow UO_2 core covered with Al_2O_3, (2) a hollow UO_2 body coated both externally and internally with Al_2O_3, (3) a core of Al_2O_3 or MgO (both dense and porous types tested) coated with UO_2 and this in turn covered with Al_2O_3, and (4) three small cylindrical UO_2 pellets embedded in an Al_2O_3 matrix in such a manner that they were uniformly coated. At least on a Laboratory scale all of these variations are possible.

All solid shapes and configurations were made by multiple dry pressing followed by a final hydrostatic pressing. Hollow shapes are made by the multiple dry pressing process only. Firing was done at 1750°C in a hydrogen atmosphere. Some attempts were also made to apply coatings by spraying techniques but this technique will require much more study.

To make a compression cladding with compressive stresses, a core containing 70 percent by volume of Al_2O_3 was made and coated with Al_2O_3. A ceramic bond forms between the core and coating on firing. However, these clad pellets were found to have poor thermal down-shock characteristics.

Thermal shock tests on clad pellets containing either solid or hollow alumina cores have shown poor strength values. It appears that the UO_2 shrinks onto the alumina and cracks and that these cracks then carry through the cladding. The size of the alumina core plays an important part; if it is small no breakage occurs. Pellets made with MgO cores have stood up well in thermal shock tests.

Qualitatively, no evidence of migration of UO_2 through the Al_2O_3 cladding was found even after prolonged heating at 1750°C. On the basis of available phase diagrams on UO_2-Al_2O_3 and on the work of Lang, et al, on BeO claddings which behave like Al_2O_3 there is no reason to expect migration.

4. CORROSION TESTS:

Since the most likely uses for a ceramic fuel element lie in a PWR-type of reactor, the corrosion resistance of possible ceramic coating materials in high temperature steam and water are of interest.

Table 7 summarizes the data on corrosion tests made to date. The tests were made in 335°C degassed water, using cylindrical pellets whose volume was generally approximately 0.5 cc. and surface area about 4 cm^2. These data show that BeO, ThO_2, and ZrO_2 have excellent corrosion resistace. Al_2O_3 is being studied further to determine whether minute amounts of impurities can affect its corrosion resistance.

5. STEAM SINTERING PROCESS:

5.1 Introduction

When the work on steam sintering was terminated at Armour Research Institute, a cursory research program was inaugurated at Corning to determine whether a process could be worked out for making high-density UO_2 by sintering in steam at GLOBAR temperatures. A second objective was to reduce the hydrogen requirement for the sintering process and so reduce the cost per pellet. Finally, the cause of the catalytic action of steam needed an explanation.

It was found that UO_2 pellets with a density of 10.60 gm/cc can be made by firing 4 hours at 1300°C. The only hydrogen requirement for this firing schedule is for a 2 hour, 1200°C hydrogen "soak". Thus, the cost of hydrogen per pellet can be minimized by firing in large batches. Finally, the increased sinterability of UO_2 has been traced to the oxidation of UO_2 by steam to a higher oxygen/uranium ratio. These results are discussed in more detail below.

5.2 Factors Affecting Sinterability of UO_2 in Steam

The remarkable effect of steam on fired density of ballmilled UO_2 is shown in Table 8 for pellets sintered for one hour at 1500°C. Comparing sample Nos. 1, 4, and 5 in Table 8, it can be seen that hydrogen is necessary as a pre-sintering atmosphere but not in the post-sintering atmosphere.

In addition to the effect of the pre-sintering atmosphere, the steam-sintered density is also influenced in a minor way by the post-sintering atmosphere. Thus, oxygen picked up during steam-sintering process is retained if the samples are cooled in steam. This excess oxygen results in a slightly higher density since the resulting U_4O_9 has a density near 11.3 gm/cc.

The steam-sintered density is also a function of the factors which influence the density of compacts fired in the normal manner. These are moisture and binder content, forming pressure, particle size and size distribution, and firing time and temperature. Also, there is probably a broad range of optimum conditions for the time and temperature of the hydrogen reduction process as well as an optimum for the time and temperature of steam sintering.

This section of the report covers briefly what appear to be the most important variables in developing a low-temperature process for making dense UO_2.

5.2.1 Effect of Ballmilling on Steam-Sintered Density

The importance of ballmilling in breaking up aggregates and producing finer particles has been discussed in earlier panel reports. Thus, for the present purpose it seemed sufficient to use two representative ballmilled powders with which we have had considerable experience and compare their sinterability with the -325 mesh fraction of as-received Mallinckrodt UO_2. These data are shown in Table 9.

Sample No. 1 in Table 9 represents an optimum ballmilling condition with respect to grinding efficiency and minimum contamination. Sample No. 2 represents a standard ballmilling procedure used for much of the work at Corning. These pellets were heated to 1400°C in hydrogen, then to 1500°C in steam, held there 1 hour, and then cooled in hydrogen. This is not the best firing schedule, but it is apparent that optimum ballmilling is just as important as atmosphere in the steam-sintering process. In fact, without ballmilling the beneficial effect of steam on sinterability would not be observable. This strongly suggests that steam-sintering is a surface phenomenon intimately related to the number and kind of surface contacts between indivudual grains.

5.2.2 Effect of Pre-Sintering Conditions

In order to realize the benefits of steam-sintering, ballmilled UO_2 must first be reduced in hydrogen. This is paradoxical since it was found that certain steam-sintered, steam-cooled samples contain excess oxygen to the extent of a molar oxygen/uranium ratio of 2.18. Thus it appears that the oxidation of UO_2 by steam is the cause of the increased sinterability. However, before steam can be effective, part or all of the oxygen picked up in ballmilling must be removed. Preferably this excess oxygen should be removed in hydrogen below the temperature at which UO_2 sinters in pure hydrogen so that reduction and steam-sintering occur separately.

Temperature and hydrogen concentration determine the optimum time for the pre-sintering step. For example, soaking in hydrogen for 2 hours at 1400°C is excessive but heating to 1400°C and immediately switching to steam is perfectly satisfactory. If the hydrogen is diluted with an inert gas, a longer pre-sintering time is normally needed to achieve sufficient reduction for good steam-sintering.

5.2.2.1 Effects of Intensity of Hydrogen Treatment During Pre-Sintering

The dependence of fired density on the temperature, time, and concentration of hydrogen during pre-sintering is further evidence of the need for reduction before steam can exalt the sinterability of UO_2. Table 10 shows that fired density is proportional to the intensity of the hydrogen treatment up to an optimum value. No measurements have yet been made on the optimum O/U ratio for steam-sintering. It would currently appear that 2 hours in hydrogen at 1200°C (e.g., sample 4) is sufficient to completely reduce the pellet. Accordingly, this O/U ratio is in the range 2.01 to 2.03. In this regard, samples 6 and 7, along with data on additonal samples indicate that the effect of a higher O/U ratio can be partially overcome by sintering at a higher temperature.

The most significant effect of a diluent is to impede the diffusion of hydrogen into and steam out of the pellet during reduction.

5.2.2.2 Effect of Pre-Sintering Temperature on Steam-Sintered Density

Pre-sintering temperature is probably most critical above that at which UO_2 will sinter in hydrogen. Below this temperature, nothing further happens to the UO_2 after reduction is complete. However, at hydrogen sintering temperatures densification results in a preferential disappearance of the finer particles with a consequent loss of surface and a decreased sinterability in steam. The data shown in Table 11 are consistent with this view.

It was also found that ballmilled calcined UO_2 produces lower density steam fired pellets than regular ballmilled as-received Mallinckrodt UO_2. The surface area of the two powders is 0.71 and 1.33 square meter/gram, respectively. This, along with the data in Table 9 on the effect of ballmilling suggests that the action of steam is principally a surface effect.

5.2.3 Steam-Sintered Density as A Function of Firing Time and Temperature

For this comparison, pellets were heated to 1200°C in steam, held for 2 hours in hydrogen at 1200°C, sintered in steam as indicated, and then cooled in steam. These data are shown in Table 12. These experiments show conclusively that dense UO_2 can be made by steam-sintering process at GLOBAR temperatures. Potentially, the firing schedule used to obtain these data consumes the minimum amount of hydrogen. For commercial operation, hydrogen consumption per pellet could be minimized by firing in large batches.

5.3 Oxidation of UO_2 During Steam-Sintering and Effect of POST-Sintering Atmosphere

When steam-sintered UO_2 is allowed to cool in steam from 1400°C, the compact consists of two cubic phases, UO_2 and U_4O_9, and has a molar oxygen/uranium ratio of 2.19. Since this oxygen/uranium ratio has already been shown by experiments at Bettis Field to be stable at these temperatures, the excess oxygen is more likely to be characteristic of the O/U ratio during steam-sintering than reflecting oxygen pick-up on steam cooling. If the compact is cooled in hydrogen rather than steam, the resulting O/U ratio is 2.03 and only a single UO_2 phase shows up by X-ray analysis.

These facts are interpreted to mean that the following reaction occurs between UO_2 and steam:

(1) (fast) $UO_2 + \frac{1}{X} H_2O(g) \rightarrow UO_{2+X} + \frac{1}{X} H_2$

This is a fast reaction which is driven to the right in flowing steam, subject to the tendency of the UO_{2+X} to dissociate according to the reaction:

(2) (slow) $UO_{2+X} \rightarrow UO_2 + \frac{X}{2} O_2$

Thus, UO_2 is oxidized in flowing steam because reaction (1) is faster than reaction (2). On the other hand, in flowing hydrogen reaction (2) is very rapidly driven to the right towards pure UO_2. This reversibility has been observed and the data are tabulated later in this report.

Equilibrium data for reaction (1) would simultaneously provide equilibrium data for reaction (2) since these are already available for

(3) $\frac{1}{X} H_2O = \frac{1}{X} H_2 + \frac{1}{2X} O_2$.

These measurements should be made. Accurate determination of the equilibirum ratio $(H_2)/(H_2O)$ as a function of temperature for reaction (1) is all that is needed.

5.3.1 Molar Oxygen/Uranium Ratio in Steam-Sintered UO_2

The data in Table 13 compare the molar ratio of oxygen to uranium obtained when steam-sintered pellets are cooled in hydrogen and in steam. It should be noted that all, or nearly all of the excess oxygen is taken off by hydrogen cooling. For these experiments, the power to the furnace was shut off at the end of the steam-sintering time and the furnace allowed to cool naturally, reducing the temperature to 700°C in 30 minutes.

5.3.2 Reversible Oxidation - Reduction of UO_2

The reversibility of this reaction is shown by following the weight changes of steam-sintered pellets which were alternatley heated in hydrogen and in steam. These data are tabulated in Table 14. In each case the pellets oscillate between a steam-sintered, steam-cooled and a hydrogen-sintered weight. The two states seem completely reversible. The 1750°C hydrogen-reduced pellets shrink and gain weight when re-sintered in steam. This is a direct result of the formation of the more dense (11.3 gm/cc compared to 10.96 gm/cc for UO_2) U_4O_9 during the steam treatment. When these pellets were reduced again, as shown in the last columns, they returned to their original density, diameter, and weight corresponding to the reduced form, as shown in the second columns.

5.3.3 Effect of Post-Sintering Atmosphere on Phase Separation of Steam-Sintered UO_2

When steam-sintered UO_2 is cooled in steam, the extra oxygen separates in a separate U_4O_9 phase. The two phases are distinguishable by X-ray analysis but not by low-power microscopic observation. There is considerable line broadening in the X-ray patterns, commensurate with the small crystallite size. Unit cell and overall O/U ratio are shown in Table 15. The intensity of the peaks of the respective phases is consistent with the O/U ratio and indicates that the U_4O_9 crystals outnumber the UO_2 by about 3 to 1.

This phase separation is consistent with previously reported data published both in earlier Bettis UO_2 Panel Reports and in the open literature.

TABLE I

Mean Modulus of Rupture of UO_2 Specimens Sintered at 1750°C For 1, 3, 5, & 20 Hours

Test Temperature	Modulus of Rupture (psi)				
	1 Hour	3 Hours	5 Hours	5 Hours (1400°C-1hr calcined)	20 Hours
Room Temperature	14,850 14,800 13,900	12,900	12,000	15,400	12,250
500°C	16,150 12,950	13,200	13,300	14,450	12,250
1000°C	14,500	17,000 13,650	13,550 10,950	16,750	14,200

TABLE 2

Mean Modulus of Rupture of UO_2 Specimens Sintered at 1750°C For One Hour. Tests made at Various Temperatures and With Different Conditions of Surface Finish

Test Temperature	Average Surface Roughness (Microinches)			
	105 (As Fired)**	38 (#400Al_2O_3)**	23 (A0303-1/2)**	11 (Cerium Oxide-Polished Surface)**
Room Temperature	12,500	14,850 14,800 13,900	15,800	14,700
500°C	13,400	16,150 12,950	*	*
1000°C	12,800	14,500	*	*

* Specimens failed spontaneously during heating of the testing apparatus.

** Grinding material used.

TABLE 3

Mean Modulus of Rupture
Measured at Room Temperature -
Standard and Annealed UO_2 Bars

Test Temperature (°C)	Modulus of Rupture (psi)		
	Sample No.	Standard Specimen	Annealed Specimen
Room Temperature	(1)	14,800	16,800
	(2)	13,900	14,400

TABLE 4

Mean Modulus of Rupture of UO_2
Specimens Sintered For Twenty Hours
At 1500°C, 1550°C, 1600°C, and 1750°C

Test Temperature (°C)	Modulus of Rupture (psi)			
Sintering Temp.	1500°C	1550°C	1600°C	1750°C
% Theo. Density	93.7	94.8	95.8	97%
Room Temperature	14,050	15,500	13,200	12,250
500°C		14,200		12,250
1000°C		15,500		14,200

TABLE 5

Young's Modulus Measured at Room Temperature
Of UO_2 Specimens Sintered at 1750°C
Determined By Flexure Method

Specimen No.	Hours Sintered	E ($X10^6$ psi)	Average ($X10^6$ psi)
147	1	28.65	28.15
148	1	27.65	
149	3	29.50	
150	3	29.45	28.65
151	3	27.00	
152	5	30.35	29.78
153	5	29.20	
154	20	30.90	29.75
155*	20	28.60	

* Specimen #155 was measured at Corning Glass Works by a sonic method. Results:

$E = 28.20X10^6$ psi
$\rho = 0.000308$
$V_c = 4332$ in/sec.

TABLE 6

TiO_2 %(wt.)	Binder %(vol)	Firing Conditions Temp.(°C)	Time(hr)	Density % Theor.
0.1	---	1750	1	96
0.1	10	1750	1	92-93
0.1	10	1500	1	93-94

TABLE 7

Sample Description	Cumulative Hours at 335°C	Average Corrosion Rate (inches/year)
Al_2O_3 clad on UO_2 Core	493	0.0043
Al_2O_3 (99+%)	493	.0036
BeO (99.8%)	325	.00039
ThO_2 (99%)	325	.00014
Stabilized ZrO_2 (20M % CaO)	325	.00051
MgO (99%)	Disintegrated in less than 24 hours	
Y_2O_3 (99%)	Disintegrated between 24-160 hours	
Nd_2O_3 (99.9%)	Disintegrated in less than 24 hours	

TABLE 8

Steam Sintered Density of Pellets
Fired 1 Hour at 1500°C

Run No.	Sample No.	Pre-Sintering Atmosphere	Sintering Atmosphere	Post-Sintering Atmosphere	Fired Density (gm/cc)	% Theo. Density (Based on 10.96gm/cc)
32	1	Hydrogen	Steam	Hydrogen	10.50	95.8
26	2	Hydrogen	Hydrogen	Hydrogen	9.78	89.2
32	3	Hydrogen Steam Mixture	Hydrogen Steam Mixture	Hydrogen Steam Mixture	9.84	89.8
32	4	Steam	Steam	Steam	8.77	79.9
46	5	Hydrogen	Steam	Steam	10.67	97.2

TABLE 9

Effect of Ballmilling on Steam-Sintered Density of Mallinckrodt UO_2

Sample	Description	Fired Density (gm/cc)	% Theor. Density (Based on 10.96 gm/cc)
1	Ballmilled for 20 hours	10.34	94.3
2	Ballmilled for 3 hours	10.03	91.6
3	-325 mesh "as-received" Mallinckrodt UO_2	8.21	74.9

TABLE 10

Effect of the Intensity of Hydrogen Soak on Steam-Sintered Density of Pellets Fired 1 Hour

Sample No.	Pre-Sintering Treatment			Sintering Temp. (°C)	Fired Density (gm/cc)	% Theor. Density (Based on 10.96gm/cc)
	Atmosphere	Hold-Time (hours)	Temp. (°C)			
1	8%H_2-92%N_2	4	1000	1500	10.25*	93.5
2	8%H_2-92%N_2	1	1000	1500	9.25*	84.4
3	100% - H_2	0.5	1200	1400	10.18**	92.9
4	100% - H_2	2.0	1200	1400	10.48*	95.7
5	100% - H_2	4.0	1200	1400	10.38**	94.7
6	100% - H_2	0	1400	1500	10.58**	95.8
7	100% - H_2	1	1000	1500	10.43	95.1

* Cooled in steam
** Cooled in hydrogen

TABLE 11

Effect of Hydrogen Pre-Sintering Temperature on Steam-Sintered Density of UO_2

Run No.	Pre-Sintering Time (hrs)	Pre-Sintering Temp. (°C.)	Sintering Time (hrs)	Sintering Temp. (°C.)	Fired Density (gm/cc)	% Theor. Density (Based on 10.96gm/cc)
55	2.0	1200	1	1400	10.42	95.1
62	2.0	1400	1	1400	9.53	86.9
64	2.0	1000	2	1300	10.06	91.8
69	2.0	1200	2	1300	10.32*	94.2

* Sample cooled in steam; accordingly, density is higher in comparison

TABLE 12

Effect of Steam-Sintering Time and Temperature On Fired Density of UO_2 Pellets

Time (hrs.)	Temp. (°C.)	Fired Density (gm/cc)	% Theor. Density (Based on 10.96 gm/cc)
1	1500	10.60	96.6
1	1450	10.57	96.4
1	1400	10.48	95.6
2	1400	10.57	96.4
2	1350	10.54	96.2
1	1300	10.06	91.8
2	1300	10.32	94.2
4	1300	10.60	96.7
8	1200	10.39*	94.8

* Cooled in hydrogen

TABLE 13

Excess Oxygen in Steam-and Hydrogen-Cooled 1400°C Steam-Sintered UO_2

Run No.	Sintering Time	Description	Mols O / Mols U
67-1	1 Hour	Steam sintered powder, cooled in steam	2.202
67-3	4 Hours	Steam sintered pellet, cooled in steam	2.194
68-2	1 Hour	Steam sintered pellet, cooled in steam	2.187
68-3	1 Hour	Steam sintered pellet, cooled in steam	2.183
70-2	1 Hour	Steam sintered pellet, cooled in hydrogen	2.027

TABLE 14

Weight Changes of Steam-Sintered Pellets
Alternately Heated in Hydrogen and in Steam

Steam Sintered Temp.(°C)	Initial Wt. (gm)	Initial Density (gm/cc)	Initial Diam. (in.)	After First Firing in H_2 15 Hours at 1750°C Wt. (gm)	Density (gm/cc)	Diam. (in.)	Wt. Loss (gm.)
1200	5.9142	10.40	0.4388	5.8565	10.52	0.4358	0.0577
1400	5.9561	10.41	0.4382	5.9047	10.40	0.4365	0.0511
1450	5.9102	10.57	0.4365	5.8502	10.52	0.4356	0.0491

Steam Sintered Temp.(°C)	Initial Wt. (gm)	After Re-Firing in Steam 4 Hours at 1400°C Density (gm/cc)	Diam. (in.)	Wt. Gain (gm)	After Re-Firing in H_2 15 Hours at 1750°C Wt. (gm)	Density (gm/cc)	Diam. (in.)	Wt. Loss (gm.)	O/U Ratio
1200	5.9171	10.73	0.4341	0.0606	5.8499	10.52	0.4353	0.0672	*
1400	5.9658	10.62	0.4351	0.0611	5.9035	10.40	0.4364	0.0623	2.012
1450	5.9114	10.76	0.4339	0.0612	5.8496	10.52	0.4354	0.0618	2.007

TABLE 15

Unit Cell Dimensions of The Two Phases Present in 1 Hour, 1400°C in Steam-Sintered, Steam-Cooled UO_2

Sample No.	Description	Unit Cell		O/U Ratio
		UO_2 Phase	U_4O_9 Phase	
1	Steam sintered powder	5.4684	5.4427	2.202
2	MCW UO_2 Powder, "as-received"	5.4684		2.023
3	Steam sintered pellet	5.4684	5.4437	2.194

Figure I

Modulus of Rupture of UO_2 Specimens
Measured at Room Temperature, 500°C, and 1000°C
For 1, 3, 5 & 20 Hour Sintering Times at 1750°C

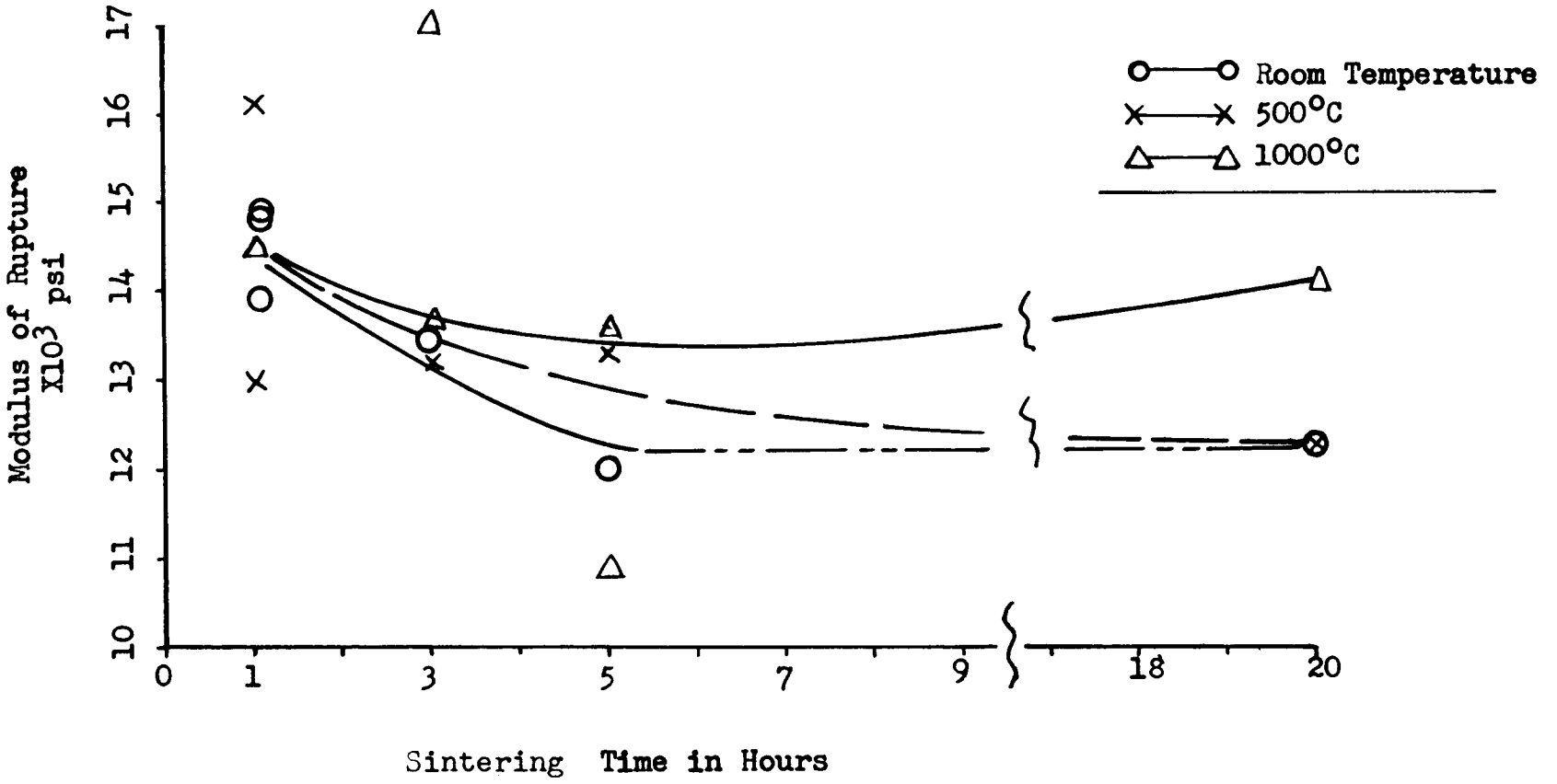

Corning Glass Works
Laboratory
UO_2 Panel Report
September 5, 1956
By: F. I. Peters

Figure II

Curves showing Relation Between
Sintering Temperature and (1)
Mean Modulus of Rupture and (2)
Percent of Theoretical Density.

UO_2 Specimens Sintered for 20 hours
Modulus of Rupture Measured at Room Temperature

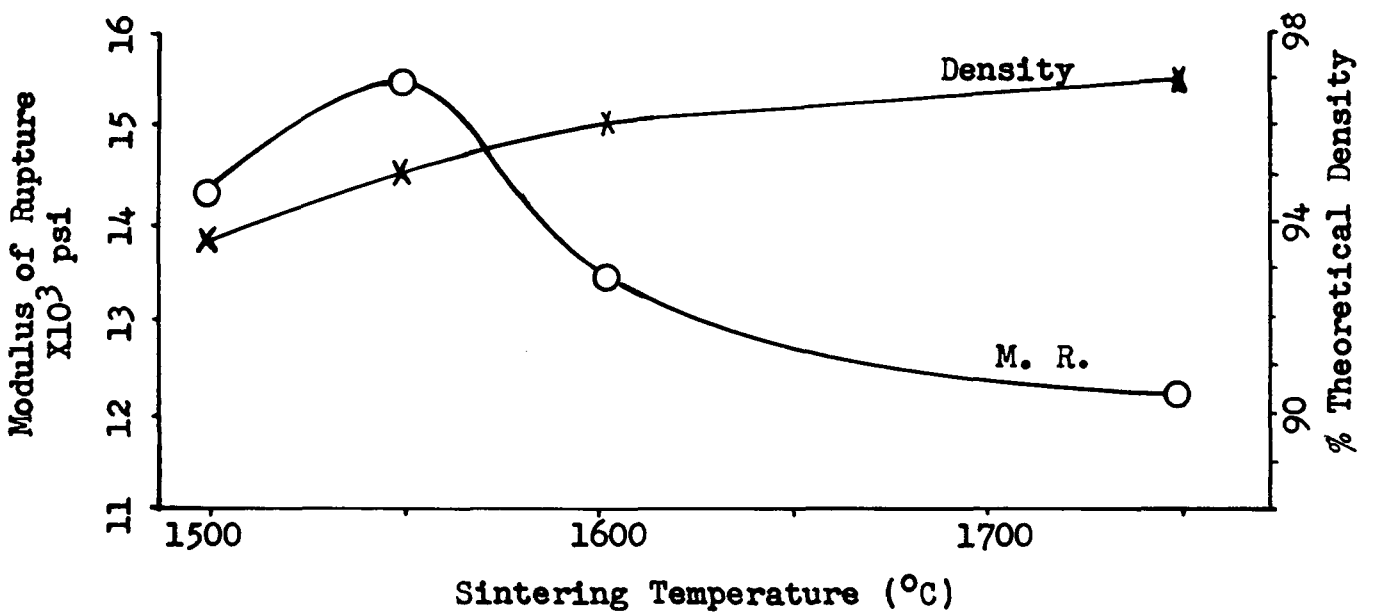

Corning Glass Works Laboratory
UO_2 Panel Report
September 5, 1956
By: F.I. Peters

TEMPERATURE CALCULATIONS FOR UO_2 FIT TOLERANCE EXPERIMENT

BY

W. E. Roake

Pile Metallurgy Unit
Pile Technology Section
ENGINEERING DEPARTMENT

May 9, 1956

General Electric Company
HANFORD ATOMIC PRODUCTS OPERATION
Richland, Washington

Operated for the Atomic Energy Commission by the
General Electric Company under Constract #W-31-109-Eng-52

TEMPERATURE CALCULATIONS FOR UO_2 FIT TOLERANCE EXPERIMENT

INTRODUCTION

Prevailing dimensional tolerances for sintered UO_2 reactor fuel components to be enclosed in metal jackets are expensively small. For instance, the PWR fuel pellet, as of November, 1955, consisted of a centerless ground UO_2 cylinder 0.3560" (+0.0005", -0.0000") in diameter and 0.3527" (±0.0008") long. This pellet was designed to fit in a Zircaloy tube 0.3585" (+0.0005", -0.0000") inside diameter. The use of UO_2 shapes as pressed, or extruded, and sintered with diameter variations controlled to a tolerance of ± 0.003" to ± 0.005" would represent a fabrication cost saving worth considering.

It is reasonable to assume that the annulus between a sintered UO_2 shape and its container will vary as a function of time of irradiation. Shrinkage from the can walls occurs with relatively low density (i.e. 85% of theoretical) sintered pieces by the mechanism of further sintering of the high temperature core during irradiation (cf. MTR Test GEH-4-3C). Contrary to this effect, the thermal expansion coefficient of UO_2 is about twice that of Zircaloy. Of possibly greater significance is the inevitable fracture of dense UO_2 due to thermal stress. Such cracking effectively relocates the annular heat transfer gap to the interior of the oxide where the higher temperatures enhance the heat transfer coefficient. Thus, possibly the worst condition, with respect to heat transfer, is when the gap is maintained at the interface between the UO_2 and the inside wall of the jacket.

Two capsules containing UO_2 with variable gap between oxide and jacket have been prepared in an effort to gain some understanding of the need for close dimensional tolerances. The range of gap is 0.001" to 0.011". These capsules, as sketched in Figure 1, are to be irradiated in the MTR and will be referred to as test GEH-3-19. This document consists of the calculation of expected temperatures and desired irradiation conditions.

OBJECTIVE

The objective of this report is to describe the method and to present the results of the prediction of core temperatures to be reached in sintered UO_2 bodies encased in Zircaloy capsules with variable clearances between UO_2 and jacket.

NOMENCLATURE

A,B,C	Constants
K_a	Coefficient of thermal conductivity of argon.
Q	Power, watts cm^{-2} of can wall surface (neglecting ends).
T_o	Maximum UO_2 core temperature, °Kelvin.
T_1	Surface temperature, UO_2, °Kelvin.
T_2	Surface temperature, inner can wall, °Kelvin.
V	Apparent volume of UO_2.
Z	Weight percent U-235 in total uranium.

a Surface area of can covering UO_2, cm^2.
a_1 Surface area of UO_2, cm^2.
b Radius of UO_2, cm.
d Flux depression.
h_w Water film heat transfer coefficient.
q Power generation or power transmitted, watts. (At steady state all power generated is transmitted.)
r Outer radius of capsule, cm.
δ Fraction of power transmitted by radiation.
ϵ Emissivity.
ϕ_o Unperturbed flux.
ρ Apparent density of UO_2.
χ Annular gap distance, cm.

DISCUSSION OF CALCULATIONS

A. Flux Depression Caused by Introduction of Capsule

The flux depression may be estimated in the manner outlined in HW-35799[1]. In this case it amounts to about 0.02.

B. Power Generation in UO_2

As in reference (1), the power generation in watts per square centimeter of can wall (excluding non-fuel bearing ends) is:

$$Q = \frac{\phi_o V \rho Z \times 4.315 \times 10^{-11}}{(100 - Z)\, a} \qquad (1)$$

or, in this case,

$$Q = 1.815 \times 10^{-12}\, \phi_o\, b^2 \qquad (2)$$

from which the following values were obtained.

TABLE I

POWER GENERATIONS FOR SPECIFIC RADII

	Q		
ϕ_o	b=0.635 cm	0.622 cm	0.610 cm
1×10^{12}	0.73	0.70	0.68
1×10^{13}	7.32	7.02	6.75
3×10^{13}	21.9	21.1	20.3
5×10^{13}	36.6	35.1	33.8
1.48×10^{14}	108.4	104.0	100.

In this case, 108.4 watts cm^{-2} of can surface (excluding ends) is equivalent to 1.375 kw $inch^{-1}$ length of UO_2 fuel rod.

C. Temperature Drop Across Can Wall and Water Annulus*

Calculated in the manner outlined in reference (1), the temperature, T_2, of the inner surface of the can wall is $\Delta T_c + \Delta T_{wf} + T_w$ and is described by:

$$T_2 = 1.6795\ Q + 313,\ ^\circ \text{Kelvin} \tag{3}$$

D. Heat Transfer Across Gap Between UO_2 and Can

It is safe to assume that heat is transferred across the argon-filled gap by radiation and by conduction. Convective transfer in such a small gap is of little consequence.

1. Radiant Heat Transfer

For purposes of this calculation it was assumed that

$$\epsilon_{UO_2} = \epsilon_{Zr} = 0.89 \tag{4}$$

at significant temperatures. A ten percent reduction in ϵ raises the maximum core temperature by 90°C when, for instance, $\chi = 0.011"$ and $Q = 100$.

From reference (2),

$$q = 5.728 \times 10^{-4} \frac{a_1 \epsilon_1}{2-\epsilon_1} \left[\left(\frac{T_1}{100}\right)^4 - \left(\frac{T_2}{100}\right)^4 \right] \text{ watts} \tag{5}$$

substituting equation (3)

$$Q\delta = 3.585 \times 10^{-4} \left[\left(\frac{T_1}{100}\right)^4 - \left(\frac{313 + 1.6795\ Q}{100}\right)^4 \right] \tag{6}$$

2. Conductive Heat Transfer

The thermal conductivity of argon is:

$$K_a = 1.69 \times 10^{-5} + 5.138 \times 10^{-7}\ T \quad \text{Wcm}^{-1}\ ^\circ\text{K}^{-1} \tag{7}$$

then,

$$(1 - \delta) Q \chi = \int_{T_2}^{T_1} K_a dT = \Big|_{T_2}^{T_1} 2.569 \times 10^{-7}\ T^2 + 1.69 \times 10^{-5}\ T \tag{8}$$

*$h_w = 2.273$ watt $cm^{-2}\ ^\circ C^{-1}$
$h_{Zr} = 1.402 \times 10^{-1}$ watt $cm^{-1}\ ^\circ C^{-1}$

Now, since

$$Q = Q\delta + Q(1-\delta),$$

we have, on rearranging,

$$Q\chi = 3.585 \times 10^{-4}\chi \left[\left(\frac{T_1}{100}\right)^4 - \left(\frac{313 + 1.6795\ Q}{100}\right)^4\right] + 2.569 \times 10^{-7}\ T_1^{\,2} + 1.69 \times 10^{-5} T_1 - 7.1947 \times 10^{-7} Q^2 - 2.9741 \times 10^{-4} Q - 3.0458 \times 10^{-2} \qquad (9)$$

or

$$3.585 \times 10^{-12}\chi\ T_1^{\,4} + 2.569 \times 10^{-7} T_1^{\,2} + 1.69 \times 10^{-5}\ T = 2.852 \times 10^{-11} Q^4\chi + 2.127 \times 10^{-8}\ Q^3\chi + (7.1947 + 59.44\chi) \times 10^{-7}\ Q^2 + (2.9741 + 10{,}007\chi) \times 10^{-4}\ Q + 3.4408 \times 10^{-2}\chi + 3.0458 \times 10^{-2} \qquad (10)$$

This neglects, of course, the argon pressure variations, which are not well known. According to data presented by Deissler and Eian[3], the thermal conductivity of argon is constant within the range of pressures and temperatures anticipated in these capsules, thus the neglection is acceptable.

The Q^3 and Q^4 terms in equation (10) may safely be omitted. Values in Table 2 were calculated in this manner. These are plotted in Figure 2. For the curve of $\chi^* = 0.000$ the UO_2-Zr interface heat transfer coefficient was assumed equal to the water film heat transfer coefficient.

TABLE II

HEAT TRANSFER ACROSS ANNULAR GAP

T_1, °K	χ =	Q			
		0.001"	0.003"	0.006"	0.011"
500		1.02(?)	5.2	4.3	1.7
1000		87	34	19	12
1500		207	89	56	39
2000		378	182	122	93
2500		614	328	238	195
3000		881	545	425	365

At UO_2 surface temperatures above 500 K the data from Table II can be empirically described by an equation of the type

$$T_1 = A \log (Q + B) - C \qquad (11)$$

Values for these constants as determined graphically are listed in Table III.

TABLE III

VALUES FOR CONSTANTS OF EQUATION (11)

$T_1 = A \log (Q + B) - C$

X Inches	A	B	C
0.001	3345	200	7247
0.003	2490	65	3953
0.006	2065	30	2489
0.011	1780	18	1641

E. Maximum Core Temperature of UO_2

From the data of Loeb, Kingery, et al[4,5], the maximum UO_2 core temperature can be estimated in the manner outlined in reference (1). The maximum temperature is so described by the equation:

$$T_o = [A \log (Q + B) - C + 77] \left[e^{\frac{rQ}{73.796}}\right] - 77 \qquad (12)$$

from which values plotted in the curves of Figures 3 and 4 have been computed.

F. Irradiation Conditions

A choice of Q = 56.3 watts per square centimeter will, if these calculations are reasonably correct, provide for a maximum core temperature of 2880°C in the area of an annulus of 0.011". This corresponds to the melting point of UO_2. Peak core temperatures at this power level are calculated to be 1408°C and 2662°C for annuli of 0.001" and 0.006", respectively (these reflect high power levels due to larger diameter of fuel).

Total heat generation per capsule is approximately 2.85 kilowatts. For this power level an unpertubed flux 8.32×10^{13} nv is required. One 18-day MTR cycle at this flux should be sufficient for the purpose of this experiment.

WE Roake
by RJK

Pile Metallurgy Unit
Pile Technology Section
ENGINEERING DEPARTMENT

REFERENCES

*(1) Roake, W.E.; "Temperature Calculations for UO_2 Capsule Irradiation Experiment", HW-35799, January 20, 1955 (SECRET).

(2) Perry, J.H.; "Chemical Engineers' Handbook", New York, McGraw-Hill Book Co. Inc., (1950), p. 484.

(3) Deissler, R.G., and Eian, C.S.; "Investigation of Effective Thermal Conductivities of Powders", NACA-RM-E-52 CO 5, June 24, 1952 (UNCLASSIFIED).

(4) Loeb, A.L.; "Thermal Conductivity, VIII, A Theory of Thermal Conductivity Of Porous Materials", NYO-3647, September 20, 1953, (UNCLASSIFIED), p. 2-18.

(5) Kingery, W.D., et. al., "Thermal Conductivity, X, Data For Several Pure Oxide Materials Corrected to Zero Porosity", NYO-3647, September 20, 1953, (UNCLASSIFIED).

* See appendix.

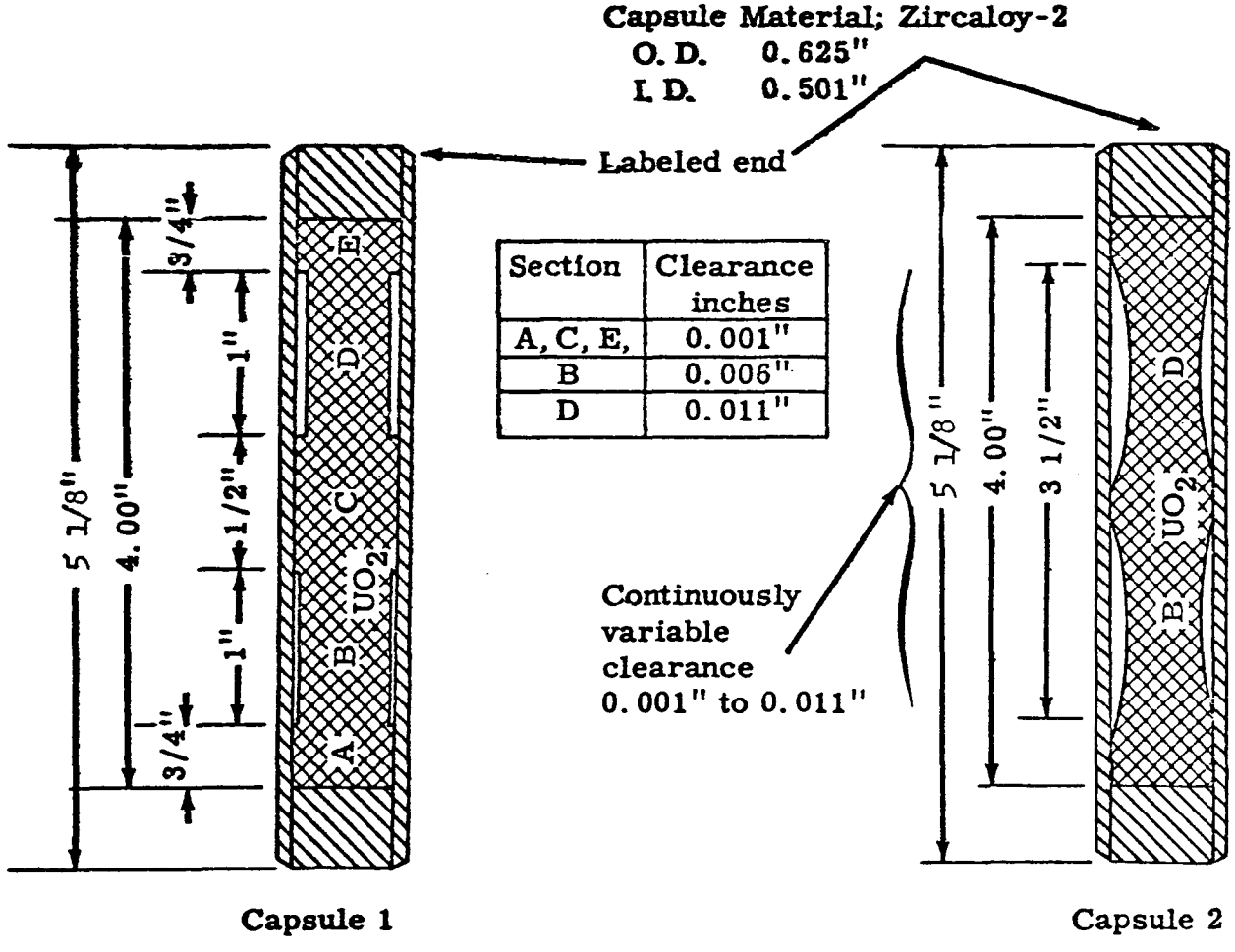

CAPSULES FOR FIT TOLERANCE EXPERIMENT

FIGURE 1

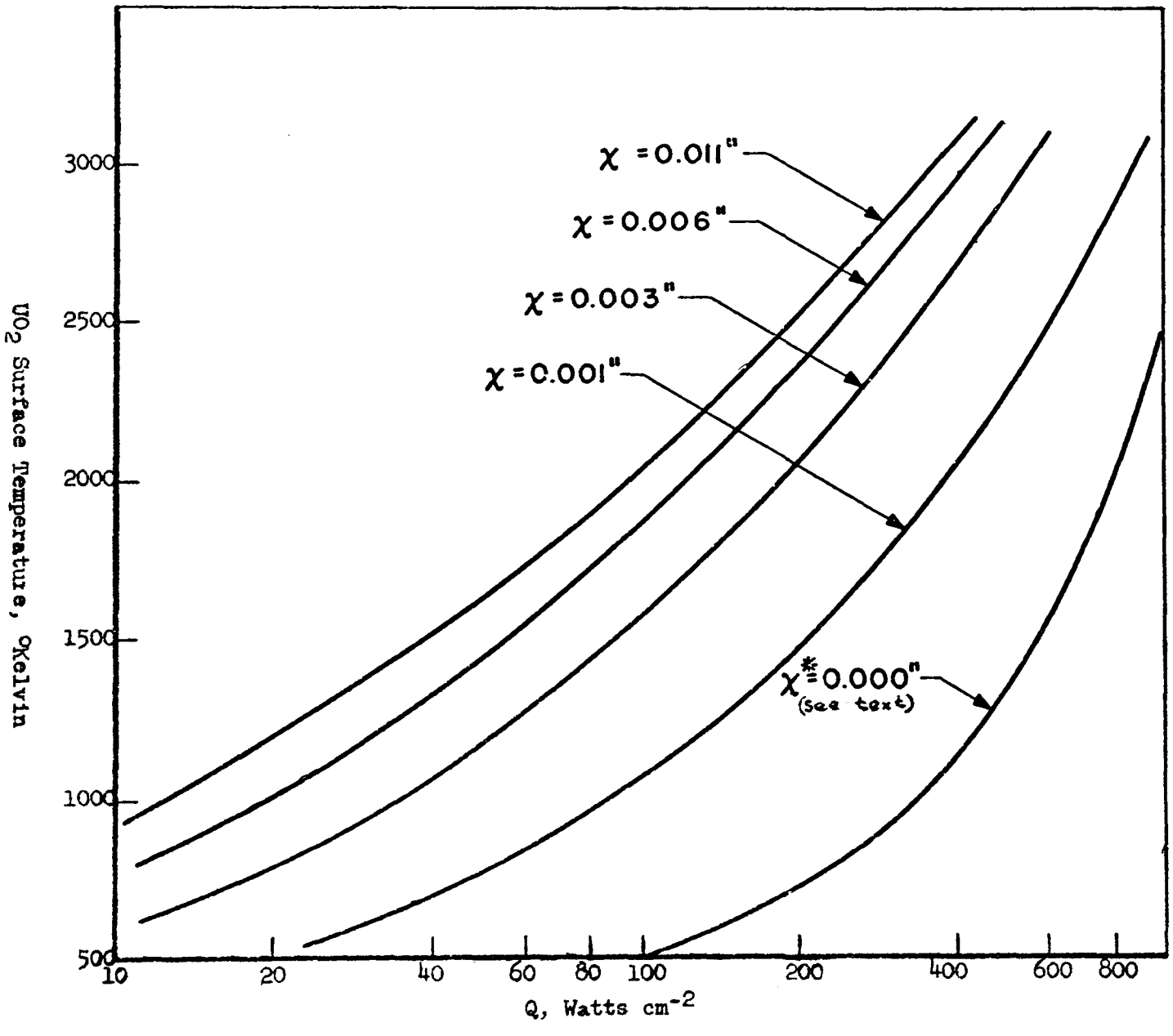

FIGURE 2

Calculated UO_2 Surface Temperature of Test Capsules

FIGURE 3

CALCULATED CORE TEMPERATURES OF TEST CAPSULE

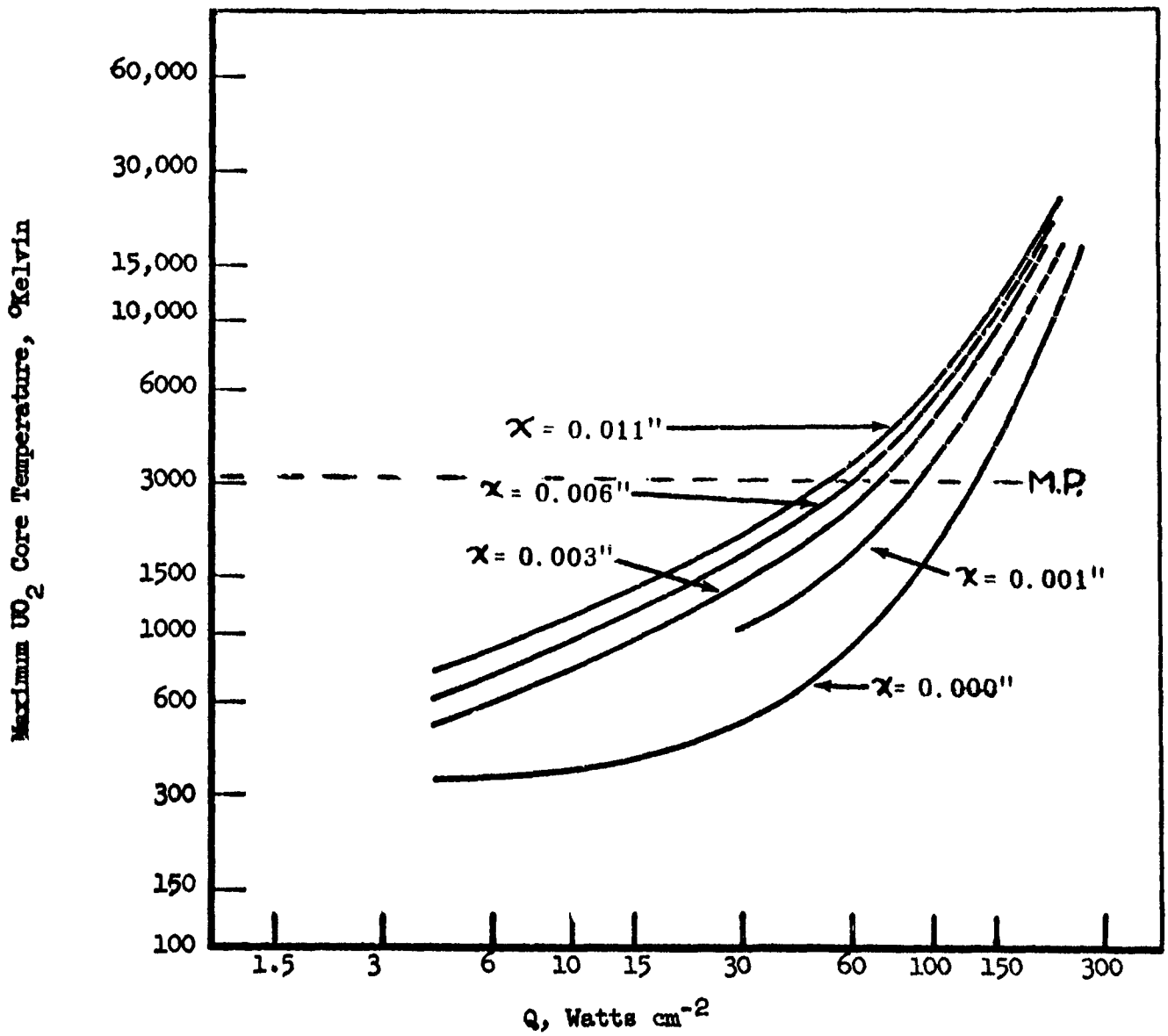

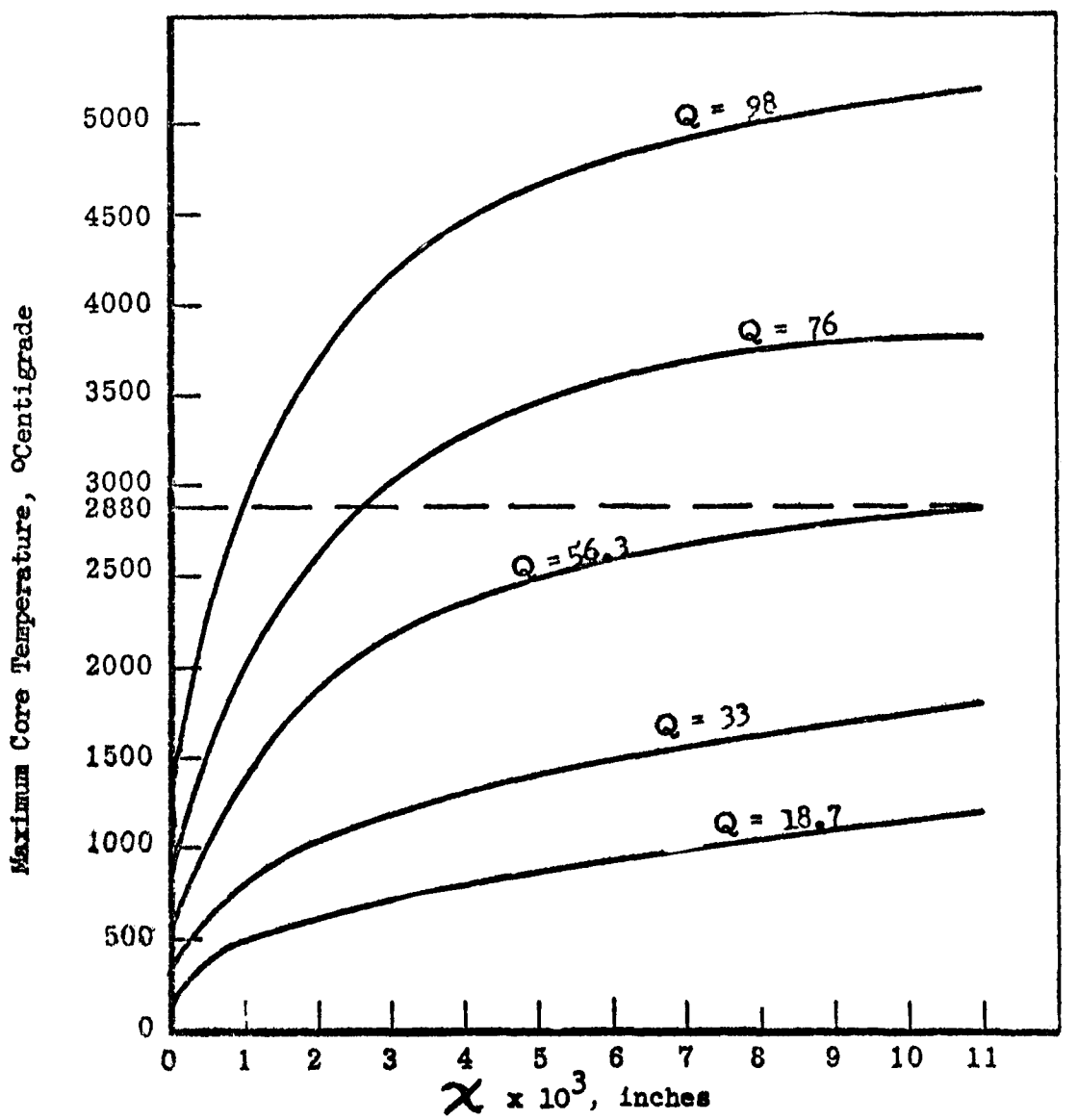

FIGURE 4

Calculated Core Temperature Of Test Capsules
Cross Plot of Figure 3

APPENDIX

A. Flux Depression Caused by Introduction of Capsule

The flux depression, (d), was estimated by simple comparison with the flux depression calculated in a U-Mg matrix slug.

$$\frac{\phi_o - \bar{\phi}\ \text{oxide}}{\phi} = \frac{(\Sigma\ V)\ \text{oxide}}{(\Sigma\ V)\ \text{matrix}} \frac{\phi_o - \bar{\phi}\ \text{matrix}}{\phi}$$

$$d \sim 0.02$$

B. Power Generation in UO_2

$$P \text{ watts} = \frac{\bar{\phi} \Sigma_f V}{3 \times 10^{10}} = \frac{(1-d)\ \phi_o\ N_{25} \bar{\sigma}_f\ V}{3 \times 10^{10}}$$

Since $N_U = N_{UO_2} = \frac{\rho}{M} \times 6.023 \times 10^{23}$

and $N_{28}/N_{25} = \frac{(100-Z)\ (235.1)}{Z \times 238.1}$

and $1-d = 0.98$

then $P = \frac{\phi_o\ V_p\ Z}{100-Z} \times 4.315 \times 10^{-11}$

or, power generation in watts per square centimeter of can wall (excluding non-fuel bearing ends) is:

$$Q = \frac{\phi_o\ V_p \rho Z\ \ 4.315 \times 10^{-11}}{(100-Z)\ a}$$

$$Q = 1.815 \times 10^{-12}\ \phi_o b^2$$

C. Temperature Drop Across Can Wall and Water Annulus

1. Temperature Drop Across Can Wall

$$\Delta T_c = \frac{Qt}{K_{Zr}\ A} = \frac{0.15748}{0.1402}\ Q = 1.2395\ Q$$

APPENDIX

where Q = power, watts per cm^2

t = can wall thickness, cm.

K_{Zr} = Thermal conductivity of Zircaloy

= 1.402×10^{-1} watt cm^{-1} $^oC^{-1}$

2. Temperature Drop Across Water Film

$$\Delta T_{wf} = \frac{q}{A\ h_w} = \frac{Q}{h_w} = 0.43995\ Q$$

where $h_w = 2.273$ watts cm^{-2} $^oC^{-1}$

Q = watts cm^{-2}.

3. Inner Can Wall Surface Temperature, T_2

$$T_2 = \Delta T_c + \Delta T_{wf} + T_w = 1.6795\ Q + 313\ ^oK$$

where T_w = water temperature in ^oK.

E. Maximum Core Temperature of UO_2

Thermal conductivity of UO_2, 85% theoretical density. From Loeb, Kingery, et. a

$$K_s = \frac{110.8 \times 0.85}{t + 350}\ W\ in.^{-1}\ ^oK^{-1}$$

$$= \frac{36.988}{T + 77}\ W\ cm^{-1}\ ^oK^{-1}$$

Since $$\frac{q'\ b^2}{4} = \int_{T_1}^{T_o} \frac{36.988}{T + 77}\ dT$$

where q' = watts generated per cm^3 fuel

b = outer radius of fuel

then, $$\Delta T = (T_1 + 77)\left[e^{\frac{q'\ b^2}{147.95}} - 1\right]$$

or $$T_o = (T_1 + 77)\left[e^{\frac{q' b^2}{147.95}}\right] - 77$$

Since $q' = \frac{2r\,Q}{b^2}$, $Q =$ watts cm^{-2} outer surface of capsule.

then $$T_o = (T_1 + 77)\left[e^{\frac{2r\,Q}{147.95}}\right] - 77$$

but $T_1 = A \log (Q/B) - C$ for fixed values of χ

So $$T_o = \left[A \log (Q + B) - C + 77\right]\left[e^{\frac{rQ}{73.98}}\right] - 77$$

THE MELTING POINT OF URANIUM DIOXIDE[1]

L. G. Wisnyi and S. W. Pijanowski

KNOLLS ATOMIC POWER LABORATORY
Schenectady, New York

In recent years it has become quite apparent that the melting point of uranium dioxide has not been confirmed to any degree in the literature. O. Ruff[2] in 1911 reported 2176°C, while E. Friederich[3] in 1925 placed it between 2500 and 2600°C. A more recent determination in 1953 by W. A. Lambertson[4] fixed the melting point at 2878 ± 22°C. However, in 1955 R. Ackermann[5] observed a much lower melting temperature of 2405°C.

A small tungsten ribbon furnace was constructed for the melting point determinations and proved successful in a hydrogen or helium atmosphere. Temperature was controlled manually and measured with a Leeds and Northrup optical pyrometer. The heating element, which was in the form of a "V", acted as the container and also provided for black body conditions (emissivity $\cong$ .95). The lower emissivity of the material to be melted made it visible at all times below its melting point. At the melting point the sample, being liquid, would appear to have vanished and the temperature of the ribbon at the apex of the "V" was recorded as the apparent melting point.

As a result of six successful determinations the melting point of uranium dioxide (as obtained from Mallinckrodt) was noted to fall between 2710°C as a minimum and 2790°C as a maximum. All readings were compensated for the window absorption and the optical pyrometer calibration. The latter correction is relative to the melting point of pure Al_2O_3, which is accepted by the authors as a secondary standard at 2040°C[6] (National Bureau of Standards reports 2049 ± 2°C[7].

In summary, the average figure of 2750°C is considered to be the melting temperature of uranium dioxide.

Effort is continuing in order to establish the exact oxygen content of the melted uranium dioxide, and to narrow the observed 80 degree spread. Results will be reported in a later resume.

---

*Operated by the General Electric Company for the United States Atomic Energy Commission.

References

(1) KAPL-1564, "Metallurgy Report of the Technical Department", March, April, May, 1956, p. 19.

(2) O. Ruff and O. Goeche, "Uber das Schmelzen und Verdampfen unserer sogenannten hoch feuerfesten Steff", Angem Chem., 24, 1459-61 (1911).

(3) E. Friederich and L. Sittig, "Lower Oxides of High Melting Point", anorg. u allgem. chem. 145, 127-40 (1925).

(4) W. A. Lambertson and M. H. Mueller, "Uranium oxide phase equilibrium systems II, UO_2 - MgO", J. Am. Ceram. Soc. 36, 332 (1953).

(5) R. Ackermann, ANL-5482. "The High Temperature, High Vacuum Vaporization and Thermodynamic Properties of Uranium Dioxide", 1955, p. 100.

(6) A. S. Russell, "Alumina Properties", Aluminum Company of America, 1953, p. 10.

(7) S. M. Lang, F. P. Knudsen, C. L. Fillmore, and R. S. Roth, "High Temperature Reactions of Uranium Dioxide with Various Metal Oxides", NBS Circular 568, 1956, p. 28.

SUMMARY REPORT OF UO_2 PROGRAM AT MALLINCKRODT CHEMICAL WORKS FOR SEPTEMBER 28, 1956

This report covers the activities at MCW on the UO_2 program from June 1, to September 1, 1956. In particular, it presents information concerned with investigations of various methods of preparing UO_2 powders utilizing existing MCW materials and processes. In addition, in keeping with the request made of panel members at the June 19, 1956 meeting to think of possible new and improved materials for core II, a description of a Flame Fusion fuel element fabrication technique is presented.

Powder Preparation and Evaluation Studies:

During the past three months various methods of preparing UO_2 powders were examined and the UO_2 powders made by each method were evaluated for possible effects on the density of fuel element pellets made by the Bettis Field process. As enumerated below the method of preparing UO_2 powders for evaluation varied from simple milling operations on normal MCW UO_2 to variations in the manner in which uranyl nitrate solutions are converted to UO_3. Uranium dioxide powders were made as follows:

1. Vacuum denitration of uranyl nitrate to yield popcorn like UO_3 which is then reduced to fine particle UO_2.

2. Milling of normal MCW UO_3 with water and uranium rods in a rubber lined mill to produce a hydrated UO_3 that upon reduction yields a fine particle UO_2.

3. Dry milling of normal MCW UO_3 with tungsten carbide balls in a rubber lined jar mill followed by stirring in cold water to hydrate prior to reduction to UO_2.

4. Micronizing of normal MCW UO_3 using air as the hydraulic fluid followed by reduction to UO_2.

5. Reduction of normal Port Hope UO_3 to UO_2.

6. Milling of normal MCW UO_2 for various periods in water using uranium rods and rubber lined jar mills.

7. Micronizing normal MCW UO_2 using air as the hydraulic fluid.

8. Normal MCW UO_2 as supplied to WAPD for core I.

Comparisons of the densities obtained with pellets pressed at 63 TSI from the UO_2 powders prepared by the above methods are shown in Table I and Table II.

Table I

COMPARISON OF PELLET DENSITIES OBTAINED WITH VARIOUS TYPES OF UO_2

UO_2 History	ρ_G,%	ρ_F,%	$\Delta\rho$,%
1. Produced from vacuum denitrated uranyl nitrate	54.9	89.4 (a)	34.5
2. Produced from UO_3 hydrated by milling with water for 28 hours using uranium balls and a rubber lined jar	53.3	85.2	31.9
3. Produced from UO_3 which was milled dry with tungsten carbide balls in a rubber lined jar and then hydrated by stirring in cold water.	55.2	86.4	31.2
4. Produced from micronized UO_3.	56.5	85.9 (a)	29.4
5. Produced from Port Hope UO_3.	55.7	83.6	27.9
6a. Normal MCW UO_2 milled with water for 2 hours using uranium balls and a rubber lined jar.	59.7	77.5	17.8
6b. Same as 6a except the UO_2 was milled for 12 hours.	59.5	77.5	18.0
6c. Same as 6a except the UO_2 was milled for 48 hours.	58.7	78.9	20.2
7. Micronized normal MCW UO_2.	55.8	83.8	28.0
8. Normal MCW UO_2 (control)	59.6	77.6 (a)	18.0

ρ_G = green density
ρ_F = fired density - 1400°C for 2 hrs. in H_2, air and steam.
$\Delta\rho$ = fired density - green density = pellet densification, percent of the theoretical density of UO_2.
(a) = fired in H_2 and steam

Table II

COMPARISON OF PELLET DENSITIES OBTAINED WITH UO_2 POWDERS MILLED FOR VARIOUS TIMES WITH URANIUM BALLS IN A RUBBER LINED JAR MILL.

Hours Milled	ρ_G,%	ρ_F,%	$\Delta\rho$,%
2	58.4	75.9	17.5
4	57.6	75.5	17.9
8	59.1	77.5	18.5

Table II (continued)

COMPARISON OF PELLET DENSITIES OBTAINED WITH UO_2 POWDERS MILLED FOR VARIOUS TIMES WITH URANIUM BALLS IN A RUBBER LINED JAR MILL.

Hours Milled	ρ_G,%	ρ_F,%	$\Delta\rho$,%
12	59.1	77.2	18.2
16	58.2	76.4	18.2
20	58.5	76.7	18.3
24	58.1	77.8	19.8
48	59.1	78.5	19.4
72	58.6	77.9	19.3
96	58.9	77.1	18.2

The highest fired pellet density, as shown in Table I, was obtained with the UO_2 made from vacuum denitrated uranyl nitrate. Substantial increases in pellet densities were obtained with all specially processed UO_2 powders as compared with pellets of normal MCW UO_2, except in the cases for both dry and wet milled normal MCW UO_2.

As shown in Table II, the optimum milling time for increasing the pellet density was 48 hours. This conclusion was confirmed by the excellent work of Mr. T. J. Burke of WAPD, Bettis Field where he conducted a careful separate study of the effect of dry ball milling in rubber lined mills on the density of pellets made from MCW UO_2. Mr. Burke's data also indicated that 48 hour milled UO_2 fired at 1725°C for 5 hours would produce pellets of approximately the same density as obtained with a 10 hour firing cycle. This reduction in firing time could more than compensate for increased costs due to milling.

Analytical results on carbon contamination indicate that the use of virgin mills lined with neoprene or tygon raises the carbon values to over 500 ppm. However, continued use of the mills lowers carbon contamination to about 50 ppm. It has been noted that powders milled in tygon lined mills do not press as well as those milled in neoprene lined mills.

Microscopic examination at 600X showed that the UO_2 made from vacuum denitrated uranyl nitrate consisted of irregular shaped platelets with rather sharp edges. In general, the average particle size of the UO_2 powders was decreased considerably by milling for long periods of time. Milling of UO_3 with water and micronizing of either UO_3 or UO_2 also produced UO_2 powders of very small average particle size. A preliminary microscopic examination of the micronized powders indicated that a considerable portion of this product would consist of irregular submicron particles.

Other approaches to obtain greater pellet densification included the use of various types of furnace atmospheres during sintering and the use of an additive to the UO_2 powder. A comparison of the influence of titania, steam, and air on pellet densification for different milling times is presented in Table III.

Table III

PELLET DENSIFICATION AS A FUNCTION OF FURNACE ATMOSPHERES AND TITANIA - FIRED AT 1400°C FOR TWO HOURS

Furnace Conditions Hours Milled	Pellet Densification, Percent of Theoretical			
	T + H	S + H	T + S + H	A + S + H
0	12.7	18.0	19.1	19.6
4	12.4	17.9	19.1	19.7
24	14.3	19.8	20.6	23.0
96	14.9	18.2	19.2	19.5

T = 0.2 w/o Titania added
S = Steam
H = Hydrogen
A = Air

The most effective treatment of those tested was the use of air, steam, and hydrogen. The addition of titania apparently increased the densification by about 1% when steam and hydrogen were used but no results are available for the case when titania was used with air, steam and hydrogen.

It is expected that better evaluation of UO_2 powders will be possible in the near future at MCW as the installation of pellet fabrication and testing facilities is nearing completion. Meanwhile, our efforts continue in the direction of learning more about how we might produce UO_2 powders of improved pressing and sintering characteristics for the production of UO_2 fuel elements of maximum density.

Flame Fusion Studies:

A flame fusion technique, similar to the Verneuil process for making monocrystalline highly refractory corundums and spinels, is being investigated as a means for minimizing sintering difficulties with presently available powders and for producing fuel elements of maximum density. Possible advantages of the flame fusion method over current fabricating techniques are:

1. Complete or partial fusion of UO_2 may be accomplished to yield polycrystalline or the ultimate-monocrystalline fuel elements as desired.

2. Elimination of pellet or fuel element forming operations such as compacting, extruding or casting is expected. Flame fusion requires only high temperature flames for the production of dense fuel elements.

3. The growth of long (several inches) one piece UO_2 fuel elements ranging from 1/8 inch to an inch or more in diameter may be achieved.

4. Flame fusion is adaptable to the production of normal or highly enriched UO_2 fuel elements. The addition of refractory additives such as Al_2O_3, ThO_2, BeO, SiO_2, and other high temperature materials to UO_2 may be readily accomplished.

Initial experiments using a hydrogen-arc as the heat source were encouraging in that several small buttons of fused UO_2 were produced. These experiments indicated that:

1. UO_2 behaves much like corundum under flame fusion conditions and should be fuseable on a continuous basis into long UO_2 rods.

2. Granules (50μ - 150μ) of dense appearing UO_2 can be grown from normal (72% through 325 screen) MCW powder.

Further experiments using a methane-hydrogen-oxygen flame in a special burner resulted in the growth of a tapered polycrystalline triangular cross section boule of UO_2 measuring roughly 1 inch high by about 1/2 inch along each side. The temperatures obtained with the CH_4-H_2-O_2 flames were judged to be 100-200°C lower than that required for good fusion growth conditions.

An X-ray diffraction examination of a representative specimen of the initial black boule produced with the CH_4-H_2-O_2 flame showed that the boule consisted of high purity UO_2. Microscopic examination of the boule indicated that densities of 100% of theoretical were obtained where the surface of the boule appeared to have been fused. This most dense material was found to extend from the fused surface into the interior of the boule for about 1/4 inch. The microscopic examination also revealed that the individual crystals of UO_2 varied from about 10μ to 300μ, with the largest crystals found near the fused side.

It is anticipated that the experience gained with these experimental flame fusion units will permit design of a flame fusion unit capable of producing fused fuel elements of interesting and desirable physical and chemicals properties.

Submitted By

B. M. Henderson

Contribution for the

UO_2 PANEL SPONSORED BY W.A.P.D.

for September 28, 1956

S. M. Lang

NATIONAL BUREAU OF STANDARDS

Not approved for publication in other than Resume' VII of the WAPD UO_2 Panel

A. PHYSICAL PROPERTY DATA

Some data have been developed during a classified study, sponsored by WADC, that is concerned with gaining an understanding of the oxidation and volatilization of UO_2 through a study of the thermodynamics and kinetics of the reactions. Of interest, also, to this panel are data that have been determined for some reactions of UO_2 with other oxides.

1. Phase Relations:

Some ten binary systems, containing UO_2 as one component, are being studied to determine and identify the nature of the reactions that might occur. In each of the systems, the 20-, 40-, 60-, and 80-mole percent UO_2 mixtures were prepared and heat-treated in tungsten crucibles at temperatures from 1300° to 2100°C in a helium or argon atmosphere. The systems are:

$BaO-UO_2$	$Cr_2O_3-UO_2$
$CaO-UO_2$	$Fe_2O_3-UO_2$
CeO_2-UO_2	$Nb_2O_5-UO_2$
$SrO-UO_2$	TiO_2-UO_2
$Y_2O_3-UO_2$	$ZnO-UO_2$

All of the proposed heat treatments for the ten systems under investigation have been completed. In order to expedite those heatings, the systems were divided into two groups according to their anticipated minimum melting points: the low-temperature systems--those containing Cr_2O_3, Fe_2O_3, Nb_2O_5, TiO_2, and ZrO; and the high-temperature systems--those containing BeO, CaO, CeO_2, SrO, and Y_2O_3.

The samples of each system in each of these groups were heated simultaneously. For the low-temperature group, the heat treatments began at 1300°C; for the high-temperature groups they began at 1600°C. All were heated for one hour at 100° temperature intervals. Mixtures were eliminated from successive heatings if they showed signs of melting or volatilization (more than 1% weight loss). In general, the $Cr_2O_3-UO_2$ mixtures were heated separately, especially at the higher temperatures.

$Fe_2O_3-UO_2$: The maximum temperature attained prior to bloating and development of vesicular structure was 1300°C for the $2Fe_2O_3:3UO_2$ and $Fe_2O_3:4UO_2$ mole ratio mixtures. All showed an unknown phase in addition to UO_2, except the $Fe_2O_3:4UO_2$ mixture that showed $UO_{2.2}$ in addition to UO_2.

Nb_2O_5-UO_2: The maximum temperature attained prior to melting or deforming was 1300°C for the $2Nb_2O_5:3UO_2$ and $Nb_2O_5:4UO_2$ mole ratio mixtures. All showed UO_2 plus one or two unknown phases, except mixture $4Nb_2O_5:UO_2$ that showed only two unknown phases similar to the unknown phases present in the others.

TiO_2-UO_2: The maximum temperature attained prior to melting was 1500°C for all compositions. All showed UO_2, TiO_2, and an unknown compound in amounts varying with composition, except mixture $TiO_2:4UO_2$ that showed no free TiO_2.

ZnO-UO_2: The maximum temperature attained prior to melting or indications of reaction with the tungsten crucible was 1500°C for the $ZnO:4UO_2$, and $2ZnO:3UO_2$ mole ratio mixtures. All showed UO_2 plus an unknown phase (not necessarily the same for each composition), except mixture $4ZnO:UO_2$ that showed only UO_2, and mixture $3ZnO:2UO_2$ that showed $UO_{2.2}$ and an unknown phase.

Cr_2O_3-UO_2: The maximum temperature attained prior to melting or excessive weight loss was 1800°C for the $Cr_2O_3:4UO_2$, $3Cr_2O_3:2UO_2$, and $4Cr_2O_3:UO_2$ mole ratio mixtures.

BaO-UO_2: The maximum temperature obtained without excessive weight loss or volume distortion was 1900°C for the $BaO:4UO_2$, $2BaO:3UO_2$, and $3BaO:2UO_2$ mole ratio mixtures. Some showed weight gains up to 1.2% at lower temperatures.

CaO-UO_2: The maximum temperature attained without excessive weight loss was 1900°C for the $2CaO:3UO_2$ and, probably, the $CaO:4UO_2$ mole ratio mixtures. Some showed weight gains as high as 0.6% at lower temperatures.

SrO-UO_2: The maximum temperature attained prior to melting or excessive weight loss was 2000°C for the $SrO:4UO_2$ mole ratio mixture. Some showed weight gains as high as 3.6% at lower temperatures.

CeO_2-UO_2: The maximum temperature attained without excessive weight loss or rea ction with the tungsten crucible was 2100°C for the $CeO_2:4UO_2$ and $2CeO_2:3UO_2$ mole ratio mixtures.

Y_2O_3-UO_2: The maximum temperature attained with no weight loss in excess of 1% above that sustained at the lower temperatures was 2100°C for all compositions. The initial weight loss increased with increasing Y_2O_3 content for all mixtures.

2. Thermodynamic Vapor-Pressure Data:

One of the problems of the research project is to determine the equilibrium vapor pressures at various temperatures for uranium oxides containing varying amounts of oxygen. A low-temperature tensimeter, similar to that described by Hoekstra and Katz (Jour. Amer. Chem. Soc., 74, 1683 (1952)), is being used for this study. There is under construction a very high-temperature Knudsen cell apparatus for the same type of measurements, and a few modifications of the tensimeter. During the last panel meeting, there was some discussion of the theory and procedure that is used with the tensimeter. These points are reviewed in this report.

There are two situations in which the tensimeter is used: (1) when solid phases are heated or cooled with an excess of oxygen for the purpose of changing their compositions, and (2) when solid phases are heated or cooled in static vacuum (no pumping) for the purpose of determining their equilibrium vapor pressures at various temperatures. In the former case, corrections must be applied to the observed pressures, because of the expansion or contraction of the excess oxygen as the reaction vessel is heated or cooled, when the manometer system is maintained at room temperature. These corrections are functions of initial oxygen pressure (amount of excess oxygen), the temperature of the reaction vessel, and any variations in room temperature. In the second case, determination of the equilibrium vapor pressures, no corrections are applied, providing that there is a sufficient number of solid phases for the system as a whole to be in univariant equilibrium.

It might appear that corrections would be necessary in any case, because of the large thermal gradient between the reaction vessel in the furnace and the manometers at room temperature. That these corrections are not necessary in the case when equilibrium measurements are made is shown by the following. Consider reactions of the type:

Higher oxide = lower oxide + oxygen ..... (1)

This is a two-component system; that is, any two of the three materials define the system. There are, however, three phases present. Applying the equilibrium phase rule, not the "condensed" phase rule, only one degree of freedom exists. This is described by saying that the system is "univariant", and it means that, when a given temperature is selected, the value of the pressure is uniquely determined. Practically speaking, this means that, as long as two solid phases are present, the equilibrium pressure cannot be changed. Any

attempt to do so, for example by heating or cooling parts of the apparatus, or even changing the volume (assuming now a definite temperature of the solid phases), would cause the solid phases to so change their proportions as to just offset the attempt to change the pressure. At univariant equilibrium, then, the pressure is a single-valued function of the temperature.

Referring again to equation (1), consider the special case where the higher oxide forms a solid solution with the lower oxide. There is still the same number of components required to define the system, but now the number of phases has been reduced by one, since a solid solution, like all solutions, is a single homogeneous phase. The phase rule shows that there are now two degrees of freedom. This is called a "bivariant" system and means that, at a given temperature, the pressure is not uniquely determined, for it now depends not only on the temperature but also on the composition of the solid solution. Thus, if one uses any equation in a bivariant situation that assumes that vapor pressure is a function of temperature only, the results will not be meaningful.

Consider the information that is obtained when an oxide is heated or cooled with a large excess of oxygen. This situation may be represented by the following equation:

higher oxide + excess oxygen $\longrightarrow$
lower oxide + oxygen + oxygen excess ..... (2)

The system in this case is no longer one of two components, for it is apparent that the excess oxygen, though it does not increase the number of phases, constitutes an extra component. It is as though an inert gas were added to the system; the solid phases cannot adjust their proportions to affect its pressure, and the observed pressure is no longer a function of temperature only. It depends also on the amount of excess oxygen, that will behave according to its own properties (coefficient of thermal expansion, etc.) as the system is heated or cooled. It is apparent then that, if the amount of oxygen entering or leaving the solid phases is to be determined in such situations, the observed pressures must be corrected for variations in the pressure of the excess oxygen with temperature. This is so because the observed pressure is the sum of the pressures of the oxygen involved in the reaction and the excess oxygen. That is, the amount of excess oxygen initially present must be known in terms of pressure, and by calibration experiments it must be determined how this pressure varies with initial amount, temperature, and variations

in room temperature. Corrected back to a standard room-temperature pressure, this corrected pressure can be subtracted from the observed pressure. Only then will the pressure of the oxygen involved in the reaction be known.

From the known pressure of oxygen involved in a reaction of this type and the known volume of the tensimeter, the amount of oxygen involved in the reaction can be calculated. This is done by assuming the validity of the ideal gas law,

$$PV = \frac{w}{NW} RT \quad \ldots\ldots\ldots\ldots\ldots\ldots\ldots\ldots\ldots\ldots \quad (3)$$

Because everything is known but w, the amount of oxygen involved in the process is readily determined. From this and the known starting weight of the solid phases, the change in composition of the solid phases can be calculated from the vapor-pressure measurements. The criterion of equilibrium was arbitrarily set as constancy of observed pressure for a period of one hour.

In treating the vapor-pressure data obtained, simple charts of pressure vs temperature would be useful. However, the thermodynamic constants could not be obtained. It is then necessary to treat the data so that it will permit the calculation of such constants.

At equilibrium, the free energies of all the phases in a system are mutually equal. This may be indicated as

$$dF_1 = dF_2 = \ldots\ldots\ldots dF_n \quad \ldots\ldots\ldots\ldots\ldots\ldots\ldots\ldots \quad (4)$$

The free energy of any given phase, for example dF_1 in the equation above for phase 1, may be defined as

$$dF_1 = dE_1 + d(P_1V_1) - d(T_1S_1) \quad \ldots\ldots\ldots\ldots\ldots\ldots \quad (5)$$

Since E + PV is defined to be ΔH, the heat content, this equation also gives the relationships among the various thermodynamic properties, F, H, E, and S. By substituting equation (5) into equation (4), imposing conditions corresponding to unvariant equilibrium, and with suitable manipulation, the Clapeyron equation may be deduced:

$$\frac{d \ln p}{d\left(\frac{1}{T}\right)} = -\frac{\Delta H}{R} \quad \ldots\ldots\ldots\ldots\ldots\ldots\ldots\ldots\ldots \quad (6)$$

where R is the gas constant in calories per degree per mole and ΔH is the change in heat content of the system, which is the heat adsorbed or evolved in the process being considered.

The property ΔH is itself temperature dependent, varying with the change in the heat capacities of products and reactants. This is indicated by the Kirchhoff equation

$$\left[\frac{d(\Delta H)}{dT}\right]_P = \Delta C_p \quad \ldots\ldots\ldots\ldots\ldots\ldots\ldots\ldots (7)$$

where ΔC_p is the change in heat capacities at a particular pressure. This variation in the value of ΔH for the type of process being investigated and in contrast to the heat content values of elements, is very slight and, therefore, is generally neglected. Then, the term $-\Delta H/R$ of equation (6) can be treated as a constant. Thus, equation (6) states that the equilibrium pressure is a function of the temperature only, so it can only be applied where that is true, namely, at univariant equilibrium. It is also apparent that equation (6) is of the form

$$y = mx \quad \ldots\ldots\ldots\ldots\ldots\ldots\ldots\ldots\ldots\ldots\ldots\ldots (8)$$

which is the equation of a straight line whose slope is m, corresponding in this case to $-\Delta H/R$. That is to say, if ln p is plotted against 1/T, a straight line is obtained whose slope is $-\Delta H/R$, from which the value of ΔH may be calculated.

Knowing ΔH and remembering that $H = E + PV$, equation (5) may be rewritten in Δ form

$$\Delta F = \Delta H - T\Delta S \quad \ldots\ldots\ldots\ldots\ldots\ldots\ldots\ldots (9)$$

and it is apparent that, if ΔF could be deduced, ΔS would be determined and all the thermodynamic constants would be known. The standard free energy change, ΔF°, of these processes may be calculated from the relationship

$$\Delta F^\circ_T = -RT \text{ in } K = - RT \ln P_{O_2} \quad \ldots\ldots\ldots\ldots\ldots\ldots (10)$$

where R is the gas constant in calories per degree absolute per mole, T is the temperature in degrees absolute, and K is the equilibrium constant for the process, being numerically equal to the vapor pressure in the particular cases of the vacuum decomposition of UO_{2+x} and vacuum desorption of adsorbate on oxides.

From the known values of ΔH and the calculated values of ΔF°, the corresponding entropy change, ΔS, can be obtained from the relationship

$$\Delta F^\circ_T = \Delta H - T\Delta S^\circ \quad \ldots\ldots\ldots\ldots\ldots\ldots\ldots\ldots (11)$$

for any given temperature. This, then, is the treatment of the data that will relate the equilibrium vapor pressure-temperature data to the thermodynamic constants.

There is an obvious practical value of plotting the data according to the Clapeyron equation (ln P versus 1/T). When a straight line is obtained, unvariant equilibrium conditions exist and the number of phases present can be deduced. Moreover, a straight line may easily be extrapolated, so that from vapor-pressure measurements at lower temperatures, estimates can be made of the vapor pressures at higher temperatures, without measuring them. This extrapolation must be done carefully, for over a large temperature range the variation of ΔH with temperature causes a departure from a straight line and, more important, the value of ΔH pertains to a particular process and an unwarranted extrapolation can be made to a temperature where another process is occurring. This, unfortunately, is the case with UO_{2+x}. Its decomposition under 1000°C yields a linear portion on a ln P versus 1/T graph. The corresponding ΔH value refers to the process

$$UO_{2+x} \longrightarrow UO_2 + x/2\ O_2 \quad \ldots\ldots\ldots\ldots\ldots\ldots\ldots\ldots\ (12)$$

If extrapolated to 2000°C, where the primary process is the congruent vaporization of UO_2, the results would be meaningless.

Because vapor pressures are being measured, the systems are not condensed ("condensed" means only solids and liquids, or investigations carried out at a constant, usually atmospheric, pressure). Hence, for a binary system, the true representation of the phase equilibria would be a space model, with one axis for pressure, one for temperature, and one for composition. The effort involved to complete a study of such a system may be appreciated from the fact that it has never been done for any system.

From a series of determinations of equilibrium pressures at various temperatures for a series of initial compositions, the data may be so arranged as to yield P-T, P-X, and T-X planes in the total P-T-X diagram. Additional data are being gathered for the system UO_{2+x}-O_2, because of its importance, that will permit the construction of a few such planes.

In these determinations, only one initial composition has been used. At increasing temperature, then, both pressure and composition of the condensed phases changes (the total composition remains constant, because the work is done in a closed system). Thus, the pressure-temperature relationship, if plotted simply as pressure versus temperature, would

twist in space. For the ln P versus 1/T graphs, the variation in composition of the condensed phases is irrelevant, for pressure depends only on the temperature for a given total composition. In the case where composition is plotted against temperature, for UO_{2+x}, it may be considered that the line that twisted in P-T-X space has been projected on any arbitrary pressure plane (moving the projection plane does not change the shape of the projection). Such a graph is not an "isobar", strictly speaking. It would be properly described as "a projection of X versus T for values of P between two limits, on an arbitrary P-plane".

(a) The system UO_{2+x}:

Three samples of UO_{2+x} were heated in static vacuum in the temperature range 25° to 1000°C. These samples were:

A. $UO_{2.03}$, Norton fused material;

B. $UO_{2.16}$, NH_3 precipitated (ORNL); and,

C. UO_{2+x}, Mallinckrodt, 88.0% U (WAPD).

Equilibrium vapor-pressure measurements were made at approximately 100°C temperature intervals. The data were plotted according to the Clapeyron equation and are presented in Figure 1. From these, the following deductions were made:

(1) The initial vacuum decomposition of each UO_2 material is bivariant, indicating the formation of a solid solution between the original UO_{2+x} and its solid decomposition product.

(2) At a temperature between 200° and 500°C, depending on the initial composition, the UO_{2+x} solid solution splits into two solid phases, α and β UO_2 (Ackerman, ANL-5482, Sept. 14, 1955). This is indicated in Figure 1 by the linear portion of the log p versus 1/T plot.

(3) When the temperature was maintained constant for 15 hours at 1000°C for samples B and C, the observed pressure of oxygen increased, as indicated by points D and E of Figure 1. This indicates that true equilibrium was not attained, or that a new process had begun.

(4) The ΔH values corresponding to the decomposition in the two solid-phase regions were calculated from the slopes of the lines in Figure 1. These values and those for ΔF and ΔS are listed in Table 1.

Figure 1
Vacuum Heating of Various Uranium Dioxides

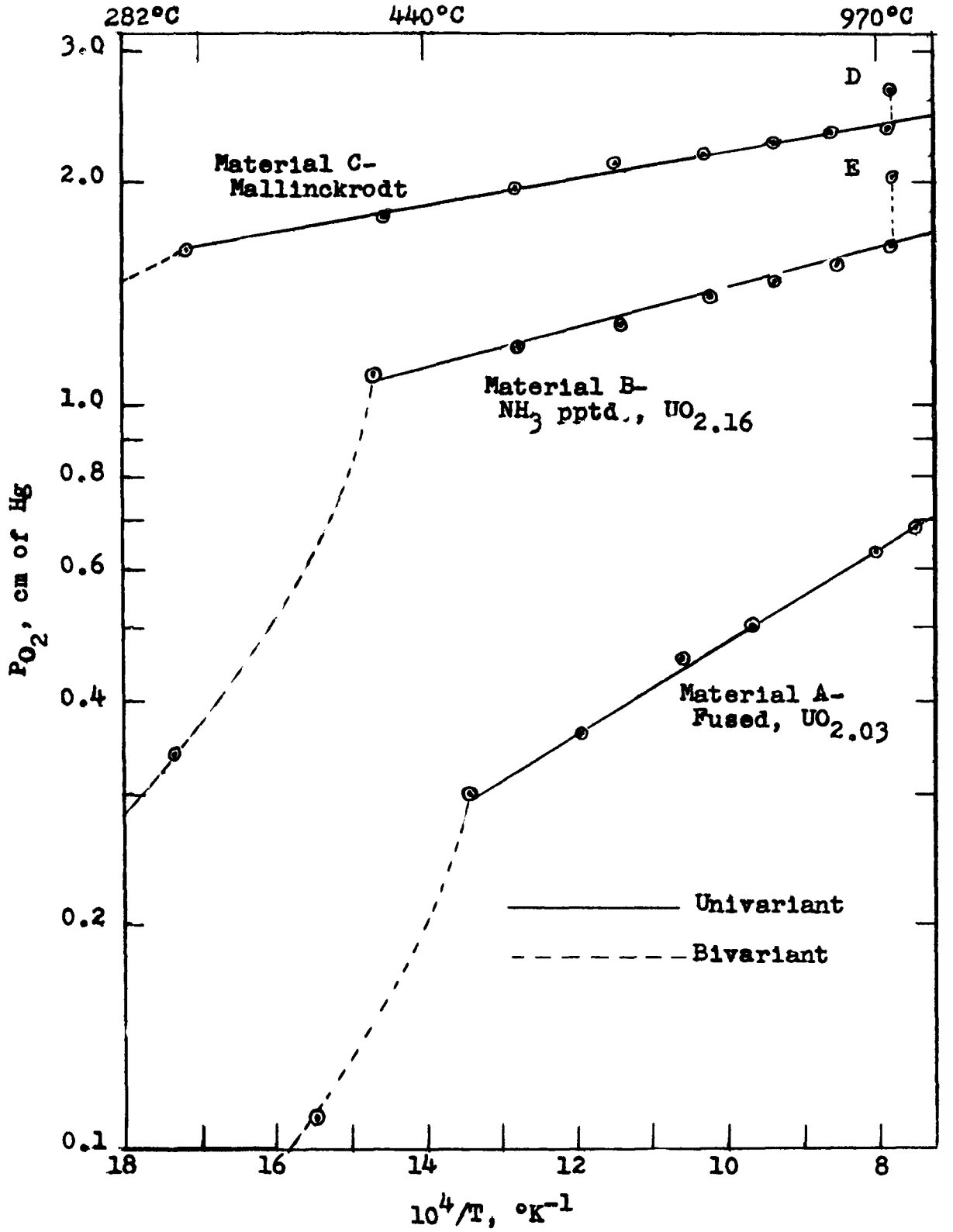

National Bureau of Standards

TABLE 1

Thermodynamic Constants - Decomposition of UO_2 and Desorption of Surface Phases

Decomposition of --- a/		Thermodynamic Constants -- b/				
		ΔH	ΔF°_{773}	ΔF°_{1273}	$-\Delta S^\circ_{773}$	$-\Delta S^\circ_{1773}$
		kcal/mole	Kcal/mole	Kcal/mole	cal/°/mole	cal/°/mole
$UO_{2.03}$	(A)	+ 3.13	5.32	8.77	6.88	6.88
$UO_{2.16}$	(B)	+ 1.37	5.06	8.31	6.54	6.52
UO_{2+x}	(C)	+ 0.81	4.82	7.93	6.24	6.23

a/ These materials are the same as those of Figure 1:

(A) - Norton fused, $UO_{2.03}$

(B) - Ammonia-precipitated, $UO_{2.16}$

(C) - Mallinckrodt, UO_{2+x}

b/ The subscripts of ΔF° and ΔS° indicate the temperatures in degrees absolute at which the values pertain.

NOTE: Please substitute this table of correct values for the one given on the same page of the NBS report in WAPD Resume' VII.

Smlang

These vapor-pressure data for the various types of UO_2 are not the vapor pressures of gaseous UO_2 over solid UO_2 but, rather, the vapor pressure of oxygen released in excess of $UO_{2.00}$. Because of a preliminary treatment, it is assumed that the gas phase evolved during these experiments is oxygen, but it could also be composed of both the liberated oxygen and other adsorbed phases that might be evolved. Other work indicates that some oxides tenaciously hold adsorbants even at temperatures of 1000° and 1100°C. In order to prevent any confusion as to the interpretation of these results, the vapor pressure-temperature diagram for UO_{2+x} is given on Figure 2. This shows the relationship of the data obtained in this investigation, line OA, for the vapor pressure of oxygen (+ X?) released in excess of $UO_{2.00}$ to the vapor pressure over UO_2, line OB, and that over liquid UO_2, line BC. The latter curves are based mainly on the work of Ackerman.

Because the volume as well as the pressure of oxygen may be determined with the tensimeter, the change in composition of the solid phases with temperature may be calculated, assuming the ideal behavior of the gas. A T-X diagram was determined for material B because it had the greatest initial O/U ratio and because its composition was better known. This is presented in Figure 3, which represents a projection on an arbitrary isobar, since pressure also varies with composition and temperature. The point E indicates the composition after 15 hours of heating at 1000°C. A new information supplied by this treatment of the data is:

(5) When UO_{2+x} is heated in vacuum, the overall composition of the condensed phases approaches $UO_{2.00}$ at 1000°C.

An X-ray diffraction powder pattern of sample A was obtained before any treatment, and after being heated at 1000°C in the tensimeter in excess oxygen. The a_o parameter increased from 5.4689 to 5.4702 Angstroms as a result of the heat treatment. Although the direction of this change was expected, it was concluded that

(6) The change in cell dimension with composition of UO_{2+x} is too small to be used as a quantitative criterion of composition.

Figure 2
Vapor Pressure-Temperature Relationships in the System UO_{2+x}

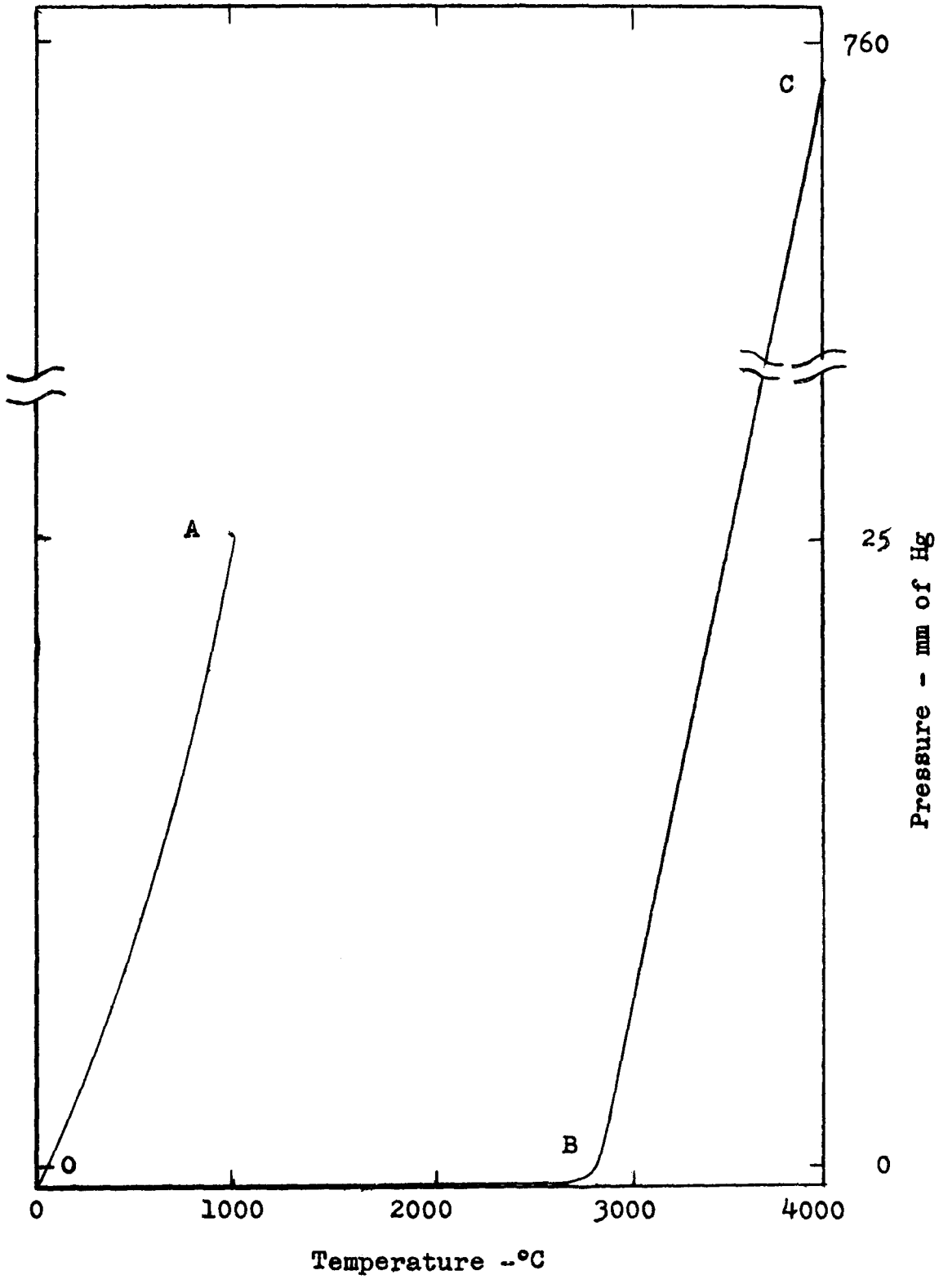

National Bureau of Standards

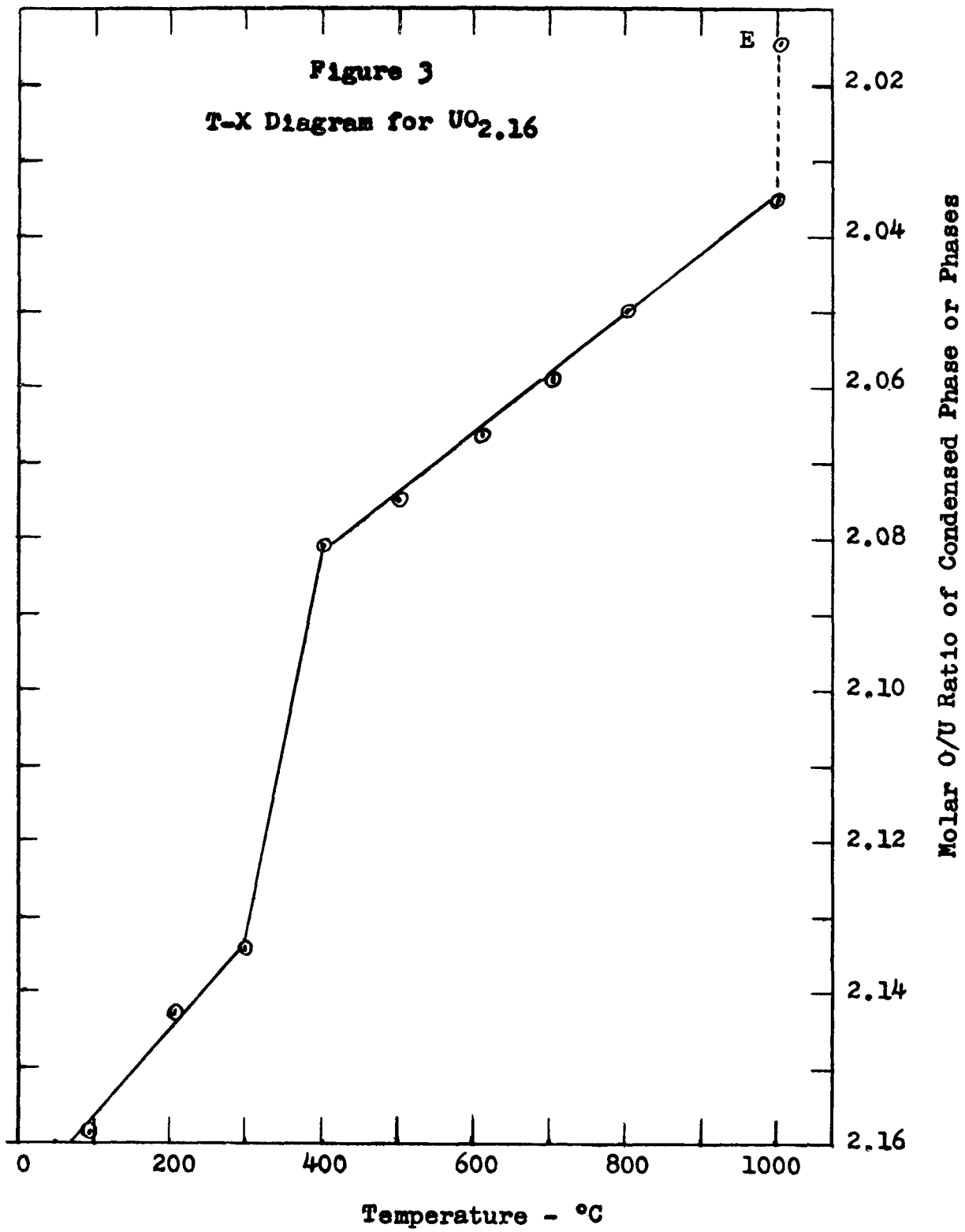

Figure 3

T-X Diagram for $UO_{2.16}$

National Bureau of Standards

A final experiment consisted of maintaining a sample of UO_{2+x} at 1000°C under dynamic vacuum for one-half hour. The sample was then cooled to room temperature, and reheated in static vacuum to 1000°C. There was no measurable vapor pressure. It is concluded that

(7) $UO_{2.00}$ is stable up to 1000°C in vacuum; that is, a UO_{2-x} phase does not form.

(b) The system UO_{2+x}-O_2:

The system was first studied under optimum oxidizing conditions, by heating UO_{2+x} in 76 cm of Hg pressure of dry oxygen. In view of the known complexity of the oxidation of this material, vapor-pressure readings were taken at approximately 50°C temperature intervals. The data are presented graphically in Figure 4. The following deductions and observations were made:

(1) The oxidation of UO_{2+x} is rapid at low temperatures. At about 350°C, the composition of the solid is $UO_{2.50}$;

(2) The overall composition of the solid remains at $UO_{2.50}$ until a temperature above 600°C is attained; and,

(3) At some temperature between 600° and 700°C, the overall composition of the solid phases begins to increase with temperature, but when maintained at 1000°C for 24 hours had not attained $UO_{2.67}$ (U_3O_8). (This figure cannot be compared to figures in the literature that were prepared from studies of condensed systems.)

The assumption is generally made in the literature that UO_{2+x} will quantitatively oxidize to U_3O_8 at about 750°C, when heated in air or oxygen, and, indeed, a frequently used method of quantitative analysis of UO_{2+x} (Ackerman, ANL-5482, Sept. 14, 1955) is based on this assumption. Hoekstra, et al (Hoekstra, Siegel, Fucks, and Katz, Jour. Phys. Chem., 59 (2) 136 (1935)) state that, when any lower oxide is heated with a partial pressure of 150 mm or greater of oxygen, the oxide goes quantitatively to exactly U_3O_8.

The experiments reported here were performed using sample weights of from 10 to 30 mg, and in either 200 or 760 mm of oxygen pressure, yet quantitative conversion to U_3O_8 was not accomplished. This could be due to the fact that the original composition of the oxide (from which all subsequent calculations are made) was not accurately established. However, Figure 3 and the textual discussion show that the original oxide ($UO_{2.16}$)

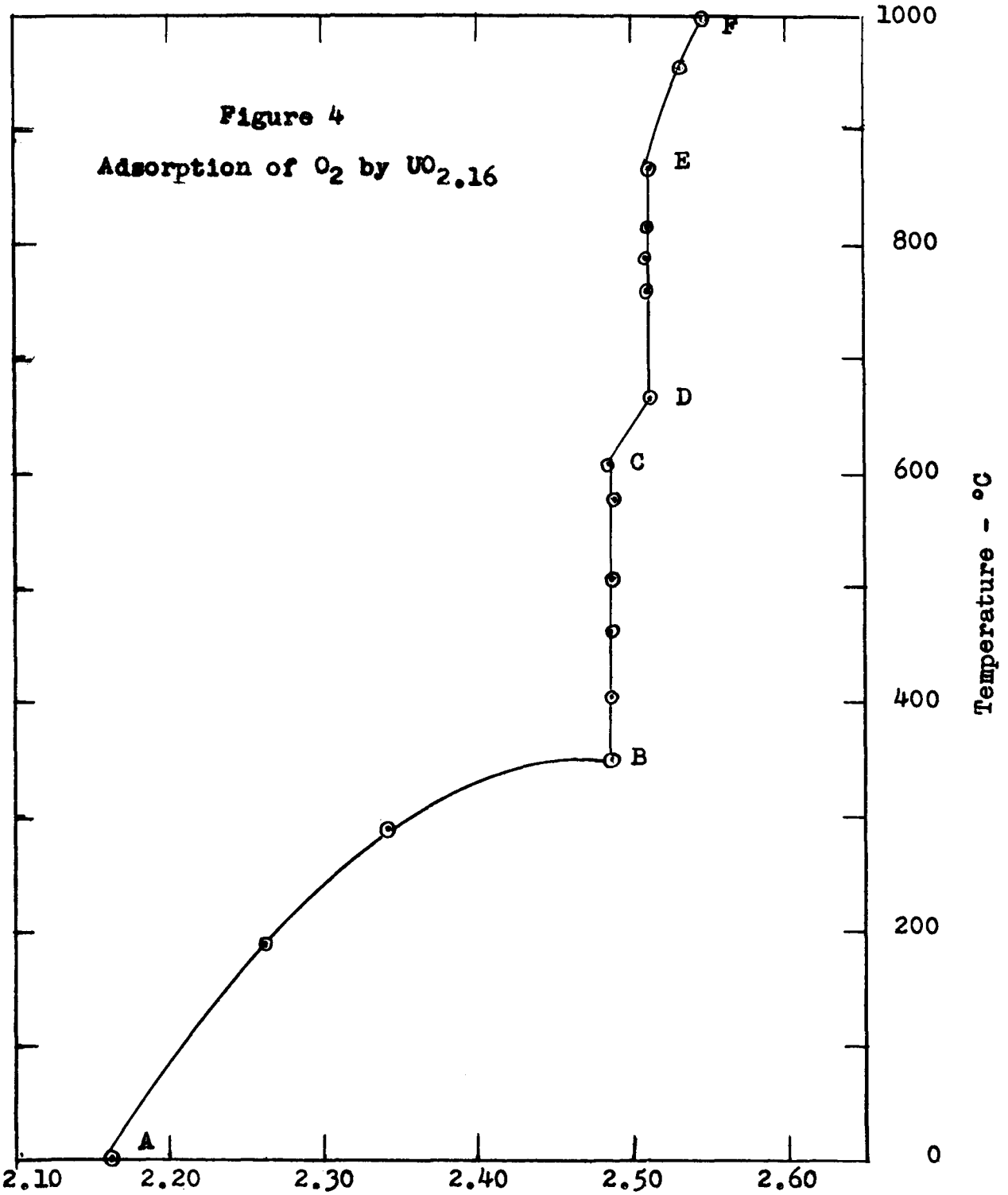

National Bureau of Standards

was decomposed to almost $UO_{2.0}$ and that, therefore, the composition of $UO_{2.16}$ used in these calculations is very nearly correct. Another series of experiments were made in which the sample weights were reduced, and it was found by trial and error that, when the sample weight was 3 mg or less, quantitative conversion to U_3O_8 was attained in a reasonable time--one hour. However, this may have been fortuitous for, with such a small sample, the inaccuracy in weighing the sample is a very large part of the total change resulting from the reaction.

These data show that there are three further experimental procedures that should be used to establish whether or not a quantitative conversion does occur. The first would be to maintain the sample at temperature for a long period of time--perhaps three or four weeks--to permit true equilibrium conditions to be attained. The second would be to use an enlarged-end reaction vessel in which a larger sample could be used. This, however, would require a high oxygen pressure to enable the use of the current differential manometer and, as a result of the high pressure required, would probably cause a change in the reaction system. The third would be to perform a total oxygen analysis both before and after such oxidations. In most analytical analyses, oxygen is determined by difference. This is inherently a poor procedure for a case such as the present where the percentage of O_2 is of prime importance. We are, therefore, planning to add a unit to our tensimeter for the direct analysis of total oxygen, using the reaction

$$UO_2 + 2BrF_3 \rightarrow O_2 + Br_2 + UF_6$$

in which the bromine and the hexafluoride will be condensed (Hoekstra and Katz, Anal. Chem., 25 (11) 1608 (1953)).

An interpretation of Figure 4 has been made. The portion of the line between A and B represents the continuous change of the UO_2 solid solution, a bivariant condition. Univariant conditions exist between the points B and C where two solid phases, perhaps U_4O_9 and UO_{2+x} (so-called alpha and beta UO_2) are continuously changing so that the total composition remains constant at $UO_{2.50}$. Bivariance occurs again between points C and D wherein there is, presumably, a transformation of one of the solid phases to yield a new assemblage of solid phases, probably U_4O_9 and U_3O_{8-x}. This causes the univariant condition, between points D and E. At point E there is a reaction in the solid to yield a single phase, causing a bivariant condition.

The possibility that dry air or air that contained some water vapor might be a better oxidant than pure dry oxygen was investigated. The results obtained indicated that these are comparable oxidants.

A study of this system under conditions that will define univariant portions and, hence, give the number and composition of solid phases at various temperatures has been initiated. Such a study consists of forming intermediate compositions between $UO_{2.00}$ and $UO_{2.67}$ by heating $UO_{2.00}$ in oxygen to a specific temperature, quenching to room temperature, evacuating, then reheating in static vacuum, and determining the equilibrium vapor pressures of these intermediate phases. It is anticipated that this will be done in the tensimeter without physically disturbing the sample. Such information will permit the construction of P-X diagrams, from which an elucidation of the number and composition of the phases present at equilibrium at specific temperatures can be made.

3. Kinetic Data:

The formation of phases that occur in a reaction, such as oxidation and possibly volatilization, is based upon thermodynamic equilibrium data as a function of dissociation pressure, while the rate of formation usually is based upon diffusion rates and impurities. Therefore, to understand the behavior of UO_2 with regard to oxidation and volatilization, its stability must be considered not only under equilibrium, but also under kinetic conditions. Although the experimental evidence required for an understanding of the kinetics of reactions may be obtained in many ways, particular emphasis was placed on the application of a continuous weight-change balance and differential thermal analysis unit. In measuring weight changes and interpreting DTA patterns, it is necessary to differentiate between the various processes that may occur. For example, the oxidation of UO_2 may be viewed as proceeding through the following series of reactions

$$UO_2 \rightarrow UO_{2+x} \rightarrow \begin{pmatrix} U_4O_9 \\ + \\ UO_{2+x} \end{pmatrix} \rightarrow \begin{pmatrix} U_4O_9 \\ + \\ U_3O_{8-x} \end{pmatrix} \rightarrow U_3O_{8-x} \rightarrow$$

$$U_3O_8 \rightarrow UO_2$$

This shows that it is not sufficient to know the equilibrium phases that exist in a particular temperature range, but it is also necessary to have some knowledge of the rates at which these phases are formed. The reaction rates and the activation energies of the oxidation of UO_2 to the U_3O_8 structure are being determined for the various types of UO_2 described earlier. However, in the application of the DTA method for the calculation of these kinetic data, the available equations have been developed only for first order reactions. There is not sufficient reliable information available on the oxidation of UO_2 to evaluate the order of the reactions involved. Therefore, we are currently studying the time, gas pressure, and particle-size dependence of isothermal weight-gain data to determine the order and to provide the necessary data for, at least, an empirical relation if higher orders are involved.

In addition to these determinations, it seems desirable to investigate the conflicting DTA reports that have been presented by ORNL and others and those from AERE (Harwell). American and Canadian patterns show only two peaks in the DTA curve, although some patterns indicate a slight ridge on the first one, while the AERE patterns show three distinct and separate peaks. Table 2 gives some data recently determined at NBS.

The work from England was discussed with Dr. Peter Murray (AERE - Harwell) during his recent visit to this country. He has consistently found the three reactions using both the U.K. oxide ($UO_{2.13}$) and the Mallinckrodt oxide ($UO_{2.03}$). He attributed these peaks to the following reactions (the temperature, of course, being dependent upon the heating rate):

at about 270°: $UO_2 \rightarrow UO_{2.2}$

at about 390°: $UO_{2.2} \rightarrow U_3O_8 + UO_{2+x}$

at about 450°: $U_3O_8 + UO_{2+x} \rightarrow U_3O_8$

TABLE 2

DTA - Weight Change Data for Various Types of UO_2 [a]

UO_2 Material	Heating Rate	DTA Sample					Max. Wt. Gain [d]	
		Wt.	Ref. Standard [b] Material	Wt.	1st Peak [c]	2nd Peak [c]	Temp.	Quan.
	°C/min	gm	----	gm	°C	°C	°C	%
Fused-$UO_{2.03}$	2.5	1.500	ThO_2	1.000	260	400	430	3.47
" "	1.3	1.500	ThO_2	1.000	320	420	510	3.35
Mallinckrodt-UO_{2+x}	1.6	1.000	Al_2O_3	0.200	260	380	380	3.88
	2.0	1.500	ThO_2	1.500	275	420	480	3.82
	2.1	1.000	ThO_2	1.000	272	435	455	3.78
	7.1	1.000	Al_2O_3	0.200	270	420	485	3.79
	10.0	1.000	Al_2O_3	0.200	290	440	475	3.76
	11.1	1.000	ThO_2	1.000	335	430	518	3.65
	12.0	1.500	ThO_2	1.000	315	435	490	3.79
	12.0	1.000	ThO_2	1.000	325	475	520	3.77
	13.0	1.000	ThO_2	1.000	315	420	485	3.73

a/ These are preliminary data developed during the incorporation of various equipment modifications for the normal air atmosphere apparatus.

b/ ThO_2 is Lindsay chemically-precipitated material that had been calcined at 1200°C and stored in a desiccator.

c/ Both DTA-peaks are exothermic, the second usually of much greater magnitude.

d/ Weight change began decreasing after these temperatures were attained.

In addition, the U.K. weight-gain determinations indicate incomplete conversion to U_3O_8, similar to our work; and, the reduction of U_3O_8 to UO_2 occurring at quite low temperatures; it appears to be measurable as low as 500° to 600°C. If the weight losses that are recorded in this temperature range when the samples are maintained for periods of up to 7 hours are true manifestations of the dissociation, then the understanding that now exists on the kinetic processes of the oxidation of UO_2 must be revised. However, with the present knowledge, there appears to be no better explanation than those which are now available.

B. FABRICATION DATA

In a study directed toward an understanding of the factors determining the strength and other desirable physical properties at high temperatures for UO_2 and the development of optimum properties in bulk shapes of that material, some fabrication data are available. Most of the information that has been secured during the course of this investigation has been included in the minutes of the Joint US - Canadian Conference on UO_2. This information is in addition to that described in that report.

The supply of peroxide- and ammonia-precipitated UO_2, referred to as lot I, has been exhausted. All of the fabrication, sintering, and mechanical property data described in the Joint US - Canadian Conference on UO_2 and that described previously at various WAPD UO_2 panel meetings was determined using the lot I materials. The peroxide- and ammonia-precipitated UO_2 in use at the present time was made by ORNL for NBS and will be referred to as lot II.

(1) Molding Additives:

Specimens were prepared by blending either peroxide- or ammonia-precipitated UO_2 and 0.2 percent by weight of technical grade aluminum stearate in a boron carbide mortar and tumbling in a jar for two hours. Cylindrical specimens were pressed in a steel mold at 4,000 psi and isostatically repressed at 45,000 psi. Specimens were heated for one hour in an atmosphere of static helium at temperatures of 1600°, 1800°, 2000°, and 2100°C. For comparison purposes, specimens of the materials prepared without stearate addition were heated at 2000°C under the same conditions.

The use of aluminum stearate as a lubricant in the pressing operations appears to have definite advantages, particularly in the case of ammonia-precipitated UO_2. The ammonia-precipitated material, without additives, has very uneven shrinkage, when formed in the same manner as described above, with the result that bar specimens warp badly and cylindrical specimens have concave sides, even when isostatic pressing is used. Many specimens exhibit laminations or cracks after the maturing heat treatments. These defects probably are due to the poor flow characteristics during pressing of this very fine-grained material. The addition of 0.2 percent by weight of aluminum stearate seems to eliminate these undesirable effects entirely and, in addition, contributes slightly to the improvement in bulk density of the matured specimens; when matured at 2000°C, porosity of the ammonia-precipitated material was reduced from 8.1 percent to 6.3 percent. No trouble had been experienced previously with warping or laminations in the peroxide-precipitated UO_2, but the addition of the aluminum stearate reduced the porosity of specimens matured at 2000°C from 10.9 to 6.3 percent. The average values of density and porosity are reported in Table 3.

Table 3

Density and Total Porosity of Ammonia- and Peroxide-Precipitated UO_2 from Lot 11 with 0.2 Percent by Weight of Aluminum Stearate Additions

Material	Maturing Temperature a/	Bulk Density	Total Porosity b/
	°C	g/cm³	%
H_2O_2 pptd., no addition c/	2000	9.80	10.9
" " , 0.1 Al Stearate d/	1600	7.70	29.7
" " , " " " d/	1800	9.65	12.0
" " , " " " d/	2000	10.27	6.3
" " , " " " d/	2100	10.36	5.5
NH_3 pptd., no addition c/	2000	10.14	8.1
" " , 0.1 Al Stearate d/	1600	9.93	9.4
" " , " " " d/	1800	10.23	6.7
" " , " " " d/	2000	10.28	6.3
" " , " " " d/	2100	10.22	6.8

a/ All heatings for one hour in static helium.

b/ Calculated as $\left(1 - \frac{\text{abs. density}}{\text{theor. density}}\right) \times 100$, theoretical density taken as 10.96

c/ Values represent average of six specimens.

d/ Values represent average of two specimens.

Pieces of physical test specimens were mounted in lucite and polished for examination. All of the specimens examined were matured at 2000°C for one hour in static helium. In the case of the ammonia-precipitated material, no visible effect due to the use of aluminum stearate could be noted. The major difference in appearance between the ammonia- and peroxide-precipitated materials was in the appearance of the pore structure. The "as received" particle size of these materials appears to be less than one micron, extensive grain growth, after heat treatment was noted in all specimens. The general characteristics of the matured specimens were as follows:

Material	Grain Size	Pore Structure
NH_3 pptd.	50 - 80 microns	grouped in clusters
NH_3 pptd. + 0.2% aluminum stearate	50 - 80 microns	grouped in clusters
H_2O_2 pptd.	15 - 30 microns	randomly distributed
H_2O_2 pptd. + 0.2% aluminum stearate	30 - 60 microns	randomly distributed

(2) Chemical Additives

The following table gives some results of microscopic examinations of various types of UO_2 with regards to the effects of additions of TiO_2 and Al_2O_3 on total porosity and grain development:

Material	Addition	Total Porosity at -- 1600°C	Total Porosity at -- 1900°C	Visible Grain Development at 1600°C	Visible Grain Development at 1900°C	Remarks
	wt.%	%	%			
Steam Oxidized	None	28.7	26.1	No	No	Very porous structure
	0.75 TiO_2	17.1	11.4	No	Yes	Some 50-100 micron grains
	1.50 Al_2O_3	27.7	12.5	No	Yes	Some 50-100 micron grains, pores larger than with TiO_2.
Hydrogenated Steam Oxidized	None	28.3	20.7	No	No	Very porous structure.
	0.75 TiO_2	12.3	7.1	No	Yes	Some 50-100 micron grains.
	1.50 Al_2O_3	25.4	7.8	No	Yes	Some 50-100 micron grains, pores larger than with TiO_2.
Peroxide Precipitated	None	29.4	11.3	No	No	
	0.75 TiO_2	5.6	7.1	Yes	Yes	
	1.50 Al_2O_3	18.9	7.0	No	Yes	
Ammonia Precipitated	None	12.1	9.2	No	Yes	Small pores at 1600°, grains usually less than 50 microns at 1900°.
	0.50 TiO_2	8.6	9.2	Yes	Yes	Grains less than 30 microns at 1600°, 40-60 microns at 1900°.
	1.33 Al_2O_3	15.1	8.1	No	Yes	Some 50-100 micron grains

C. MECHANICAL PROPERTY DATA

The supply of peroxide- and ammonia-precipitated UO_2, referred to as lot I, has been exhausted. All of the fabrication, sintering, and mechanical property data described in the Joint US-Canadian Conference on UO_2 and that described previously at various WAPD UO_2 panel meetings was determined using the lot I materials. The peroxide- and ammonia-precipitated UO_2 in use at the present time was made by ORNL for NBS and will be referred to as lot II.

(1) Flexural Strength of Peroxide- and Ammonia-precipitated UO_2

The room temperature flexural strengths of peroxide- and ammonia-precipitated UO_2 with 0.2 percent by weight of aluminum stearate, and peroxide-precipitated UO_2 with and without 0.25 percent by weight of TiO_2 from lot II are summarized in Table 4. This table also includes flexural strength data obtained on earlier groups of specimens prepared from lot I of peroxide- and ammonia-precipitated UO_2 with and without additions.

The room temperature flexural strength, 12,990 psi, obtained with specimens from lot II of peroxide-precipitated UO_2 without additions is essentially the same as that obtained with the lot I of peroxide-precipitated UO_2, 12,400 psi. The coefficient of variation of strength is also approximately the same, 13 and 13.6 percent. The bulk density of specimens of lot II appears to be slightly higher, and the "t" test (for significant difference between means) indicates that, at the 95% confidence level, the average bulk density of this group of specimens is significantly greater than that of lot I. It has been found that there is no significant difference between different headings, and it seems logical to attribute the slight bulk density difference to minor variations between different lots of UO_2.

The use of 0.2 percent by weight of aluminum stearate as a lubricant in the pressing operation did not show any effect on the flexural strength of the peroxide-precipitated UO_2, 12,680 psi, obtained with the addition and 12,990 psi obtained without the addition. However, the average bulk density was increased from 10.17 to 10.37 g/cm^3 and the variability was decreased slightly. The fact that the strength remained the same while the porosity decreased may be explained by the fact that the grain size of specimens prepared with stearate addition was greater than the grain size of specimens prepared without additions of the stearate.

The average flexural strength of the peroxide-precipitated UO_2 containing 0.25 percent by weight TiO_2 was 14,520 psi. At the 95% confidence level, this is not significantly different from the values of flexural strength obtained from the peroxide-precipitated material with and without aluminum stearate additions, 12,990 and 12,680, respectively. However, the strength is significantly greater at the 95% confidence level than the average strength obtained from lot I of peroxide-precipitated UO_2 with TiO_2 addition.

Table 4
Summary of Room Temperature Flexural Strength and Bulk Density Results for NH_3- and H_2O_2-precipitated UO_2

Material	Heat Treatment a/	No. of Specimens	Modulus of Rupture			Density		
			Average	S.D. b/	C.V. c/	Average	S.D. b/	C.V. c/
	°C	---	psi	psi	%	g/cm^3	g/cm^3	%
NH_3 ppt.								
Lot I	2000	12	11,100	1,230	11.1	9.84	0.07	0.74
Lot II + Al stearate	2000	11	10,870	1,164	10.7	10.26	.02	.23
H_2O_2 ppt.								
Lot I	2000	6	12,400	1,610	13.0	10.04	.07	.71
Lot II	2000	15	12,990	1,770	13.6	10.17	.03	.32
Lot II + Al stearate	2000	8	12,680	1,730	13.6	10.37	.02	.19
Lot I + 0.25% TiO_2	1600	7	10,400	2,800	26.9	10.39	.10	.92
Lot II + 0.25% TiO_2	1600	15	14,520	2,400	16.7	10.38	.03	.28

a/ Heat-treated for one hour in an argon atmosphere at the temperature given.

b/ S.D. = standard deviation.

c/ C.V. = coefficient of variation = (S.D./average) x 100.

The room temperature strength of specimens of the ammonia-precipitated UO_2, prepared with 0.2 percent by weight aluminum stearate, was found to be 10,870 psi. This value compares favorably with the value of 11,100 psi found for the material from lot I without additions. Specimens prepared from the unadulterated material warped very badly with the result that all had to be prepared with large dimensions to provide sufficient material to grind flat specimens. Specimens prepared with the stearate addition did not exhibit any such warpage. Also, the total porosity of the specimens that were prepared using the aluminum stearate addition was 6.4 percent as compared to 10.2 percent for the unadulterated specimens of lot I. A portion of this difference may be attributed to differences between the two lots of UO_2, since total porosities of 8.1 percent were obtained without additions with lot II.

(2) Elastic Constants:

The moduli of elasticity of specimens of ammonia-precipitated UO_2 (approximately 93% of theoretical density) were determined as a function of temperature over the range of from 25° to 825°C in vacuo. The data obtained from different specimens sawed from a large bar were in good agreement and duplicate determinations on the same specimen revealed that the material of the support wires, i.e., platinum or tungsten, had no apparent effect on the various determinations. The modulus of elasticity values were found to decrease, but not linearly, with increasing temperature. At 825°C, the value had decreased to approximately 1,625 kilobars from the room temperature value of 1,823 kilobars. Figure 15 shows these data.

Five specimens of ball-milled Mallinckrodt UO_2 (Lot 39-225), normal uranium dioxide, were received from the Corning Glass Works. The fabrication information, supplied by Corning, is as follows: "A weight gain of 3.66% on ignition to U_3O_8 of the 'as received' material corresponds to $UO_{2.048}$, if the only impurity is assumed to be oxygen. A weight gain of 3.80% of the fired material on ignition corresponds to $UO_{2.024}$. Spectrographic examination of the 'as received' material shows traces of aluminum, calcium, copper, iron, silicon, magnesium, manganese, nickel, lead, and tin. A binder addition of one weight percent Carbowax 20-M was made during granulation of the material. The specimens were fired at 1750°C for 3 hours in a Harper molybdenum-wound tube (3" I.D. x 36") furnace. The atmosphere used was deoxygenated dry hydrogen flowing at a rate of 30 ft. per hour."

The following values for the elastic constants, and other data, were determined for these five specimens of Mallinckrodt normal UO_2 (lot 39-225) as fabricated by the Corning Glass Works :

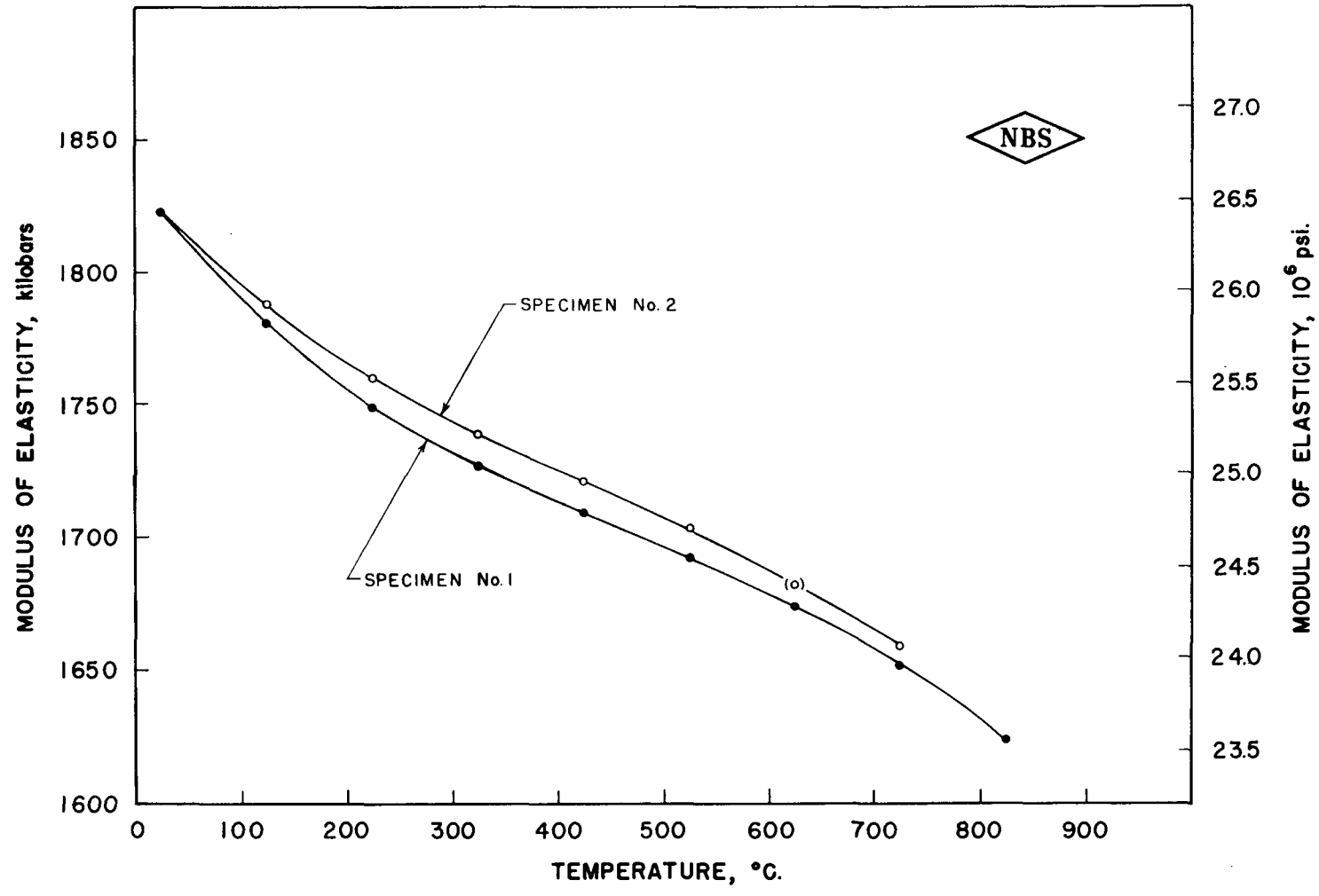

Figure 5

MODULUS OF ELASTICITY vs. TEMPERATURE, IN VACUO

AMMONIA PRECIPITATED URANIUM DIOXIDE

Property	Average Value	Standard Deviation	Coefficient Variation
	Kilobars*	Kilobars*	%
Modulus of Elasticity:			
Longitudinally	1929	8	0.42
Flexurally, wide	1936	9	.46
Flexurally, thin	1930	12	.64
Shear Modulus	741	3	.39
Poisson's Ratio:			
From Long. E	0.302	0.002	0.7
From Flex., wide E	.306	.002	.7
From Flex., [illegible] E	.302	.005	1.6
Bulk Modulus	1620	21	1.3
Velocity of Sound, m/sec.	4314	7	0.17
Bulk Density, g/cm^3	10.37**	0.02	0.16

* 1 kilobar = 14,503.8 $lb/in.^2$ = 10,197.16 kg/cm^2

** About 94.6% of theoretical density.